UNIVERSITA' DEGLI STUDI DI PADOVA

Sede Amministrativa: Università degli Studi di Padova

Dipartimento di Scienze Sperimentali Veterinarie

SCUOLA DI DOTTORATO DI RICERCA IN SCIENZE VETERINARIE

INDIRIZZO: Scienze Biomediche Veterinarie e Comparate

CICLO XXI

ORGANIZATION OF THE CETACEAN FRONTAL AND INSULAR CORTICES: CYTOARCHITECTURE, CHEMOARCHITECTURE, AND NEURONAL SPECIALIZATIONS

Direttore della Scuola: Ch.mo Prof. Massimo Morgante

Supervisore: Ch.mo Prof. Bruno Cozzi

Co-Supervisore: Ch.mo Prof. Patrick R. Hof

Dottorando: Camilla Butti

Table of contents

Abstract

The brain of cetaceans is very large in both absolute and relative size and possesses an extremely convoluted cortex. The understanding of how the brain of these mammals fully adapted to an aquatic life is organized is important to shed light on the processes that shaped the evolution of the mammalian brain in general, including humans. Three cortical regions, the anterior cingulate (ACC), anterior insular (AI), and frontopolar cortices (FPC) have been shown to be involved in high-level cognitive function in primates and thus, the understanding of their structural organization in cetaceans is particularly meaningful given the wide evidence of their cognitive abilities. Cytoarchitecture, chemoarchitecture based on the distribution of the calcium binding (CaBP) protein calretinin, glia/neuron ratio, and neuronal specializations were assessed in the ACC, AI, and FPC of a series of cetaceans representative of the main families such as the bottlenose dolphin (*Tursiops truncatus*, Odontoceti, Delphinidae), Risso's dolphin (*Grampus griseus*, Odontoceti, Delphinidae), harbor porpoise (*Phocoena phocoena*, Odontoceti, Phocoenidae), killer whale, (*Orcinus orca*, Odontoceti, Delphinidae), beluga whale (*Delphinapterus leucas*, Odontoceti, Monodontidae), sperm whale (*Physeter macrocephalus*, Odontoceti, Physeteridae), pigmy sperm whale (*Kogia simus*, Odontoceti, Kogiidae), Amazon river dolphin (*Inia geoffrensis*, Odontoceti, Iniidae), minke whale (*Balaenoptera acutorostrata*, Mysticeti, Balaenopteridae), and humpback whale (*Megaptera novaeangliae*, Mysticeti, Balaenopteridae). Other species including the pigmy hippopotamus (*Hexaprotodon liberiensis*, Cetartiodactyla, Hippopotamidae), Florida manatee (*Trichecus manatus latirostris*, Sirenia, Trichechidae), Atlantic walrus (*Odobenus rosmarus rosmarus*, Carnivora, Odobenidae), African savannah elephant (*Loxodonta africana*, Proboscidea, Elephantidae), black rhinoceros (*Diceros bicornis*, Perissodactyla, Rhinocerotidae), rock hyrax (*Procavia capensis*, Hyracoidea, Procavidae), lowland streaked tenrec (*Hemicentetes semispinosus*, Afrosoricida, Tenrecidae), and black and rufous elephant shrew (*Rhynchocyon petersi*, Macroscelidea, Macroscelididae), were used for comparative purposes in different parts of this study. The results show that 1) Order-specific differences in the organization of the neocortex occur among cetaceans; 2) Cetaceans share structural features of the neocortex with the artiodactyls, both at a structural and neurochemical level; 3) The glia-neuron ratio of the cetacean neocortex corresponds to what is expected for their brain size; 4) The specific cortical regions investigated contain, in most of the available cetaceans species, a neuronal specialization observed with the same pattern of distribution only in great apes and humans, the Von Economo neurons. Overall these results are

further evidence for an organization of the cetacean neocortex, which, although very different from that of primates, displays complexity, challenging the classical view of its homogeneous and simple structure. Specifically, the extended development of regions involved in high-level cognitive processes such as the ACC, AI, and FPC, their diverse cortical organization, and the presence of a specific neuronal specialization, all suggest that specific evolutionary selective pressures acted on these cortical regions and thus on their functions. Based on the evidence reported in the present thesis, the brain of cetaceans can be considered of a complexity comparable to that of primates, and an evolutionary alternative to the generation of complex behaviors.

Riassunto

L'encefalo dei cetacei è caratterizzato dal notevole volume e dalla complessità ed estensione della superficie neocorticale. La conoscenza dell'organizzazione delle strutture cerebrali di questi mammiferi completamente adattati alla vita acquatica è di primaria importanza per comprendere i meccanismi che stanno alla base dell'evoluzione del sistema nervoso centrale dei mammiferi, incluso l'uomo. In particolare, le tre regioni corticali costitute dalla corteccia cingolata anteriore (ACC), dalla insula anteriore (AI) e dalla corteccia frontopolare (FPC) hanno un ruolo primario nei processi di alto livello cognitivo nei primati e, quindi, lo studio della loro organizzazione corticale nei cetacei assume una particolare importanza in ragione delle capacità cognitive ampiamente documentate in queste specie. La citoarchitettura, la chemoarchitettura basata sulla distribuzione della proteina legante il calcio (CaBP) calretinina (CR), il rapporto cellule della glia-neuroni (GNI) e le specializzazioni neuronali di ACC, AI e FPC sono state studiate in alcune specie, rappresentanti delle maggiori famiglie di cetacei, che includono il tursiope (*Tursiops truncatus*, Odontoceti, Delphinidae), il grampo (*Grampus griseus*, Odontoceti, Delphinidae), la focena (*Phocoena phocoena,* Odontoceti, Phocoenidae), l'orca (*Orcinus orca*, Odontoceti, Delphinidae), il beluga (*Delphinapterus leucas*, Odontoceti, Monodontidae), il capodoglio (*Physeter macrocephalus* , Odontoceti, Physeteridae), il capodoglio nano (*Kogia simus*, Odontoceti, Kogiidae), l'inia (*Inia geoffrensis*, Odontoceti, Iniidae), la balenottera minore (*Balaenoptera acutorostrata*, Mysticeti, Balaenopteridae) e la megattera (*Megaptera novaeangliae*, Mysticeti, Balaenopteridae). Specie selezionate che includono l'ippopotamo nano (*Hexaprotodon liberiensis*, Cetartiodactyla, Hippopotamidae), il lamantino della Florida (*Trichecus manatus latirostris,* Sirenia, Trichechidae), il tricheco (*Odobenus rosmarus rosmarus* Carnivora, Odobenidae), l'elefante africano (*Loxodonta africana*, Proboscidea, Elephantidae), il rinoceronte nero (*Diceros bicornis,* Perissodactyla, Rhinocerotidae), la procavia (*Procavia capensis,* Hyracoidea, Procavidae), il tenrec striato di pianura, (*Hemicentetes semispinosus,* Afrosoricida, Tenrecidae), e il toporagno elefante di Peters (*Rhynchocyon petersi*, Macroscelidea, Macroscelididae) sono state utilizzate, in una prospettiva comparata, in diverse parti della presente tesi. I risultati qui riportati dimostrano che 1) Esistono differenze ordine-specifiche nell'organizzazione corticale dei cetacei; 2) Esistono similitudini strutturali e chimiche nell'organizzazione corticale di cetacei e artiodattili; 3) Il rapporto cellule della glia-neuroni nella corteccia dei cetacei è conforme a quanto previsto sulla base delle dimensioni dell'encefalo; 4) Le specifiche regioni corticali esaminate nella

presente tesi contengono, nella maggior parte delle specie di cetacei, una particolare specializzazione neuronale, osservata con la medesima distribuzione solo nell'elefante e nelle scimmie antropomorfe filogeneticamente più vicine all'uomo: i neuroni di Von Economo. In conclusione, i risultati qui riportati costituiscono una ulteriore evidenza del fatto che l'organizzazione corticale dei cetacei, anche se molto diversa da quella dei primati, è caratterizzata da una specifica complessità che sfida la visione di semplicità e monotonia classicamente associata alla struttura della corteccia cerebrale di questi mammiferi marini. In particolare, il notevole sviluppo di regioni corticali associate a complessi processi cognitivi, quali ACC, AI e FPC, l' eterogeneità dell'organizzazione corticale, e la presenza di definite specializzazioni neuronali, suggeriscono che queste regioni corticali, e le loro funzioni, siano state plasmate da specifici processi evolutivi. Sulla base dei risultati riportati nella presente tesi, l'encefalo dei cetacei può essere considerato di complessità paragonabile a quella dei primati, ed una alternativa evoluzionistica per la produzione di comportamenti strutturati.

List of publications

Publications are listed in chronological order:

I. **BUTTI C**, CORAIN L, COZZI B, PODESTÀ M, PIRONE A, AFFRONTE M, ZOTTI A (2007)
Age estimation in the Mediterranean bottlenose dolphin, *Tursiops truncatus* (Montagu, 1821) by bone density of the thoracic limb.
Journal of Anatomy, **211** (5):639-646.

II. MARINO L, **BUTTI C**, CONNOR RC, FORDYCE RE, HERMAN LM, HOF PR, LEFEBVRE L, LUSSEAU D, MCCOWAN B, NIMCHINSKY EA, PACK AA, REIDENBERG JS, REISS D, RENDELL L, UHEN MD, VAN DER GUCHT E, WHITEHEAD H (2008)
A claim in search of evidence: reply to Manger's thermogenesis hypothesis of cetacean brain structure.
Biological Reviews, **83** (4):417-440.

III. SHERWOOD CC, STIMPSON CD, **BUTTI C**, BONAR CJ, NEWTON AL, ALLMAN JM, HOF PR (2009)
Neocortical neuron types in Xenarthra and Afrotheria: implications for brain evolution in mammals.
Brain Structure and Function, **213** (3):301-328.

IV. HAKEEM AY, SHERWOOD CC, BONAR CJ, **BUTTI C**, HOF PR, ALLMAN JM (2009)
Von Economo neurons in the elephant brain.
The Anatomical Record, 292 (2): 242-248.

V. **BUTTI C**, SHERWOOD CC, HAKEEM AY, ALLMAN JM, HOF PR (2009)
Total number and volume of Von Economo neurons in the cerebral cortex of cetaceans.
Journal of Comparative Neurology, **515** (2):243-259.

List of figures

List of tables

Abbreviations

ac	anterior commissure
ACC	anterior cingulate cortex
AI	anterior insular cortex
aq	aqueduct
C	cerebellum
cc	corpus callosum
cr	cruciate sulcus
crs	coronal sulcus
dlPFC	dorsolateral prefrontal
ec	cortex
EG	ectosylvian sulcus
en	ectosylvian gyrus
es	entolateral sulcus
FI	ectosylvian sulcus
FPC	frontoinsular cortex
g	frontopolar cortex
IC	genu of the corpus callosum
la	inferior colliculus
lc	lateral sulcus
LL	limbic cleft
LG	limbic lobe
LGN	lateral gyrus
MGN	lateral geniculate nucleus
OFC	medial geniculate nucleus
P	orbitofrontal cortex
pc	pons
PLL	posterior commissure
PG	parlimbic lobe
s	perisylvian gyrus
SC	sylvian fissure
	superior colliculus
SG	suprasylvian gyrus
sp	splenium
ss	suprasylvian sulcus

Chapter 1

General introduction

Review of cetacean evolutionary history, taxonomy, and classification

Cetaceans diverged from terrestrial mammals about 55 million years ago (Gingerich and Uhen, 1998; Gingerich et al., 2001), and from their common ancestor of primates about 95 million years ago (Kumar and Hedges, 1998; Bromham et al., 1999). According to the fossil record, early cetaceans, the Archeocetes, were a group of non-echolocating non-filter-feeders, inhabiting marine and fresh waters (Clementz et al., 2006) that arose from terrestrial mammals such as hippopotamuses, raoellids, and mesonychids (Geisler and Sanders, 2003; O'Leary and Gatesy, 2007; Thewissen et al., 2007; Fordyce, 2008a). Archeocetes diversified in the early Eocene between 45-53 million years ago (Fordyce, 2008a), but it is only in the late Eocene, 38-40 millions years ago, that the Basilosauridae, a family with morphological features, and feeding and hearing capacities comparable to early odontocetes and mysticetes, appeared (Uhen, 2004; Gingerich, 2005; Fordyce, 2008a). The early Oligocene, about 35 millions years ago, is marked by the appearance of the Neoceti that, in the late Miocene, about 10-12 million years ago, gave origin to the modern odontocetes and mysticetes. However, only the early Pliocene, 8-10 million years ago, is characterized by the appearance of the main crown genera (Fordyce, 2008a). The oldest baleen-bearing mysticetes date to the mid-Oligocene, about 28-29 million years ago, a period of great diversification of Mysticeti (Geisler and Sanders, 2003; Fitzgerald, 2006). The oldest odontocetes are found in the early Oligocene, about 32 million years ago (Fordyce, 2002). Sperm whales (*Physeter macrocephalus* and *Kogia* spp.) are considered the most basal extant odontocetes (Bianucci and Landini, 2006; Fordyce, 2008b).

Table 1. Latest classification of extant cetaceans. Modified from (Rice, 2008)

Order CETARTIODACTYLA

Infraorder CETACEA

Parvorder MYSTICETI
- Superfamily Balaenoidea
  - Family Neobalaenidae
  - Family Balaenidae
- Superfamily Cetotherioidea
  - Family Eschrichtiidae
- Superfamily Balaenopteroidea
  - Family Balaenopteridae

Parvorder ODONTOCETI
- Superfamily Physeteroidea
  - Family Physeteridae
  - Family Kogiidae
- Superfamily Ziphioidea
  - Family Ziphiidae
- Superfamily Platanistoidea
  - Family Platanistidae
- Superfamily Inioidea
  - Family Pontoporidae
  - Family Inidae
- Superfamily Lipotoidea
  - Family Lipotidae
- Superfamily Delphinoidea
  - Family Delphinidae
  - Family Phocoenidae
  - Family Monodontidae

The classification and phylogenetic position of cetaceans has always been a contested field given the different and frequently divergent conclusions drawn from morphological and molecular studies.

However, recent data provide both molecular (Nikaido et al., 1999; Shimamura et al., 1999) and morphological (Gingerich et al., 2001; Thewissen et al., 2001; Geisler and Sanders, 2003; Boisserie et al., 2005) evidence for the inclusion of cetaceans within the Artiodactyla (even-toed ungulates) and for a sister-taxon relationship between cetaceans and hippopotamuses (family

Hippopotamidae) (Gatesy, 1997; Boisserie et al., 2005; Agnarsson and May-Collado, 2008). The currently accepted classification groups Cetacea (dolphins, whales, and porpoises) and Artiodactyla in the taxon Cetartiodactyla. Accordingly to this latest classification the taxon Cetacea is an Infraorder that includes the two Parvorders Mysticeti (baleen whales) and Odontoceti (toothed whales) as shown in Table 1. The two living clades of cetaceans include 14 species in 4 families for Mysticetes, and 74 species in 10 families for Odontocetes, in the current classification (Rice, 2008).

General organization of the cetacean brain

Surface configuration, cortical organization and main general features

The cetacean telencephalon is rotated rostroventrally, characterized by a rostrocaudal foreshortening, and increased height and width compared to the general mammalian brain shape, reflecting modifications that the skull of cetaceans underwent over the 50 million years of adaptation to the aquatic environment (Marino, 2008). Odontocetes lack an olfactory bulb and tract completely, although a vestigial bulb is present in late embryonic and early fetal stages (Oelschläger and Buhl, 1985; Oelschläger and Kemp, 1998). In mysticetes these structures are present but poorly developed (Kojima, 1951; Breathnach and Goldby, 1954; Jacobs et al., 1971; Morgane et al., 1980; Oelschläger and Oelschläger, 2008; Oelschläger et al., 2008). One of the most fascinating characteristics of the cetacean neuroanatomy is the size and the extreme folding of the neocortex (Kojima, 1951; Breathnach and Goldby, 1954; Morgane et al, 1980; Hof and Van der Gucht, 2007; Oelschläger and Oelschläger, 2008). Compared to terrestrial mammals, cetaceans have extensive parietal and temporal regions with a degree of regional parcellation comparable to that of primates and carnivores (Felleman and Van Essen, 1991; Hof et al., 1992, 2000, 2005; Glezer and Morgane, 1993; Scannell et al., 1995; Glezer et al., 1998; Hof and Sherwood, 2005; Hof and Van der Gucht, 2007; Marino et al., 2007, 2008), as well as a well-developed frontal cortex (Hof et al., 2005; Hof and Van der Gucht, 2007). It is worth noting that although a cortical region homologous to the primate prefrontal cortex has not been functionally identified in cetaceans, the frontopolar cortex is extremely expanded and shows a very different cytoarchitecture compared to the adjacent motor fields (Hof and Van der Gucht, 2007). The limbic lobe is extensive and it includes well-developed cingulate, insular, and parahippocampal cortices (Jacobs et al., 1979; Morgane et al., 1980; Hof and Van der Gucht, 2007). In contrast to the extreme development of the neocortex, the paleocortex (rhinencephalon) and archicortex (hippocampal formation) are very reduced although the hippocampal formation contains all its subregions (dentate gyrus, hippocampus proper, and subiculum), as well as a large entorhinal cortex (Breathnach and Goldby, 1954; Filimonoff, 1965; Jacobs et al., 1979; Morgane et al., 1982; Hof et al., 2005; Hof and Van der Gucht, 2007), providing evidence that the cetaceans learning and memory pathways are likely organized very differently than those in terrestrial mammals.

In general the cetacean cortex is agranular owing to the lack or underdevelopment of a layer IV. The general layering pattern is characterized by a thick layer I, a densely populated layer II that contains extraverted neurons with dendrites extending into layer I, a wide pyramidal layer III, a layer V containing large pyramidal neurons and a multiform layer VI (Morgane et al., 1988; Glezer and Morgane, 1990; Hof et al., 2005; Hof and Van der Gucht, 2007). Moreover, layer V in specific cortical regions comprising the anterior cingulate, the anterior insular and the frontopolar cortices, contains, in almost all species examined thus far, a unique population of projection neurons, the Von Economo neurons, suggested to play a crucial role in social and cognitive processes (Hof and Van der Gucht, 2007; Butti et al., 2009; see Chapter 4 for details). The ventricular system of the cetacean brain reflects the configuration of the cerebral hemispheres with an anteroposterior compression leading to a reduced space between the anterior and inferior horn

and the reduction in size of the anterior horn, the lateral extension of the inferior horn, the lack of a posterior horn, the foreshortening and dorsoventral elongation of the third ventricle as well as a "swollen" appearance of the aqueduct (Breathnach and Goldby, 1954; McFarland et al., 1969; Oelschläger and Oelschläger, 2008). The corpus callosum, the major brain commissure, has in cetaceans a smaller midsection area relative to brain mass if compared to other mammals (Tarpley and Ridgway, 1994), and shows a variation in fibers size and density along its length (Keogh and Ridgway, 2008), features that have been linked to the degree of functional independence of the cerebral hemispheres in cetaceans (Tarpley and Ridgway, 1994). The anterior commissure is extremely reduced owing to the reduction of the olfactory system, whereas the posterior commissure is very well developed (Oelschläger and Oelschläger, 2008). The basal ganglia are characterized by the extreme development of the striatum and by an extensive claustrum (Breathnach and Goldby, 1954; Schwerdtfeger et al., 1984; Hof and Van der Gucht, 2007; Oelschläger and Oelschläger, 2008).

In the diencephalon, the thalamus is extensive (Langworthy, 1932; Breathnach and Goldby, 1954; Kruger, 1959; Oelschläger and Oelschläger, 2008), and of particular interest is the large size of the anteroventral (AV) and mediodorsal (MD) nuclei given their extensive connections with limbic structures and prefrontal cortex, as well as the larger size of the medial geniculate nucleus (MGN) relative to the lateral geniculate nucleus (LGN), reflecting the important development of the auditory system in cetaceans (Kruger, 1959; Oelschläger and Oelschläger, 2008; Oelschläger et al., 2008). For the same reason, the inferior colliculus (IC) is larger than the superior colliculus (SC) in several species, especially echolocating ones (Ries and Langworthy, 1937; Breathnach and Goldby, 1954). Finally, the facial, trigeminal, and vestibulocochlear nerves are very well developed in cetaceans (Breathnach, 1960).

The cetacean cerebellum is very large and accounts for about 15-20% of total brain mass (Breathnach, 1960; Marino et al., 2000). A correlation between the extreme expansion of the neocortex and the cerebellar size as well as the involvement in acousticomotor processing as a possible cause for the hyperthrophy of the cerebellum have been suggested (Schwerdtfeger et al., 1984; Marino et al., 2000; Oelschläger and Oelschläger, 2008).

Recently, the use of magnetic resonance imaging (MRI) technique, a common diagnostic tool in human medicine, shed light on several quantitative features of the brain of several species of cetaceans such as the beluga whale, *Delphinapterus leucas* (Marino et al., 2001a), the fetal and adult common dolphin, *Delphinus delphis* (Marino et al., 2001b, 2002; Oelschläger et al., 2008), the bottlenose dolphin, *Tursiops truncatus* (Marino et al., 2001c), the harbor porpoise, *Phocoena phocoena* (Marino et al., 2003b), the dwarf sperm whale, *Kogia simus* (Marino et al., 2003a), the spinner dolphin, *Stenella longirostris orientalis* (Marino et al., 2004c), the killer whale, *Orcinus orca* (Marino et al., 2004b), and the Atlantic white-sided dolphin, *Lagenorhyncus acutus* (Montie et al., 2007, 2008). These studies provide quantitative data on the spatial arrangement and proportion of systems and structures within the cetacean brain, highlighting once again their particularities.

Gyral pattern and localization of cortical areas

The remarkable development of the cetacean neocortex results in a complex pattern of gyrification. Although the gyral pattern of the cetacean neocortex retains general features similar to that of ungulates and carnivores, with a variable series of circular gyri and sulci capping a more or less verticalized (pseudo)sylvian fissure, the macroscopic organization of the gyri differs considerably. The gyral pattern of the cetacean brain is characterized by a prominent and almost vertical sylvian fissure (s; in fact, technically a pseudosylvian fissure) that is surrounded concentrically towards the vertex of the hemisphere by the ectosylvian (es), suprasylvian (ss), lateral (la), and entolateral (en) sulci, respectively (Fig. 1) (Jacobs et al., 1979; Morgane et al., 1982; Hof and Van der Gucht, 2007; Oelschläger and Oelschläger, 2008; Oelschläger et al., 2008). The caudal cortical domain

comprised between the ectosylvian and the suprasylvian sulci, the ectosylvian gyrus, corresponds to the secondary auditory field; almost the entire rostrocaudal extent of the cortex comprised between the suprasylvian and entolateral sulci, the suprasylvian gyrus, forms a belt along the vertex of the hemisphere that correspond to the primary auditory field (Ladygina and Supin, 1970; Sokolov et al., 1972; Popov and Supin, 1976; Ladygina and Supin, 1977; Ladygina et al., 1978; Morgane et al., 1980; Morgane et al., 1986; Popov and Supin, 1986; Morgane et al., 1990; Hof et al., 1992, 1995; Revishchin and Garey, 1996; Fung et al., 2005; Poth et al., 2005; Oelschläger and Oelschläger, 2008) the cortex located between the lateral and the entolateral sulci, at the vertex of the hemisphere, in the lateral gyrus, corresponds to the primary visual field (Sokolov et al., 1972; Ladygina and Supin, 1977; Ladygina et al., 1978; Morgane et al., 1988; Garey et al., 1989; Revishchin, 1989; Glezer and Morgane, 1990; Morgane et al., 1990; Hof et al, 1995; Revishchin and Garey, 1996; Poth et al., 2005). On the rostroventral extent of the cortex originates the cruciate sulcus that extends rostrocaudally delineating the boundaries between the primary motor and primary somatosensory fields (Kesarev and Malofeeva, 1969; Lende and Welker, 1972; Sokolov et al., 1972; Ladygina and Supin, 1977; Glezer, 2002; Poth et al., 2005). The remainder of lateral surface of the hemisphere has been proposed to be occupied by "association cortices" connecting the auditory, somatosensory and motor fields (Oelschläger and Oelschläger, 2008). Maps of the sensory cortical fields in the brain of cetaceans are shown in Figure 2.

Cetacean brain evolution

Modern cetaceans possess the largest brains in absolute size and relative to body size including the largest of vertebrate brain, that of the sperm whale, *Physeter macrocephalus* (Odontoceti, Physeteridae) with an average brain mass between 8,000 and 10,000 g (Jerison, 1973; Marino, 1998; Marino, 2004; Marino, 2008; Oelschläger and Oelschläger, 2008).

If the anatomical and physiological adaptations of cetaceans (reviewed in Reidenberg, 2007) are considered to be the direct consequence to the challenge of an aquatic lifestyle, the increase in brain size and complexity is now widely recognized to be the result of selective pressures acting specifically on social and cognitive capabilities (Herman, 1980; Connor, 2007; Connor et al., 1992; Marino et al., 2004, 2007, 2008). Fossils show evidence that extreme modifications in cranial morphology occurred during cetacean evolution and that the process of telescoping[1] and migration of the narial apertures on the dorsal apex of the skull (Klima, 1999) lead to the modern cetacean skull anatomy. As such, the morphology of the cetacean brain reflects these anatomical changes in cranial morphology with structural modifications such as foreshortening along the beak-fluke axis and lateral widening (Marino, 2008).

The brain does not fossilize and it is only the study of skull endocasts[2] at different time points during evolution that provides an informative, albeit not optimal, rendering of the structural changes in external morphology and size that the cetacean brain underwent during evolution. The use of modern techniques, such as computed tomography (CT), on cetacean natural endocasts (Marino et al., 2003c) provided evidence for two major events of brain size increase during cetacean evolution: the first occurred when the odontocetes diverged from the primitive Archeoceti, and the second occurred much later in evolution at the origin of Delphinoidea, about 15 million years ago (Marino et al., 2004). The increase in brain size was accompanied by an increase in

[1] Process by which there is an elongation of the rostral elements of the skull and a rostrodorsal movements of the caudal elements (Miller, 1923).

[2] 3D model representation of the space within a cavity, like the skull.

Encephalization Quotient (EQ)[3] that led to EQ values for many modern odontocete species comparable to those of non-human primates and in some species to values that are second only to humans (Marino, 1998; Marino, 2004). However, the expansion of the brain, and particularly the expansion of the neocortex, followed in cetaceans extremely different pathways than other large-brained mammals leading to major differences at several levels of brain organization, particularly at the neocortical level, between modern cetaceans and terrestrial mammals.

Cetacean cognition

Recent studies provide an overwhelming evidence for high cognitive abilities in cetaceans. The capacity of mirror self-recognition, first observed in humans and great apes but not in other primates (Gallup, 1970, 1977; Gallup et al., 1971; Gallup et al., 1980; Suarez and Gallup, 1981; Calhoun and Thompson, 1988; Kitchen et al., 1996; Povinelli et al., 1997; Posada and Colell, 2007) and thought to be a unique ability of these species, is now widely documented in several cetaceans such as the bottlenose dolphin (*Tursiops truncatus*), the killer whale (*Orcinus orca*) and the false killer whale (*Pseudorca crassidens*) (Delfour and Marten, 2001; Reiss and Marino, 2001) as well as in the Asian elephant (*Elephas maximus*) (Plotnik et al, 2006). Mirror self-recognition is considered an indication of self-awareness and has been related to empathy and "theory of mind" in humans and great apes (Gallup, 1982, 1985; Lewis et al, 1989; Povinelli et al., 1990; Povinelli and De Blois, 1992). Although the firm demonstration of "theory of mind" in species other than humans is far from being established, both dolphins and elephants are known to show behaviors consistent with empathy (Connor and Norris, 1982; Balfour and Balfour, 1997; Poole and Moss, 2008). Dolphins are known to have the ability to imitate sounds and behaviors (Tayler and Saayman, 1973; Richards et al., 1984; Reiss and McCowan, 1993; Hooper et al., 2006), to understand artificial language as sequences of gestural and acoustic codes, demonstrate cross-modal discriminatory abilities and understanding of syntactic features in controlled environment (Herman et al., 1984; Herman et al., 1993; Pack and Herman, 1995; Harley et al., 1996; Herman et al., 1998; Pack et al., 2002) as well as understanding of pointing gestures (Herman et al., 1999; Tschudin, 2001; Pack and Herman, 2007). Dolphins are reported to use uncertainty (Smith et al., 1995) and to display a strong short-term auditory, visual, and spatial memory, as well as long-term memory involving the structure of relationships between individuals in a specific group (Herman, 1975; Thompson and Herman, 1977; Richards et al., 1984; Reiss and McCowan, 1993; Connor, 2007).

A large body of evidence points to the formation, in the wild, of complex social structures with relationships among individuals comparable to that of chimpanzees (Connor and Smolker, 1985; Lusseau, 2007), and long lasting complex bonds and coalitions with a structural arrangements in groups such as the "fission-fusion societies"[4] (Connor, 1992; Connor et al., 2000; Lusseau and Newman, 2004; Connor, 2007; Lusseau, 2007). There is compelling evidence of extremely complex patterns of communications with repertoires composed of "signature whistles" (Tyack, 1986; Sayigh et al., 1990, 1995; Janik et al., 1994; McCowan and Reiss, 1995; Thomsen et al., 2001, 2002), different "dialects" characterizing the acoustic repertoire of different groups of dolphins (Ding et al., 1995; Deecke et al., 2000; Janik, 2000) as well as vocal learning in the form of learning of species-specific whistles and the use of specific whistles in association to specific social

[3] Measure of observed brain size relative to expected brain size derived from a regression of brain weight on body weight for a given reference group. The equation is as follow: $Em(brain) = 0.12m(body)^{2/3}$ (Jerison, 1973).

[4] Dynamic groups in which the associations among individuals are modified over time. The flexibility and multiple scales of organization of the fission-fusion societies give origins to complex higher-order social structures.

behaviors (Sayigh et al., 1990; McCowan and Reiss, 1995; Sayigh et al., 1995; Connor and Smolker, 1996; McCowan and Reiss, 2001; Rendell and Whitehead, 2001). Cultural transmission and tool use are widely documented (Deecke et al., 2000; Rendell and Whitehead, 2001; Krutzen et al., 2005), and some cetaceans species, such as male humpback whales (*Megaptera novaeangliae*), are known to produce long and structured sequences (the so-called "songs") that are characterized by a broad repertoire of variability overtime within a group of whales. Finally, episodes of copying songs elements from other individuals have been reported (Edds-Walton, 1997; Noad et al., 2000; Mercado et al., 2005;) as well as significative differences in themes and phrases of songs generated by geographically isolated populations (Helweg et al., 1998).

Because most of the experimental cognitive tests have been performed in the bottlenose dolphin (*T. truncatus*), for obvious reasons related to the flexibility of this species to adapt to the controlled environment, and evidence of different cognitive abilities related to specific behavioral pattern have been reported in the wild only in few cetacean species, the resulting evidence for complex cognitive abilities cannot be extended to the whole taxon. However, the compelling neuroanatomical characteristics and specializations shared by all the cetacean species analyzed so far (reviewed in Marino et al., 2008) give reason to think that high level cognition is an ability shared by all cetaceans rather than by few species. The large body of behavioral evidence for high cognitive abilities in cetaceans (reviewed in Simmonds, 2006; Marino et al., 2007; Marino et al., 2008), and primates, despite their extremely divergent evolutionary histories, is the evidence that advanced cognitive processes evolved in distantly related species may be considered the product of a process of convergent evolution. Cetaceans and primates are the evidence that evolution can shape different cortical organizations in distantly related species to lead to similar functional outcomes. The intriguing question that remains to be answered is how extreme differences in cortical and wiring organization that evolved under similar selective pressure, translate into comparable level of cognitive capacities.

The cortical regions of interest

General notes

This work focuses on the anterior cingulate cortex (ACC), the anterior insular cortex (AI), and the frontopolar cortex (FPC) of the cetacean brain. Given that most of the cetacean species are endangered, invasive studies are difficult if not impossible to perform. Direct experimental evidence of cortical connectivity with subcortical structures and other cortical regions is lacking, and thus, the functional significance of the cetacean brain structure can be elucidated only through the comparison with other mammals. The evidence from studies in humans, and laboratory animals including non-human primates, shows a general pattern of connectivity and contribution of these three cortical regions to behavior that can be considered general for all mammals, including cetaceans. In primates, the anterior cingulate, anterior insular, and orbitofrontal/prefrontal cortices are part of a large network of rostral structures involved in the regulation and initiation of context-dependent behaviors, that includes also the amygdala, the septum, the ventral striatum including the nucleus accumbens, and several brainstem nuclei such as the periaqueductal grey (reviewed in Devinsky et al., 1995), and that is considered to be functionally independent from the more caudally located hippocampus. The study of ACC, AI, and FPC in cetaceans is particularly intriguing given the presence in these cortical regions, similarly to what observed in humans and great apes, of a unique neuronal specialization the Von Economo neurons (see Chapter 4). Below I will introduce the three regions of interest, considering the ACC as a medial component of the PFC and, as a consequence, I will present it jointly with the PFC, while a separate paragraph will be dedicated to the AI.

The prefrontal cortex (PFC)

Structurally, the primate PFC is an architectonically heterogeneous region including dorsal, ventral, lateral, and medial (i.e., "limbic", the ACC) sectors that encompass several distinct areas (Papez, 1937; Broca, 1878; Reep, 1984; Barbas and Pandya, 1989; Weinberger, 1993; Rajkowska and Goldman-Rakic, 1995; and reviewed in Barbas, 2000; Dombrowski et al., 2001; Öngür et al., 2003). It is important to stress here that the portion of the cingulate cortex that, in primates, is considered part of the PFC is limited to its anterior extent, and specifically areas 32, 24, and 25, also known as the cingulate "executive region".

Prefrontal regions have different roles in cognitive, mnesic, and emotional processes that are underlyined by their specific pattern of connections. However, the scope of this introduction is to give an overview of the PFC as a whole and, for this reason, I will illustrate a generic pattern of connectivity that can be considered comprehensive of all the prefrontal cortical domains, unless otherwise specified.

The PFC as a whole (dorsal, ventral, lateral, and medial sectors) is interconnected with a large number of thalamic nuclei, and in particular to the mediodorsal nucleus (MD) (Vogt et al., 1979; Goldman-Rakic and Porrino, 1985; Preuss and Goldman-Rakic, 1987; Vogt and Pandya, 1987; Barbas et al., 1991; Vogt et al., 1992; Xiao and Barbas, 2002a, 2002b; Xiao et al., 2009). Connections are established with the amygdala (Aggleton et al., 1980; Porrino et al., 1981; Amaral and Price, 1984; Vogt and Pandya, 1987; Barbas and De Olmos,1990; Carmichael and Price, 1995; Ghashghaei et al., 2007; Morecraft et al., 2007; Beckmann et al., 2009), the hypothalamus (Öngür et al,, 1998a, 1998b; PriceRempel-Clower and Barbas, 1998; Freedman et al., 2000; Beckmann et al., 2009), basal ganglia (Johnson et al., 1968; Alexander et al., 1986; Graybiel et al.,1994; Joel and Weiner, 1994; Kunishio and Haber, 1994; Haber et al, 1995; Parvizi et al., 2006; Beckmann et al., 2009), claustrum (Pearson et al., 1982), periaqueductal grey (Müller-Preuss and Jürgens, 1976) and autonomic brainstem nuclei (Terreberry and Neafsey, 1983; Willett et al., 1986).

Additional connections are established with sensory and limbic cortices (Pandya and Kuypers, 1969; Künzle, 1978; Cavada and Goldman-Rakic, 1989: Barbas, 1988,1995; Barbas and Mesulam, 1981; Pandya and Van Hoesen, 1981; Mufson and Mesulam, 1982; Barbas and Pandya, 1987; Selemon and Goldman-Rakic, 1988; Carmichael and Price, 1995a,b; Barbas et al., 1999; Arikuni et al., 1988), with motor, parahippocampal and superior temporal cortices as well as the hippocampal formation (Rosene and Van Hoesen, 1977; Vogt et al., 1979; Baleydier and Mauguière, 1980; Muller-Preuss et al., 1980; Pandya et al., 1981; Jürgens, 1983; Barbas and Pandya, 1987; Vogt and Pandya, 1987a, 1987b; Musil and Olson, 1988; Barbas and Pandya, 1989; Vogt, 1992; Bates and Goldman-Rakic, 1993; Morecraft and Van Hoesen, 1993; Lu et al.,1994; Barbas and Blatt, 1995; Carmichael and Price, 1995; Carmichael and Price, 1996; Barbas et al., 1999; Cavada et al., 2000; Hatanaka et al., 2003; Luppino et al., 2003; Wang et al., 2001, 2004; Takada et al., 2004; Beckmann et al., 2009). Because the ACC itself represents one of the three regions of interest studied in the present thesis, here I will give some more specific details on its structure, pattern of connectivity and function.

From a cytoarchitectural point of view, the cingulate cortex is an extremely heterogeneous region (Vogt et al., 1995; Vogt et al., 2001; 2003). Although classically the cingulate cortex was considered to have a unitary function, evidence from lesions, electrical stimulation, imaging, and neuropathological studies in humans and experimental animals show that the cingulate cortex is characterized by a major structural and functional dichotomy with an anterior division, the "executive region", playing a role in emotions and motor functions, and a posterior division, the "evaluative region" mostly involved in visuospatial cognition and memory (Baleydier and Mauguière, 1980; Vogt et al., 1992b; Bush et al., 1998; Whalen et al., 1998). The anterior executive region of the ACC can be further divided on the basis of its cytoarchitecture, contribution to behavior, and connectivity, into two functional subdivisions: a rostroventral "affective" component, involved in affect, visceromotor, and vocalization control, including areas

25, rostral 24a-c, 32, and 33, and a caudodorsal "cognitive" component, involved in response selection, skeletomotor control, and nociception, including caudal areas 24´, 32´, and 33 (Corbetta et al., 1991; Vogt et al., 1992b; Vogt et al., 1995; Devinsky et al., 1995). Particularly, the "affect" division of the ACC (area 25 specifically) projects to the brainstem nuclei that regulates autonomic activity such as the nucleus of the solitary tract and the motor nucleus of the vagus, has projections to the periaqueductal grey and a substantial set of reciprocal connections with the amygdala (Vogt et al., 1979), whereas the "cognitive" division projects to the spinal cord, primary and supplementary motor cortices (Biber et al., 1978; Morecraft and Van Hoesen, 1992).

The PFC as a whole has been implicated in a variety of executive functions that include the ability of discriminating between conflicting thoughts, the planning of goal-directed behavior, reward and punishment expectation based on actions, the "social" control of actions, and working memory (Funahashi et al., 1989,1993; Fuster, 1993; D'esposito, 1995; Goldman-Rakic, 1995; Price et al., 1996; Miller, 1999; Barbas, 2000; Leung et al., 2005). The particular contribution of the ACC is considered responsible for somatic and autonomic responses such as vocalization, cardiovascular modulation, inhibition of somatic movements, pain and emotion, cognition, and social behaviors such as aggressiveness, mating behavior, mother-infant interaction, fear, and intraspecific interactions (Devinsky et al., 1995; Bush et al., 2000; Vogt, 2005; Medalla and Barbas, 2009).

From a pathological point of view, the PFC is implicated in several illnesses. Particularly, anatomical alterations and dysfunctions of the PFC are linked to autism, attention-deficit/hyperactivity disorder, and post-traumatic stress disorder (Bush et al., 1999; Shin et al., 2001; Seidman et al., 2006). Finally, quantitative neuronal or glial alterations, as well as morphological neuronal changes and disruption of specific networks in prefrontal regions are linked to diseases such as schizophrenia, Alzheimer's disease, and frontotemporal dementia (Hof et al., 2002; Bussière et al., 2003a,b; Seeley, 2008; Seeley et al., 2008, 2009).

In cetaceans, the frontopolar cortex is a very expanded, heterogeneous and complex cortical region, very well differentiated from the adjacent cortical fields (Hof et al., 2005; Hof and Van der Gucht, 2007). Although direct evidence of the homology of this cortical region to any specific region of the primate frontal cortex is lacking, there is a likely homology between the cetacean frontopolar cortex and the dorsolateral PFC of primates (see Chapter 5 for a detailed discussion).

The anterior insular (AI) and frontoinsular (FI) cortices

The insula is another major component of the "great limbic lobe" of Broca (Broca, 1878). It lies in the depth of the sylvian fissure under the frontal and parietal opercula, and consists of a highly heterogeneous region in cytoarchitecture and connectivity patterns. Structurally, in primates, the insular cortex is divided into three major sectors: an agranular anterior sector, a dysgranular middle sector, and a granular posterior sector (Mesulam and Mufson, 1982a). Moreover in human, an additional field is constituted by the more rostral part of the insular cortex that lies in front of the anterior insula (AI) at the junctional limit with the posterior part of the orbitofrontal cortex, the so-called frontoinsular cortex (FI; von Economo and Koskinas, 1925). Given their relevant functions for the goals of the present thesis, emphasis will be placed here to AI and FI.

With respect to their connectivity, AI and FI are interconnected with the ACC, frontal, parietal, and temporal lobes, and the enthorinal cortex (Pandya, 1981; Mesulam and Mufson, 1982b; Mufson, 1982; Augustine, 1996), and have extensive reciprocal connections with the amygdala (Aggleton, 1980; Mufson et al., 1981; Mufson, 1982; Mesulam and Mufson, 1982b). Given that FI is absent in macaque monkeys, studies on the connectivity of the FI are lacking. However, its activation in imaging studies (reviewed in Craig, 2009) suggests connections with brainstem nuclei that regulate autonomic activity.

From a functional point of view, classical and recent studies in humans and laboratory animals show evidence for a role of the AI in a large variety of viscerosensory, visceromotor, and interoceptive functions, as well as language and music processing (Showers and Lauer, 1961;

Augustine, 1996; Platel et al., 1997; Craig, 2002; Bamiou et al., 2003; Stephan et al., 2003; Crichley et al., 2004; Shelley, 2004; Critchley, 2005; Mutschler et al., 2007, 2009). Recent evidence suggest that the AI is involved in bodily self-awareness functions such as self-recognition (Craig, 2003; Karnath et al., 2005; Devue et al., 2007), sense of homeostasis, and emotional awareness (Seeley, 2007; Craig, 2009).

A recent imaging study, through the identification of two systems of resting state connectivity that include the AI and ACC, confirmed the involvement of these two cortical regions in the integration of interoceptive information with emotions and in the environmental monitoring, response selection and skeletomotor body orientation (Taylor, 2009).

The cortical regions of interest in the cetacean brain

Maps of the sampled regions displaying the limits of the ROIs in an odontocete (*T. truncatus*) and a mysticete (*M. novaeangliae*) are shown in Figure 3. Boundaries were based on comprehensive descriptions of the anatomy of the bottlenose dolphin brain by (Jacobs et al., 1971; Jacobs et al., 1979; Morgane et al., 1980, 1982; Jacobs et al., 1984; Manger et al., 1998; Hof et al., 2005) for the odontocetes and on the description of the structure of the cerebral cortex of the humpback whale brain by Hof and Van der Gucht (2007). Briefly, the cingulate cortex was identified as the cortical domain located ventrally to the splenial fissure on the midline of the hemisphere. Anterior and posterior cingulate cortices were identified on the basis of their cytoarchitecture as described in Morgane et al. (1982) and Hof and Van der Gucht (2007). The insular cortex was identified as the cortex distributed on the medial wall of the pocket formed by the sylvian fissure and the distinction between anterior and posterior insular cortices was based on cytoarchitectural criteria of (Jacobs et al., 1984; Hof and Van der Gucht, 2007). The FI was defined as the cortical domain that forms an extension from the anterior part of the insular cortex and merges with the posterior aspect of the FPC (Hof and Van der Gucht, 2007). The frontopolar cortex was identified as the cortical domain that comprehends the polar gyri at the tip of the "frontal" lobe and ventrally the cortex that merges with the FI (Hof and Van der Gucht, 2007).

Goals of the present thesis

The general goal of the present thesis is to contribute to the understanding of the cetacean cortical organization through the study of the three cortical regions ACC, AI, and FPC, in an extensive group of cetacean species using different approaches.

The specific objectives of **Chapter 2** are:

- Examine the cytoarchitecture of ACC, AI and FPC on Nissl-stained sections and define structural differences among ceteacean species.
- Define the distribution of calretinin (CR)-immunoreactive neurons in the ACC, AI, and FPC in cetaceans and compare it with select species of terrestrial and semi-aquatic mammals.

The specific objectives of **Chapter 3** are:

- Define the glia/neuron index (GNI) in the ACC and primary somatosensory (S1) cortices of a series of cetacean species.
- Use a series of selected terrestrial and semi-aquatic mammals with a large variation in brain size to determine whether there is a relationship, and of what kind, between brain size and GNI among mammals.
- Use such a relationship to determine whether the values of GNI, obtained in the present study for cetaceans, match the expected values based on their brain size.

The specific objectives of **Chapter 4** are:

- Investigate the occurrence of Von Economo neurons (VENs) in the ACC, AI, and FPC of representative species of cetaceans.
- Define the pattern of distribution of VENs among the species that possess them.
- Define the total number of VENs in ACC, AI, and FPC in these species.
- Measure the somatic volume of VENs and compare it to the somatic volume of large pyramidal cells of layer V and fusiform cells of layer VI.
- Investigate the presence of VENs in few species of large-brained terrestrial mammals.

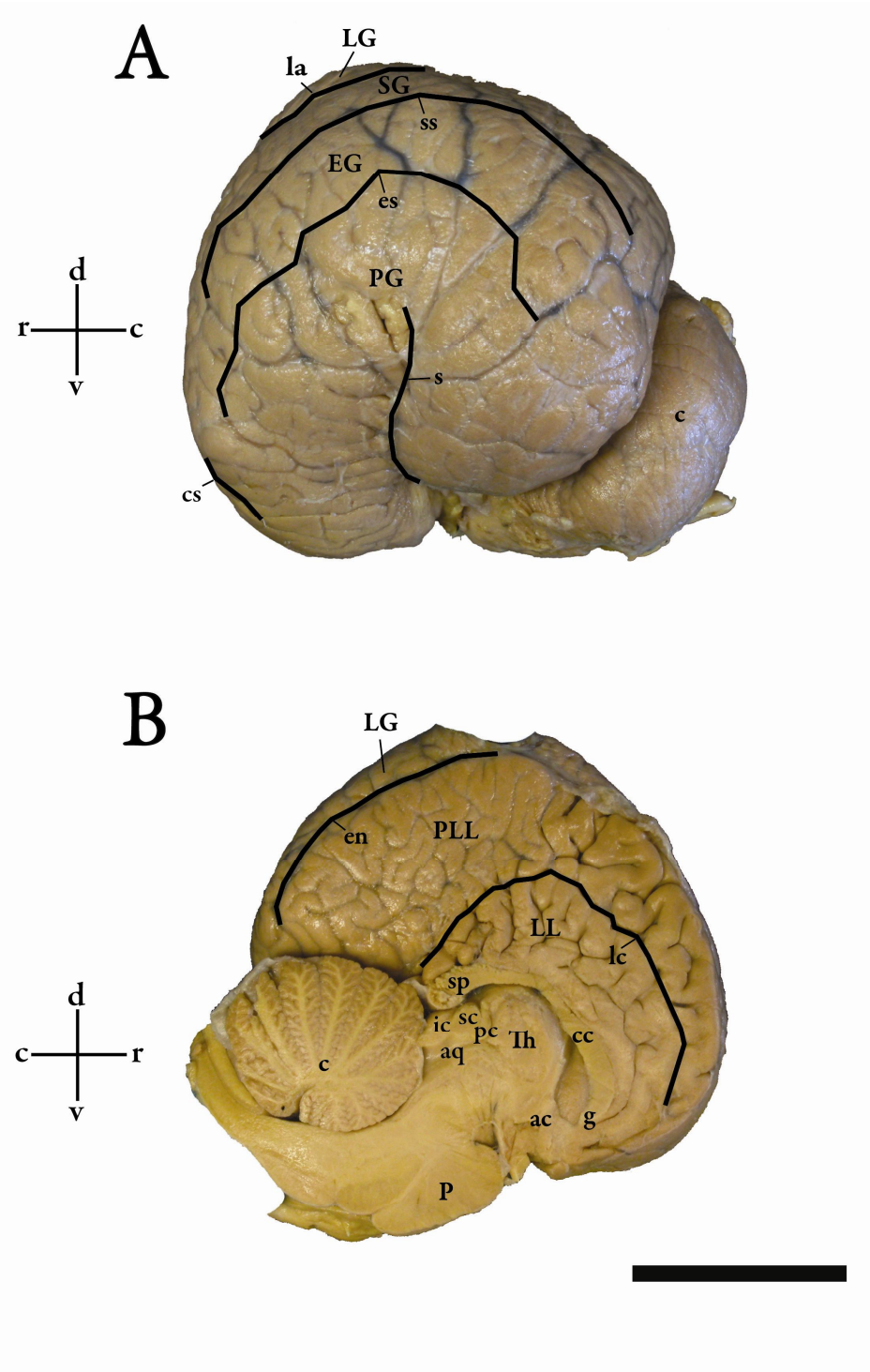

Figure 1. Lateral (A) and mediosagittal (B) aspects of the brain of the striped dolphin (*Stenella coeruleoalba*). ac, anterior commisure; aq, aqueduct; Cb, cerebellum; cc, corpus callosum; cs, central sulcus; EG, ectosylvian gyrus; en, entolateral sulcus; es, ectosylvian sulcus; g, genu of the corpus callosum; IC, inferior colliculus; la, lateral sulcus; lc, limbic cleft; LG, lateral gyrus; LL, limbic lobe; P, pons; pc, posterior commisure;PG, perisylvian gyrus; PLL, paralimbic lobe; s, sylvian sulcus; SC, superior colliculus; SG, suprasylvian gyrus; sp, splenium; ss, suprasylvian sulcus; Th, thalamus. Scale bar = 4 cm.

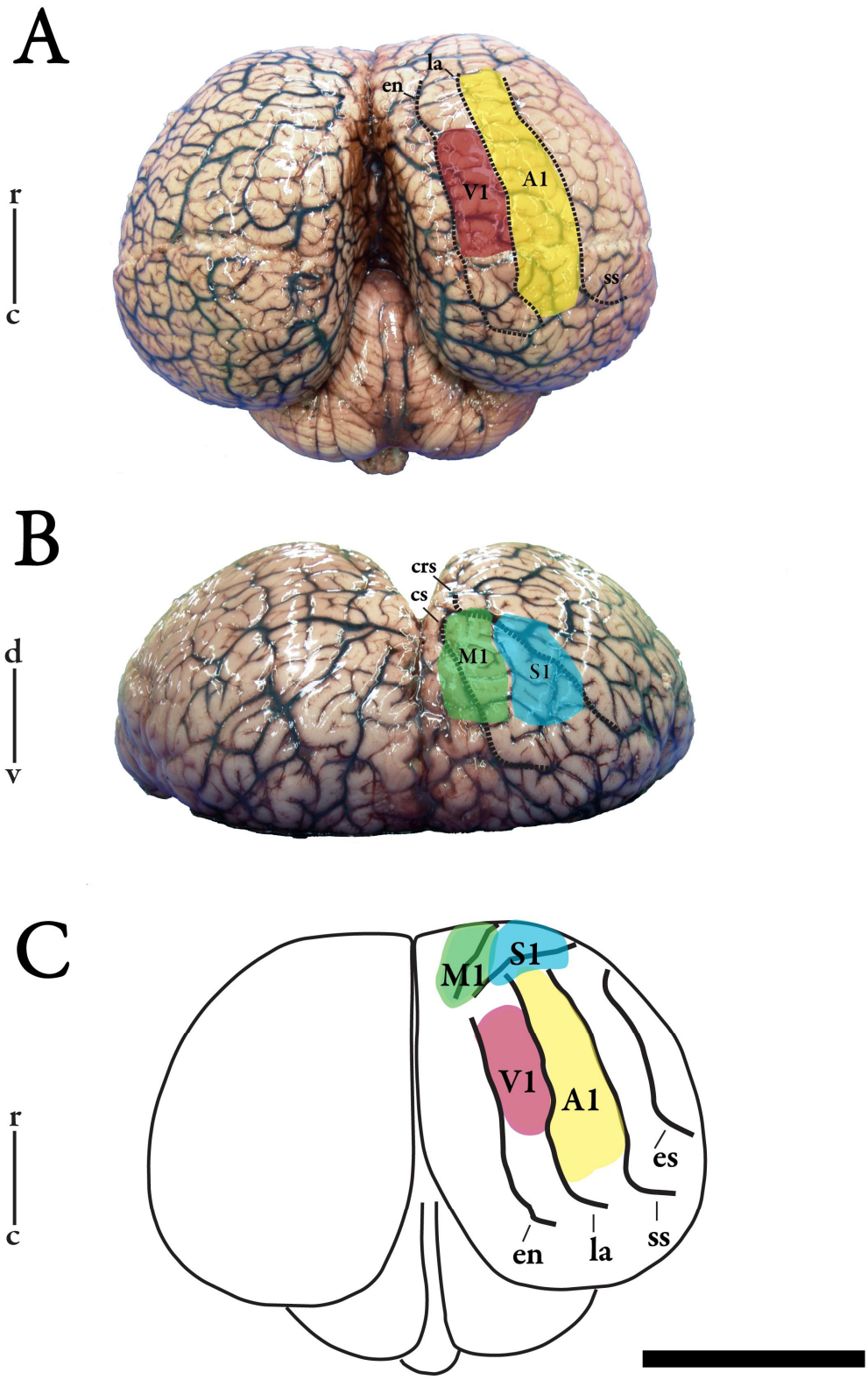

Figure 2. Dorsal (A) and rostral (B) aspects, and dorsal schematic (C) of the brain of the bottlenose dolphin (*Tursiops truncatus*) showing the localization of primary cortical areas. A1, primary auditory cortex; cs, cruciate sulcus; crs, coronary sulcus; en, entolateral sulcus; la, lateral sulcus; M1, primary motor cortex; S1, primary somatosensory cortex;V1, primary visual cortex. Scale bar = 5 cm.

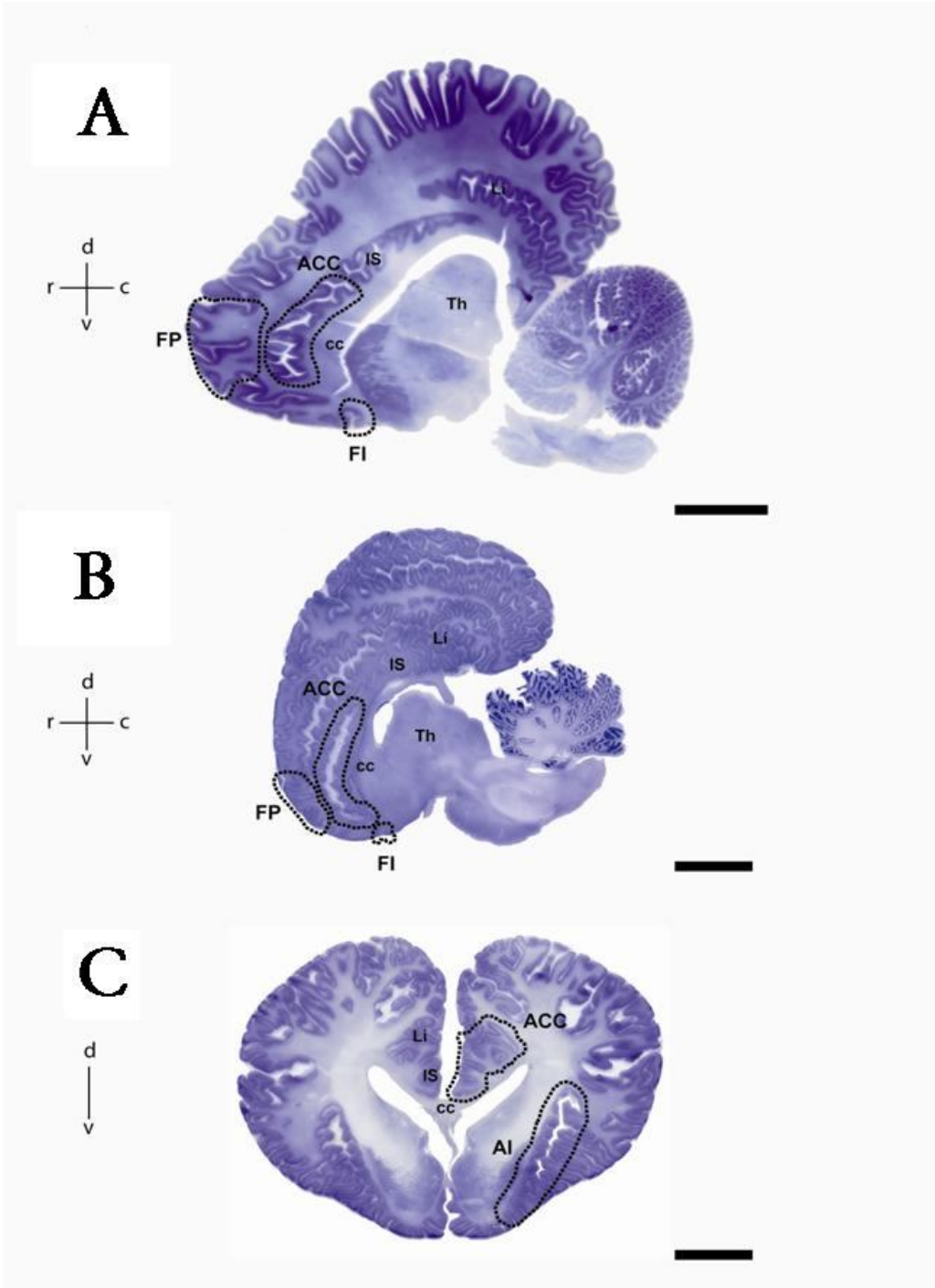

Figure 3. Nissl-stained parasagittal (A, B) and coronal (C) sections of the brain of the right hemisphere of a mysticete, the humpback whale (*Megaptera novaeangliae*) (A) and of an odontocetes, the bottlenose dolphin (*T. truncatus*) (B, C), showing the cortical regions of interest: anterior cingulate cortex (ACC), frontoinsular cortex (FI), anterior insular cortex (AI) and frontopolar cortex (FPC). The location of the regions of interest in the brain of the humpback whale and of the bottlenose dolphin are shown as representative of the mysticete and odontocete brains, respectively, as they occur within the same landmarks in either suborder. cc, corpus callosum; is, intercalate sulcus; li, limbic fissure; Th, thalamus. Scale bar = 2.5 cm.

Chapter 2

Cytoarchitecture and chemoarchitecture of the prefrontal and insular cortex in cetaceans

Introduction

The structure and organization of the cerebral cortex can be studied using different approaches. Most of the cytoarchitectural studies are carried out with the classical approach of the Nissl stain that provides information on the organization and layering patterns of the cortical plate and on the basic morphology of the neurons. However, populations of neurons with comparable morphology can be characterized by their potentially variable neurochemical profile, and as such, by different functions. It is important, thus, to combine morphological and molecular studies to obtain a more precise overview of the structure of the cortex in a given species. Several neurochemical markers have been used to identify the molecular organization of the cortex in a wide range of species and among the most used are the calcium-binding proteins (CaBPs) parvalbumin (PV), calbindin (CB), and calretinin (CR) (Hof et al., 1999, 2000). CaBPs are a large group of proteins with a high affinity for calcium ions (Ca^{2+}) that are located in the cytosol and participate in a wide range of calcium-dependent functions in a variety of tissues. Particularly, PV, CB, and CR are the most abundant in the CNS and belong to the EF-hand family, that are characterized by a consensus sequence that folds into two α-helices ("E" and "F") joined by a Ca^{2+} -binding loop, the so-called "helix-loop-helix" motif (Kretsinger and Nockolds, 1973; Persechini et al., 1989; Lewit-Bentley and Réty, 2000). PV, CB, and CR are classified as "buffer" proteins as they regulate the intracellular free calcium concentration (and thus the amplitude of calcium signals) by binding Ca^{2+} ions (Dalgarno et al., 1984).

Among these three CaBPs, PV and CB are expressed in the CNS as well as in other non-neural tissues such as the intestine, while CR is expressed selectively in the nervous system (Rogers, 1992) and is quantitatively more abundant than CB or PV. Given the features of the non-overlapping distribution patterns of these three calcium-binding proteins, PV, CB, and CR have been shown to be powerful neuronal markers to identify taxon-specific traits in comparative studies (Glezer et al., 1993, 1998; Hof et al., 1999; Hof and Sherwood, 2005).

Our knowledge of the pattern of distribution of CaBPs in the mammalian CNS and their colocalization with specific neurotransmitters is based on studies in laboratory animals and humans. These studies show that immunoreactivity to these three types of CaBPs is observed in distinct and non-overlapping subpopulations of mostly non-pyramidal cells (Hendry et al., 1989; van Brederode et al., 1990; Hendry and Jones, 1991; Andressen et al., 1993; Kubota et al., 1994; Condé et al., 1994; DeFelipe, 1997; Gonchar and Burkhalter, 1997) and is colocalized with the major inhibitory neurotransmitter, γ-aminobutyric acid (GABA) (Hendry and Jones, 1991; Rogers, 1992; reviewed in DeFelipe, 1997 and Hof et al., 1999), The CaBPs-immunoreactive neurons are thus inhibitory interneurons (reviewed in Gilbert, 1983; Conti et al., 1987; DeFelipe, 1993; Markram et al., 2004).

Studies in the rat, macaque monkey, and human show that PV-immunoreactive neurons are mainly chandelier and basket cells and are found in layers II to V (Hof and Nimchinsky,1992; Condé et al.,1994; Nimchinsky et al.,1997); CB-immunoreactive neurons are double-bouquet cells located mainly in layers II and III (DeFelipe et al.,1989) and CR-immunoreactive cells are bipolar and bitufted and are located throughout the cortical mantle but with a higher density in layers II and III. Moreover, CB- and CR-immunoreactive Cajal-Retzius cells have been described in layer I

(for a detailed review see Hof et al., 1999). Atypical CB-immunoreactive pyramidal and large fusiform cells in layers III and V as well as CB-containing fibers in layers III and V, CR-immunoreactive atypical large non-pyramidal neurons with an oblique orientation of the cell body and dendrites in deep layer I and layer VI were also observed in the primary auditory (A1) and visual (V1) cortex (Hof et al., 1999). Moreover, the cetacean A1 and V1 were reported by Glezer and colleagues (Glezer et al., 1993, 1998) to contain a higher concentration of CB- than PV-immunoreactive neurons

Of all the CaBPs, CR is the most interesting in the context of the present thesis given its specificity for the CNS and the high concentration of CR-immunoreactive neurons in comparison to the other CaBPs in the cetacean neocortex. Moreover, there is a lack of information on the distribution and morphology of CR-immunoreactive cells in the ACC, AI, and FPC in cetaceans in comparison to the data available for CB and PV.

The cetacean neocortex is characterized, in contrast to that of primates, by the presence of only five cortical layers: a very thick layer I that is far more cellular than in most terrestrial species; a densely packed layer II displaying cellular clustering in many cortical regions, particularly in the insula (Manger et al., 1998; Hof and Van der Gucht, 2007) and containing isolated, very large, inverted-pyramid-like neurons; a wide pyramidal layer III; a relatively thin pyramidal layer V containing large pyramidal cells usually distributed in small clusters, and a plesiomorphic layer VI (Morgane et al., 1988; Glezer and Morgane, 1990; Hof and Sherwood, 2005; Hof and Van der Gucht, 2007). This cortical lamination pattern with the lack of an internal granular layer IV may reflect a particular cortical wiring organization in cetaceans (Hof and Van der Gucht, 2007). Only few descriptions of the laminar and cytoarchitectonic organization of the cetacean cortex are available and they are mostly based on the structure of primary sensory areas in a small number of species, such as the bottlenose dolphin, *T. truncatus*, Risso's dolphin, *G. griseus*, and striped dolphin, *S. coeruleoalba* (Jacobs et al., 1971, 1979, 1984; Morgane et al., 1982, 1988; Hof et al., 2005; Furutani, 2008), and on a recent study that provides a detailed description of the organization of the cerebral cortex of the humpback whale, *M. novaeangliae* (Hof and Van der Gucht, 2007) . Although the latter study includes a detailed description of the cytoarchitecture of the regions of interest in the present thesis, namely ACC, AI and FPC, studies of the cytoarchitecture of these regions of interests in odontocetes species are sparse and mainly based on the brain of the bottlenose dolphin (Jacobs et al., 1984; Manger et al., 1998; Hof et al., 2005).

While several reports of the pattern of distribution of CR-immunoreactive neurons in the neocortex of laboratory animals and humans are available (Van Brederode et al., 1990; Hendry and Jones, 1991; Jacobowitz and Winsky, 1991; Baimbridge et al., 1992; Hof and Nimchinsky, 1992; Martinez-Guijarro and Freund, 1992; Résibois and Rogers, 1992; Rogers, 1992; Andressen et al., 1993; Glezer et al., 1993; Condé et al., 1994; Vogt Weisenhorn et al.,1994; Belichenko et al.,1995; Hof et al., 1995, 1996a, 1996b; Verney and Derer, 1995; Berger and Alvarez, 1996; DeFelipe, 1997; Nimchinsky et al., 1997; Glezer et al., 1998) while reports on the distribution of CaBPs in the cortex of cetaceans are sparse (Glezer et al., 1993, 1998; Hof et al.,1999, 2000) and mostly emphasizing on the visual and auditory cortices.

Only few comparative studies addressed the chemoarchitecture of the cetacean neocortex, based on the distribution of CB, CR, and PV, in the primary sensory areas of some odontocetes such as *T. truncatus*, the dwarf sperm whale (*Kogia simus*), the long-finned pilot whale (*Globicephala melas*), and the beluga (*Delphinapterus leucas*). The distribution of CB-, PV-, and CR-immunoreactive neurons in the primary visual (V1) and primary auditory (A1) cortices of the bottlenose dolphin (*T. truncatus*), dwarf sperm whale (*K. simus*), and beluga whale (*D. leucas*) (Glezer et al., 1992, 1993,1998; Hof et al., 1999). These studies provide evidence of the 96.8% of colocalization of CaBPs and GABA in the cetacean visual cortex (Glezer et al., 1993) and of a pattern of distribution of PV, CB, and CR that is very different from what observed in rodents and

primates but comparable to insectivorous bats and hedgehogs and artiodactyls (even-toed ungulates) (Glezer et al., 1993,1998; Hof et al., 1999), which is consistent with the recent inclusion of cetaceans and artiodactyls in a larger taxonomic level, Cetartiodactyla. In the case of cetaceans, areas V1 and A1 are characterized by the presence of CB-immunoreactive bipolar/bitufted neurons in layers I-II and III-V with a higher density in the latter layers; CR-immunoreactive bipolar, bitufted and multipolar neurons with a vertical orientation along the radial cortical axis and dendrites spreading to the whole thickness of the cortex are observed in deep layer I and layer II, and only sparse cells in layer III; finally, a paucity of PV-immunoreactive stellate neurons mainly located, when present, in deep layers III-V and rare sparse cells in other layers have been reported (Glezer et al., 1993,1998; Hof et al., 1999).

However, studies of the cytoarchitecture of ACC, AI, and FPC in the odontocetes and in more than one species of mysticetes are lacking. Particularly, there is no previous knowledge of the distribution of the calcium-binding proteins in the ACC, FI, and FPC in both odontocetes and mysticetes. In the present study of the cetacean neocortical structure, I investigated the cytoarchitecture, based on Nissl-stained sections, and the chemoarchitecture, based on the distribution of CR-immunoreactive neurons in the prefrontal and insular cortices of select species of cetaceans representative of the main families of Odontoceti and Mysticeti.

Materials and methods

Specimens and histological preparation

Eleven cetacean brains, including nine odontocetes, namely the bottlenose dolphin, *Tursiops truncatus* (Delphinidae); Risso's dolphin, *Grampus griseus* (Delphinidae) harbor porpoise, *Phocoena phocoena* (Delphinidae); killer whale, *Orcinus orca* (Delphinidae); beluga whale (Monodontidae), dwarf sperm whale, *Kogia simus* (Kogiidae); sperm whale, *Physeter macrocephalus* (Physeteridae), Amazon river dolphin, *Inia geoffrensis* (Iniidae), and two mysticetes including the minke whale, *Balaenoptera acutorostrata* (Balaenopteridae) and the humpback whale, *Megaptera novaeangliae* (Balaenopteridae) were used in the present study. The Florida manatee (*Trichechus manatus latirostris*, Sirenia, Trichechidae), African elephant (*Loxodonta africana*, Proboscidea, Elephantidae), pigmy hippopotamus (*Hexaprotodon liberiensis*, Artiodactyla, Hippopotamidae), Atlantic walrus (*Odobenus rosmarus rosmarus*, Carnivora, Odobenidae), and the black rhinoceros (*Diceros bicornis*, Perissodactyla, Rhinocerotidae) were investigated for comparative purposes. All brains were obtained from strandings, marinelands and zoos where the animal died of natural causes and the brain was available for prompt fixation in 4% paraformaldehyde. However, some of these specimens were part of collections and were collected several decades ago and stored in fixative since, which influenced the quality of the immunostaining. Blocks from the regions of interest were sampled from each brain using the landmarks reported in Chapter 1, cryoprotected in graded sucrose solutions from 10 to 30% in phosphate buffer saline (PBS), frozen in dry ice, and cut into 80 µm-thick sections on a sliding microtome (Leica Biosystems, Nussloch, Germany). Every 10^{th}, 20^{th}, or 50^{th} section were mounted on glass slides, stained with a solution of 0.2% cresyl violet, and coverslipped for examination. The Nissl staining protocol here used is adapted to the conditions of the postfixed tissue, has been used for all the staining events reported in the present thesis and is reported in Table 2.

Immunohistochemistry

Free-floating sections from the previously cut blocks were first treated in a solution of 0.3% hydrogen peroxide in methanol to eliminate endogenous peroxidase activity, rinsed and treated for antigen retrieval in a solution of citrate buffer pH 8.0-9.0 in a 95°C water bath for 10 minutes. After cooling at room temperature the blocking step was performed in a solution of 5% normal goat serum in PBS-B. After washes the sections were incubated in a solution of the primary

monoclonal mouse anti-CR antibody (Swant, Bellinzona, Switzerland; dilution, 1:3,000; Schwaller et al.,1993) diluted in PBS-B containing 0.3% Triton-X-100. The sections were incubated overnight at room temperature on a rotating shaker. Following the overnight incubation in the primary antibody, the sections were washed and incubated in a solution of the secondary polyclonal goat anti-mouse biotinylated antibody (Dako, Glostrup, Denmark; dilution, 1:200) for 45 minutes. After washes the sections were processed with the avidin-biotin peroxidase method using the Vectastain ABC kit (Vector Laboratories, Burlingame, CA) and the 3,3'-diaminobenzidine (DAB) peroxidase kit (Vector Laboratories,) was used as a chromogen to visualize the product of the reaction. The immunoreactivity was intensified using nickel. All the washes were made in a solution of 0.3% Triton-X-100 in PBS-B. Negative controls were run omitting the primary antibody and positive controls were constituted by whole brain slices of perfused wild type mice.

Results

Cytoarchitecture

In all of the cetacean species investigated, the ACC, AI, and FPC revealed a five-layer structure owing to the absence of an internal granular layer (layer IV). Thus, the general organization of these cortical areas is, according to previous descriptions of sensory areas of the cetacean cortex, characterized by a thick layer I, a narrow and densely packed layer II, a wide layer III, a layer V containing large pyramidal neurons and, in some regions,Von Economo neurons in most of the species (see Chapter 4 for details), and a polymorphic layer VI. The most striking differences among the species investigated were the size and density of neurons between large and smaller species, the larger species such as *M. novaeangliae*, *P. macrocephalus*, and *O. orca* having larger neurons in overall lower densities throughout the cortical plate than the smaller species. The organization of the three regions of interest, ACC, AI, and FPC, is discussed across the cetacean species for which the ROIs were available and the cyto- and chemoarchitecture of the same cortical regions in other relevant terrestrial and aquatic mammals is discussed in a comparative perspective.

Anterior cingulate cortex (ACC)

The cytoarchitecture of the ACC was investigated in a group of odontocetes including *T. truncatus*, *G. griseus*, *P. phocoena*, *O. orca*, *D. leucas*, *P. macrocephalus*, and *I. geoffrensis* and in the two mysticetes *B. acutorostrata* and *M. novaeangliae*. In general, the ACC showed a very distinct layering pattern with clear interspecific differences in cytoarchitecture. The three smaller delphinids (*T. truncatus*, *G. griseus*, and *P. phocoena*) showed a comparable and overall higher neuronal density throughout the ACC layers (Fig. 4A-C) than the larger species such as *O. orca*, *P. macrocephalus* and the two mysticetes (Fig. 4D, F). However, a low neuronal density was observed also in *D. leucas* (Fig. 4E) and *I. geoffrensis* (Fig. 4G) and could represent a feature of the monodontids and iniids. Moreover, these two species showed the thinnest cortical plate among all cetaceans and a characteristic pattern of columnarity defined in these two species by the grouping of layer V large pyramidal cells joining the thin layer VI organized in modules (Fig. 4E,G). This modular pattern was more visible in *D. leucas* in which a patchy appearance of the deep cortical layers represents the most prominent organizational feature. In the small delphinids, differences were observed in the laminar thickness and in the distribution of neurons in layer V. Particularly, in *T. truncatus* the large pyramidal neurons of layer V were grouped in small clusters of 10 to 15 neurons that gave a patchy appearance to this layer (Fig. 4A). In *G. griseus*, layer V was thicker and the large pyramidal cells were arranged in thin columns throughout the whole extent of this layer (Fig. 4B). The organization of layer V in *P. phocoena* was more homogeneous with large evenly distributed pyramidal cells (Fig. 4C). A modular distribution of the neurons in

layers V and VI was observed in *O. orca* (Fig. 4D) and *P. macrocephalus* (Fig. 4F) but the greater space between adjacent columns and the low neuronal densities accounted for a less evident pattern. In the two mysticetes, clustering and modules of layer V were observed in both *M. novaeangliae* (Fig. 4I) and *B. acutorostrata* (Fig. 4H), although with a much larger width of individual modular elements than in odontocetes. Further differences in neuronal density were appreciable between the two mysticetes such as much more densely populated layers II and V in *B. acutorostrata* than in *M. novaeangliae* (Fig. 4H,I).

Anterior insular cortex (AI)

The cytoarchitecture of the AI was investigated in an odontocete, the beluga whale (*D. leucas*), and in two mysticetes, the minke whale (*B. acutorostrata*) and the humpback whale (*M. novaeangliae*). The most remarkable feature of the organization of the AI in these cetacean species was the pattern of clustering of neurons of layer II throughout the whole extent of the cortical region. However, a different degree of clustering was observed across species. While the clusters appeared very large and extremely separated one from each other in *M. novaeangliae*, (Fig. 6C), their size and the distance between them were less pronounced in *B. acutorostrata* (Fig. 6B), and even much less in *D. leucas* (Fig. 6A), decreasing the overall appearance of the clustering pattern in this species. In all three species, AI was thin and exhibited a thick layer I, a layer III characterized by a lower neuronal density and that consisted mostly of small pyramidal neurons, a thin layer V in which large pyramidal neurons were often grouped in small clusters and a layer VI variable in thickness and well-visible columnar organization in *D. leucas*, as was the case in the ACC (Fig. 6A). In addition, all three species were characterized, in the white matter underlying the AI, by well defined claustral islands (indicated by arrows in Fig. 6A-C) that occasionally established contact with layer VI (Fig. 6A-C). The size and extension of these claustral islands was variable throughout the AI but highly comparable in all the three species.

Beside this general cortical organization, specie-specific differences were observed. Notably, while layer III in the two mysticetes was characterized by a homogeneous distribution of neurons, in *D. leucas* the small pyramidal neurons were organized in columns that often abutted the clusters of layer V and given this peculiar organization, layer III seemed, in *D. leucas*, less densely populated than in the two mysticetes. Moreover, as for the clustering of layer II, the large pyramidal neurons in layer V of *M. novaeangliae* formed clusters spanning through the whole extent of the layer, which, due to this organization, appeared thicker given the irregular vertical distribution of the clusters (Fig. 6C). Finally, layer VI in *D. leucas* was much thicker and less densely packed than in the two mysticetes (Fig. 6A).

Frontopolar cortex (FPC)

The cytoarchitecture of the frontopolar cortex (FPC) was investigated in two mysticetes (*B. acutorostrata* and *M. novaeangliae*). Its overall organization was characterized by a thick layer I, a well defined layer II that in *M. novaeangliae* showed a weak clustering pattern and a lower density of neurons, a thich layer III and a layer V characterized by pronounced clusters of pyramidal cells that, especially in *M. novaeangliae* were joined by modules of cells in layer VI. The organization of layer V appeared patchy in the two mysticetes whereas layer VI was characterized by an even distribution of multipolar neurons and a greater thickness compared to other cortical regions. In *M. novaeangliae* the overall appearance of FPC was dominated by an accentuated pattern of columnarity compared to *B. acutorostrata* (Fig. 7A,B).

Notes on the cytoarchitecture of ACC, AI, and FPC in other relevant species

The cyto- and chemoarchitecture of relevant species of aquatic and terrestraial mammals was investigated in a comparative perspective. Particularly, details are reported about the cyto- and chemoarchitecture of a semiaquatic carnivore, the Atlantic walrus (*O. rosmarus rosmarus*), of a sirenian, the Florida manatee (*T. manatus latirostris*), of an artiodactyl, the pigmy hippopotamus (*H. liberiensis*) and of a perissodactyl, the black rhinoceros (*D. bicornis*). Unfortunately, not all regions were available in each of these species and comparison with the corresponding cortical regions of the cetacean brain will be made based on tissue availability.

Anterior cingulate cortex (ACC)

Trichechus manatus latirostris

The organization of the ACC was characterized by a thick cortical plate, the absence of layer IV, and by very well developed layers V and VI. The most prominent feature was the modular organization of layer VI that could be divided into a layer VIa containing a low density of neurons and a layer VIb in which the neurons were densely packed and organized into long columns of single neurons in width that extended for the whole thickness of the layer. Often 2-3 columns were intimately related forming a larger columnar unit. The larger columns were very well defined with no cells bodies visible between two consecutive columnar structures. Layer V could be divided into a thin layer Va containing large pyramidal neurons and a thicker layer Vb containing smaller pyramidal neurons often loosely and less tightly packed. Similarly to the situation in cetaceans, layer II was thin and densely populated and lied over a thick layer III. However, the density of neurons in layer II was less homogeneous than that observed in cetaceans, and as a consequence the general appearance of this layer was discontinuous (Fig. 5A).

Loxodonta africana

Similar the situation in cetaceans and in *T. manatus latirostris*, the ACC of *L. africana* was characterized by the absence of layer IV. Layers III, V, and VI were comparable in thickness and very well developed. However, the distribution of neurons within these layers was uniform and a columnar organization such as that observed in the deep layers of *T. manatus latirostris* and some cetaceans was absent (Fig. 5B).

Odobenus rosmarus rosmarus

The ACC of this species was characterized by a thick layer I, and layer II was less densely packed and much thicker than in the cetaceans, *T. manatus latirostris*, and *L. africana*. Layer V contained very large and isolated pyramidal neurons that often grouped into large clusters and, forming wide columns, merged with the neurons of the thin layer VI. Overall, the ACC was thinner than that of *T. manatus latirostris* and *L. africana* given the less developed layers V and VI (Fig. 5C).

Anterior insular cortex (AI)

Trichechus manatus latirostris

The most prominent feature of this cortical region was the obvious clustering of layer II in which, similar to cetaceans, large groups of neuron clusters gave a patchy appearance. However, in this species, the clustering of layer II was more striking given the formation of extremely large

columns of cells starting from layer II and extending throughout the whole thickness of the cortex with the most pronounced appearance in layer II and upper layer V. Between layer II and V the columns were extremely pronounced owing to the absence of neurons between adjacent columnar structures. In the deeper layers V and VI the columnar pattern was less pronounced as the columnar element were linked to each other in a more homogeneous cellular distribution in both layers (Fig. 6D).

Hexaprotodon liberiensis

The AI of *H. liberiensis* was characterized by a very thick layer I and a layer II composed by large clusters of cells that often bulged into layer I. A thick layer III was followed by a layer V populated by very large pyramidal cells. Layer VI was very thin and loosely packed (Fig. 6E). Moreover, like in *B. acutorostrata*, layer III was divided into large vertical modules matching the width of the layer II clusters. This characteristic gave to the upper half of the AI a very pronounced columnar appearance (Fig. 6E).

Odobenus rosmarus rosmarus

The AI of *O. rosmarus rosmarus* was characterized by a very thin cortex. Layer I was thick and layer II thicker and less densely packed than the cetacean species. Moreover, layer II did not present clusters but was characterized by a rather homogeneous distribution of neurons. A thick layer III containing small pyramidal neurons was followed by a thin layer V containing mainly isolated and very large pyramidal neurons extending their axons into the upper layers and that grouped in clusters of 10-15 neurons. Only a few perikarya were visible between adjacent clusters and as such this layer had a less dense appearance than the upper cortical layers. Layer VI was thick and consisted of small multipolar neurons (Fig. 6F).

Frontopolar cortex (FPC)

Trichechus manatus latirostris

The organization of the FPC was, much like AI, characterized by the prominent thickness of layers V and VI, and the extreme modularity of the latter with thin columns of neurons extending to the white matter. However, in the FPC, the structure of layer V was more homogeneous along its thickness and could not be divided into sublayers. The organization of layer VI was heterogeneous and a loosely packed layer VIa as well as a well organized and columar layer VIb were identifiable (Fig. 7C).

Diceros bicornis

The structure of the FPC was characterized by a thick layer I, a layer II thicker and less densely packed than in cetaceans with a transition into layer III not well defined. A thin layer IV was visible and layer V was thick and consisted of pyramidal neurons that were larger than the neurons of layer III but smaller if compared to the neurons of layer V in some of the species investigated. Finally, layer VI that was variable in thickness along the cortical area and contained small multipolar neurons (Fig. 7D).

Chemoarchitecture

Given that not all cortical regions were in optimal condition to yield reliable results on the pattern of distribution of CR-immunoreactive neurons, only some cortical regions and species were used for the analysis of their chemoarchitecture. As such, the patterns of distribution and morphologies

of the CR-immunoreactive neurons in cetaceans and other relevant species will be discussed together.

Calretinin

The distribution pattern of CR-immunoreactive neurons was comparable in all of the cetacean species investigated in the present study. As reported by Glezer et al. (1998) and Hof et al. (1999) in A1 and V1 of cetaceans, CR-immunoreactive neurons in the ACC and AI were bipolar and multipolar neurons mainly located in layers II-III with vertically oriented axons and dendrites, although scattered cells were present throughout all cortical layers (Fig. 8A-I; Fig. 10 A-B). CR immunoreactivity was visualized in the cell body and in the major neuronal processes in a different degree among the investigated species, probably given the differences in the quality of the tissue. Particularly, in the ACC of *T. truncatus*, *G. griseus*, *O. orca*, and *P. macrocephalus*, the main processes of CR-immunoreactive bipolar neurons located in layer II and III featured intensely immunostained dendrites extending into layer I and deep layer III (Fig. 8A, B, D, F). Overall, the ACC of *P.phocoena, I. geoffrensis,* and *K.simus* showed bipolar and multipolar neurons in deep layer I and in layer II, but not visible processes extending to the upper and lower cortical layers. Overall, the staining pattern in these three species did not show morphological details of the neuronal processes but was mainly concentrated in the perikarya (Fig. 8C, E, G). Moreover, CR-immunoreactive extraverted neurons, previously described in V1 and A1 of *T. truncatus* (Glezer et al., 1998), were observed in layer II of the ACC of *O. orca* and *P. macrocephalus* (Fig. 8D, F). Interestingly, the ACC of *O. orca* and *B. acutorostrata,* showed very similar morphologies of large multipolar neurons in deep layer II and layer III that were not observed in other cetacean species (Fig. 8 D, H, I). However, whereas in *O. orca,* a high density of bipolar and fusiform neurons was visible, in the mysticete, *B. acutorostrata*, the large multipolar neurons represented the most abundant morphology observed.

The pigmy hippopotamus, *H. liberiensis*, the closest relative of cetaceans, showed in the ACC a pattern of distribution of CR-immunoreactive neurons very similar to that observed in the cetaceans, with cells bodies in every layers and the highest density of immunolabeled neurons observed in layers II-III (Fig. 9A, D). Given the remarkable quality of the materials, the ACC of *H. liberiensis* showed processes extending throughout all the cortical layers and fusiform bipolar and multipolar cells were observed in deep layer I, as well as layer II and III. The fusiform multipolar cells were comparable to the large fusiform multipolar cells previously described in layer V of V1 of the giraffe (*Giraffa camelopardalis*) (Hof et al., 1999).

The Atlantic walrus, *O. rosmarus rosmarus,* showed a pattern of distribution of CR immunoreactivity in the ACC very different from that in cetaceans, with the most of the CR-immunoreactive cell bodies in the deep layers III, IV and V, although CR-immunoreactive neurons occurred layers II and III (Fig. 9B). The most of the CR-immunoreactive neurons in the ACC of *O. rosmarus rosmarus* were large multipolar neurons (Fig. 9E), and large atypical CR-immunoreactive pyramidal neurons were observed in layer V (Fig. 11A).

The black rhinoceros, *D. bicornis*, showed a distribution of CR-immunoreactive neurons that resemble that observed in cetartiodactyls, with cells in all layers but the majority of CR-immunoreactive neurons in layers II-III. Interestingly, large fusiform multipolar CR-immunoreactive neurons, similar to those previously described in layer V of the primary visual cortex of the giraffe (*G. camelopardalis*) and in layers I, II, and III of the ACC of *H. liberiensis*, were observed in deep layer I of the ACC of *D. bicornis*. Additionally, large CR-immunoreactive multipolar neurons as well as neurons with a round or ovoid soma oriented parallel to the pial surface were observed in layer I, possibly representing CR-immunoreactive Cajal-Retzius neurons.

The AI of *P. phocoena* displayed bipolar CR-immunoreactive neurons in layers II-III and the same pattern of distribution was observed in the AI of *B. acutorostrata* but in this species the dominant morphology was represented by large multipolar neurons. The AI of *H. liberiensis* was

characterized by the presence, as in the ACC, of large and fusiform CR-immunoreactive bipolar and multipolar neurons in which the neuronal processes could be followed into the upper and lower layers given the optimal staining. These CR-immunoreactive neurons were mainly concentrated in layers II and III and spread their dendrites throughout the upper layer I and lower layers V and VI (Fig. 10C). The AI of *O. rosmarus rosmarus*, as its ACC, was characterized by the presence of CR-immunoreactive neurons mostly in deep layer III as well as in layers and V with a few scattered neurons in layers I and VI (Figs 9B, 10D).

Discussion

The present study compared the cytoarchitecture and the neurochemical specialization of the ACC, AI, and FPC of a range of cetaceans and select terrestrial and aquatic mammals. Although the overall organization of the neocortex of the cetacean species investigated showed a similar cytoarchitectonic structure, several order-specific differences as well as differences in the organization of the three cortical regions were observed. Generally, the organization among these cortical regions was marked by specific differences that distinguish them based on their cytoarchitecture. These findings support previous reports on the complexity and specializations of the cetacean neocortex (Glezer et al., 1993, 1998; Hof et al., 2005; Hof and Van der Gucht 2007; Marino et al., 2007, 2008; Butti et al., 2009).

In particular, among the cetacean species examined, the three cortical regions were characterized by 4 major layers-specific differences: 1) the thickness of layers II-III and V; 2) the neuronal density of layers II and III; 3) the presence or absence of columnar patterns in layers V-VI; and 4) the size of large pyramidal neurons of layer V and their degree of clustering. Moreover, among the cortical regions investigated, the AI showed the most striking cytoarchitectural organization, being dominated by a distribution of neuronal clusters in the layer II. This structural feature of AI was previously reported in *T. truncatus* (Jacobs et al., 1984; Manger et al., 1998) and in *M. novaeangliae* (Hof and Van der Gucht, 2007) and was found in the present study also in smaller odontocete species, although with a less evident pattern of clustering. Interestingly, Hof and Van der Gucht (2007) reported a marked modularity of layer II also in extensive areas of the occipital cortex in both *M. novaeangliae* and the fin whale (*B. physalus*), and proposed that such modules are shaped by thalamocortical afferents and possibly play a crucial role in shaping specific long-range connections in an energy-efficient manner. In this context, it is worth noting that the clustering pattern of layer II in AI is observed also in the closest relative of the cetaceans, *H. liberiensis*, and in another aquatic mammal, *T. manatus latirostris* but not in the semiaquatic pinniped *O. rosmarus rosmarus* or in the rhinocerotid *D. bicornis*.

Differences among odontocetes and mysticetes were observed in the variation of neuronal density between small and large species, and the high degree of modularity observed in the latter (e.g., *O. orca*, *P. macrocephalus*, and *M. novaeangliae*) compared to smaller species. The smaller mysticete analyzed, *B. acutorostrata*, showed a neuronal density more comparable to that in the larger odontocetes than to *M. novaeangliae*. However, this was a young specimen and probably not a good representative of the adult cortical organization in this species.

Although specific cortical regions were organized on a similar scheme across species, species-specific differences were appreciable. Of particular interest was the lower neuronal density, compared to species of similar brain size, observed in *D. leucas* and *I. geoffrensis*. *D. leucas* has in fact a brain mass of 2,083 g, which is comparable to that of other delphinids such as *T. truncatus* and *G. griseus*, whereas *I. geoffrensis* has a brain mass of only 634 g (Hof et al., 2005). If any pattern of cell density would have to be expected, *I. geoffrensis* should have a higher neuronal density than *D. leucas* and the two delphinids. However, this comparison is based on qualitative observations and in this context it will be interesting to perform a quantitative analysis of the neuronal density in these two species to confirm the present observations. Moreover, within the same cortical region, *G. griseus* showed a thicker layer V and a more pronounced columnar

organization in comparison to the thinner and clustered layer V of *T. truncatus.* Differences were also observed in the density of layer V neurons and in their level of columnarity between *B. acutorostrata* and *M. novaeangliae.*

Among cetaceans, the immunostaining patterns observed were consistent with previous descriptions of CR-immunoreactive populations of neurons in other cortical regions of the cetacean brain, namely A1 and V1 of *T. truncatus*, *G. melas*, *D. leucas*, and *K. simus.* Particularly, the CR-immunoreactive neurons exhibited mainly bipolar and multipolar morphologies and were located in layers II and III (Hof et al., 1999).

The distribution of CR-immunoreactive neurons was consistent throughout cortical regions and species and was found to be prevalent in the superficial layers in cetaceans and *H. liberiensis.* Although there is no information, but the present report, on the structure of the cerebral cortex of *H. liberiensis*, the observed pattern of distribution of CR in the cetacean brain is interesting given the recent morphological and molecular evidence of the phylogenetic relationship between cetaceans and hippopotamuses. *H. liberiensis*, showed a pattern of cortical organization, both structurally and for CR immunreactivity, very similar to that observed in cetaceans, being agranular with only five layers. It also exhibited mainly bipolar CR-immunoreactive neurons, distributed in the upper cortical layers giving further credence to the occurrence of shared evolutionary traits between cetaceans and ungulates. The restricted distribution of CR-immunoreactive neurons to the upper layers, together with the finding that in the cetacean V1 the 70% of the synapses is contained in layer I (Glezer and Morgane, 1990) has been proposed by Glezer et al., (1992) to be evidence for these layers as recipient of thalamocortical afferents and thus for the need of extensive modulatory and inhibitory microcircuits within them.

Unfortunately the cortex of *M. novaeangliae* did not allowed for a good immunoabeling and *B. acutorostrata* was considered as representative of the situation in mysticetes. In contrast to odontocetes, in which the ratio of CR-immunoreactive bipolar and multipolar neurons is very similar, in the mysticetes there seems to be a prevalence of multipolar CR-immunoreactive neurons. A similar situation was also observed in *I. geoffrensis*, although this specimen was not optimal for immunohistochemistry. This will require further investigations to confirm this observation in iniids.

The distribution of CR-immunoreactive neurons in the cortex of all of the cetaceans and *H. liberiensis* was similar to that in *D. bicornis*, even though there were differences in the morphology of the CR-immunoreactive neurons. *O. rosmarus rosmarus* presented a very different distribution of CR-immunoreactive neurons, that were mainly distributed in the deeper layers and showed CR-expressing large pyramidal neurons that were not observed in the other species investigated.

The two limiting factors affecting the present study are represented by the sometime lesser quality of the collection materials due to the long storage time in fixative as well as the rarity of these species that did not allow for a large group size. The present investigation, as a consequence, could not account for an assessment of intraspecific variability and for any possible effect related to age and sex. However, if we consider the present specimens as representative of the cortical organization of ACC, AI, and FPC for their species, clear patterns emerge among the cetaceans and intriguing similarities between phylogenetically related species, such as the cetaceans and *H. liberiensis*, are likely, which deserve further and more extensive analyses.

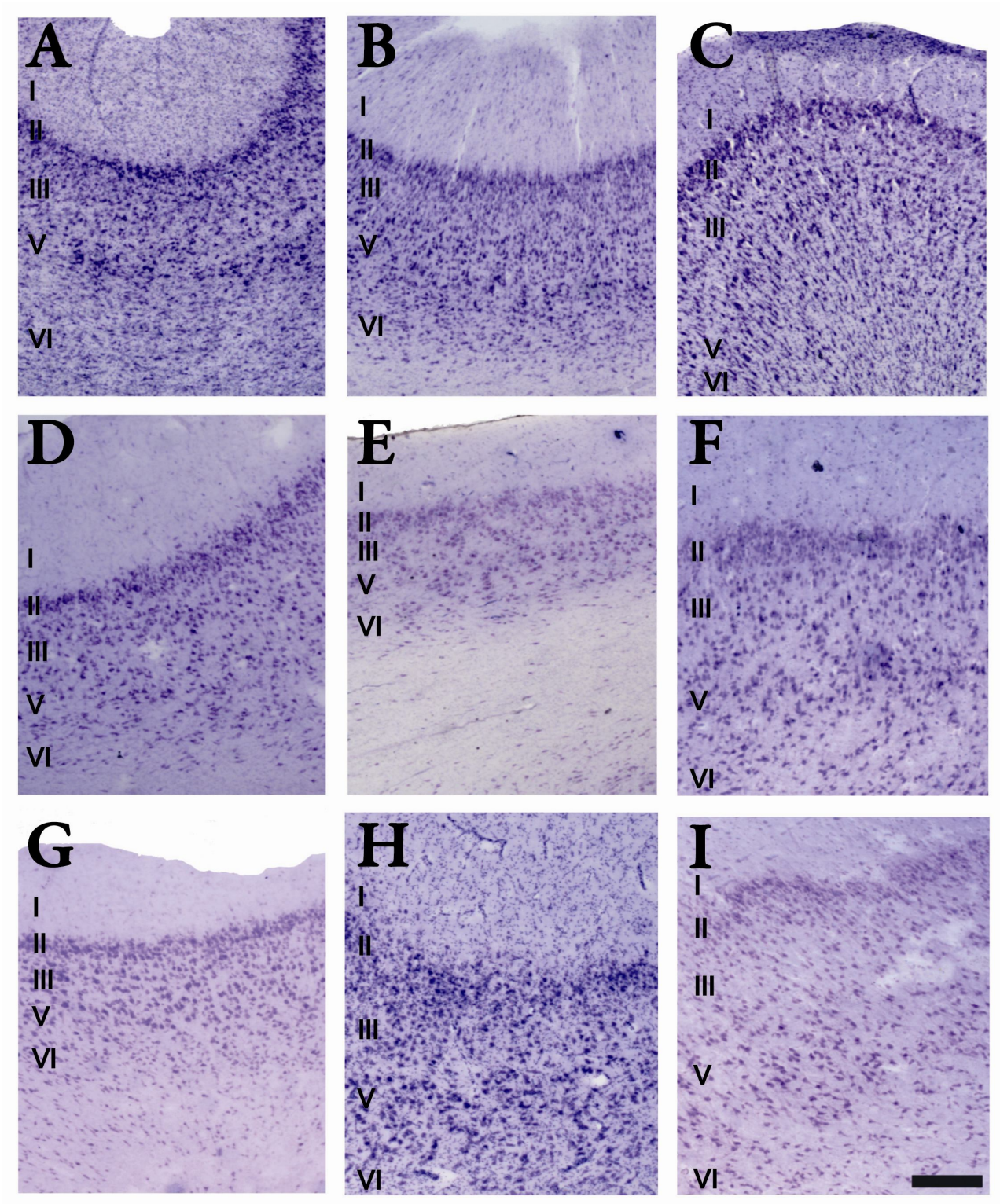

Figure 4. Comparative structure of the ACC in the brain of the odontocetes *T. truncatus* (A), *G. griseus* (B), *P. phocoena* (C), *O. orca* (D), *D. leucas* (E), *P. macrocephalus* (F), *I. geoffrensis* (G), and the mysticetes *B. acutorostrata* (H), and *M. novaeangliae* (I). Cortical layers are indicated by Roman numerals. Scale bar = 240 µm.

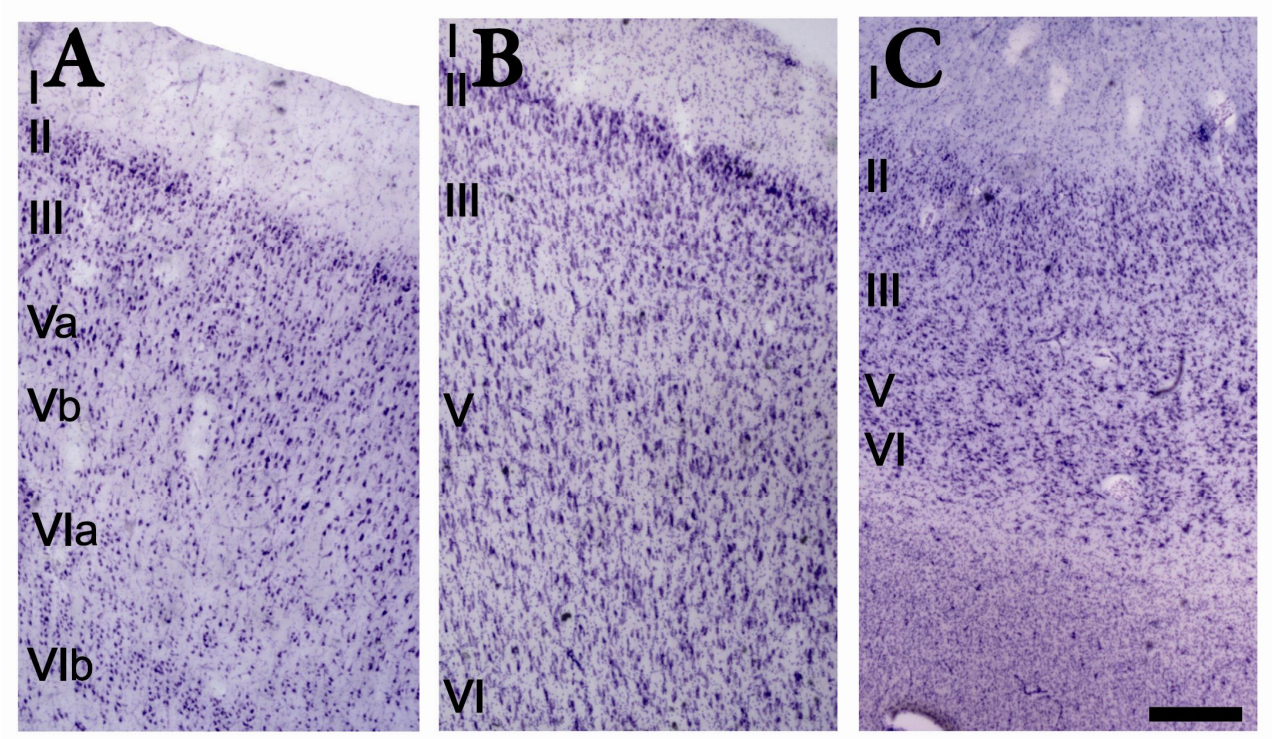

Figure 5. Comparative structure of the ACC in the brain of *T. manatus latirostris* (A), *L. africana* (B), and *O. rosmarus rosmarus* (C). Cortical layers are indicated by Roman numerals. Scale bar = 240 µm.

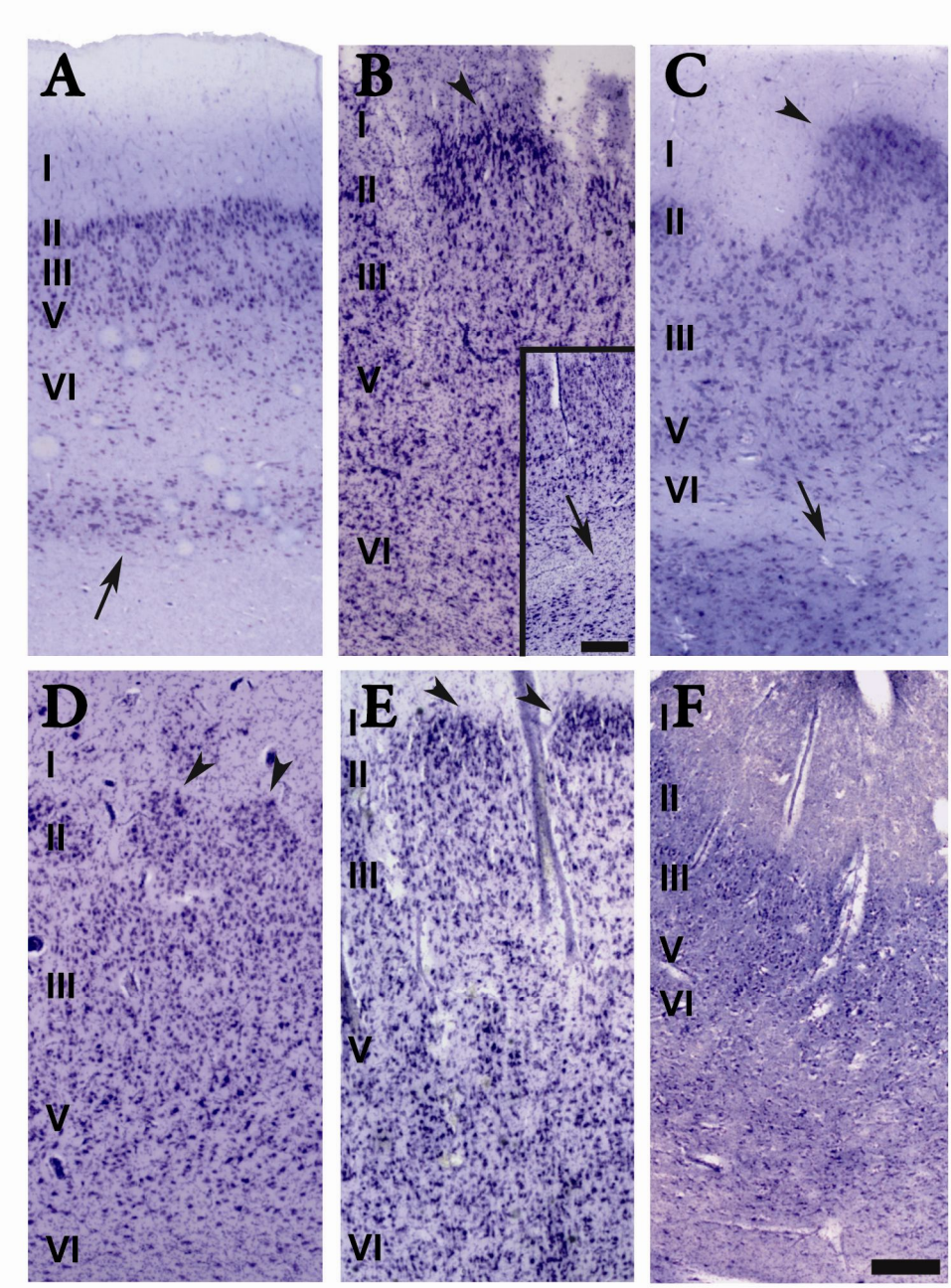

Figure 6. Comparative structure of the AI in the brain of *D. leucas* (A), *B. acutorostrata* (B), *M. novaeangliae* (C), *T. manatus latirostris* (D), *H. liberiensis* (E) and *O. rosmarus rosmarus* (F). Arrowheads indicate the clustering of layer II and arrows indicate the claustral islands in the white matter underlying the cortical plate. Cortical layers are indicated by Roman numerals. Scale bar = 240 µm

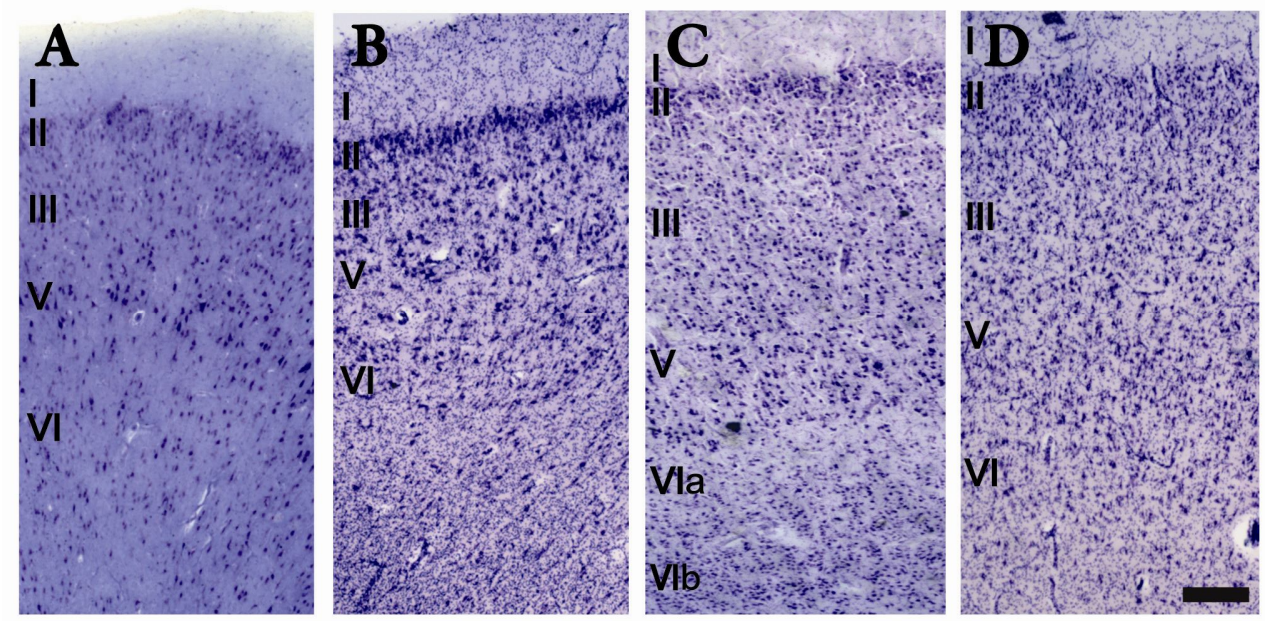

Figure 7. Comparative structure of the FPC of *M. novaeangliae* (A), *B. acustorostrata* (B), *T. manatus latirostris* (C), and *D. bicornis* (D). Scale bar= 240 μm.

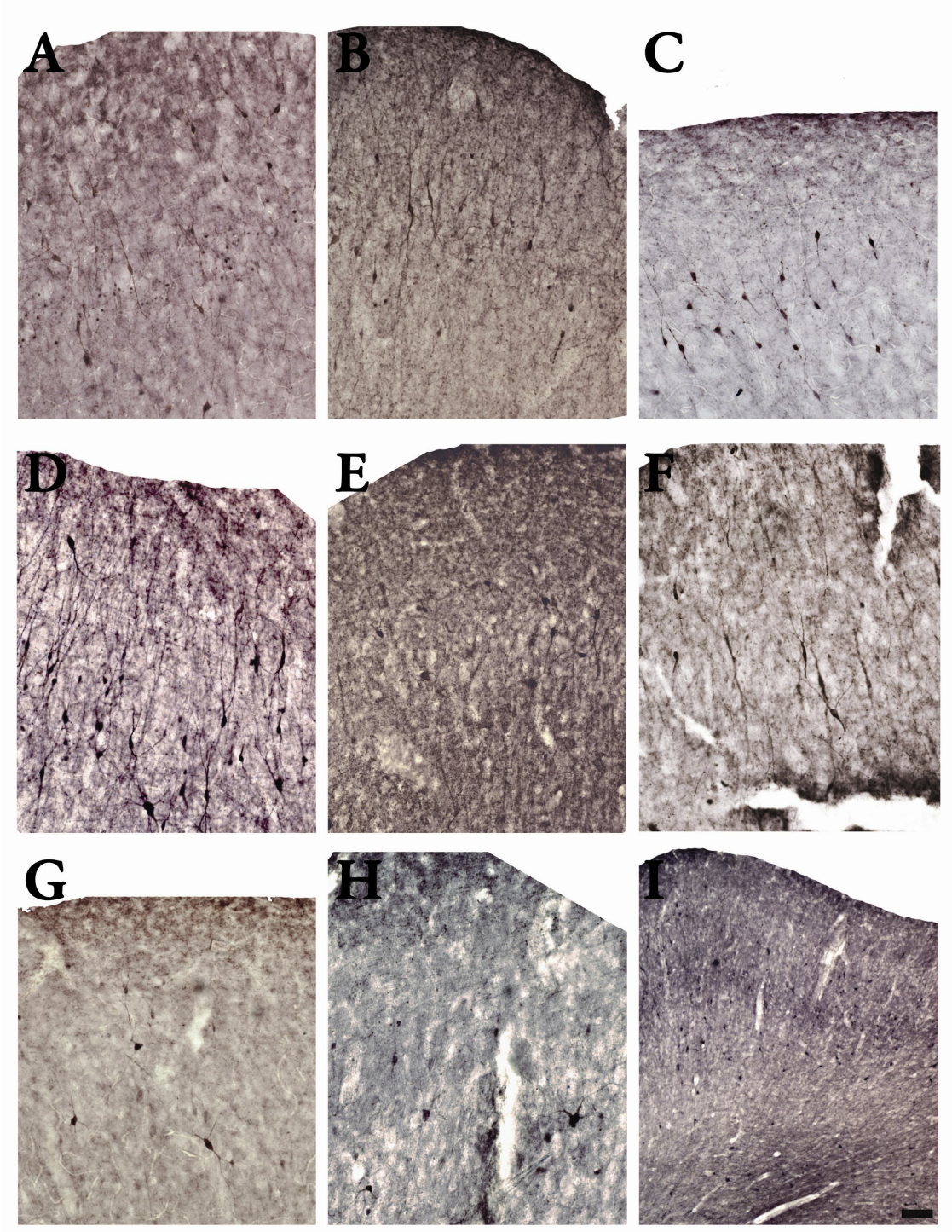

Figure 8. Comparison of distribution of CR-immunoreactive neurons in the ACC of *T. truncatus* (A), *G. griseus* (B), *P. phocoena* (C), *O. orca* (D), *K. simus* (E), *P. macrocephalus* (F), *I. geoffrensis* (G), and *B. acutorostrata* (H-I). Scale bar = 60 μm (A-H), and 240 μm (I).

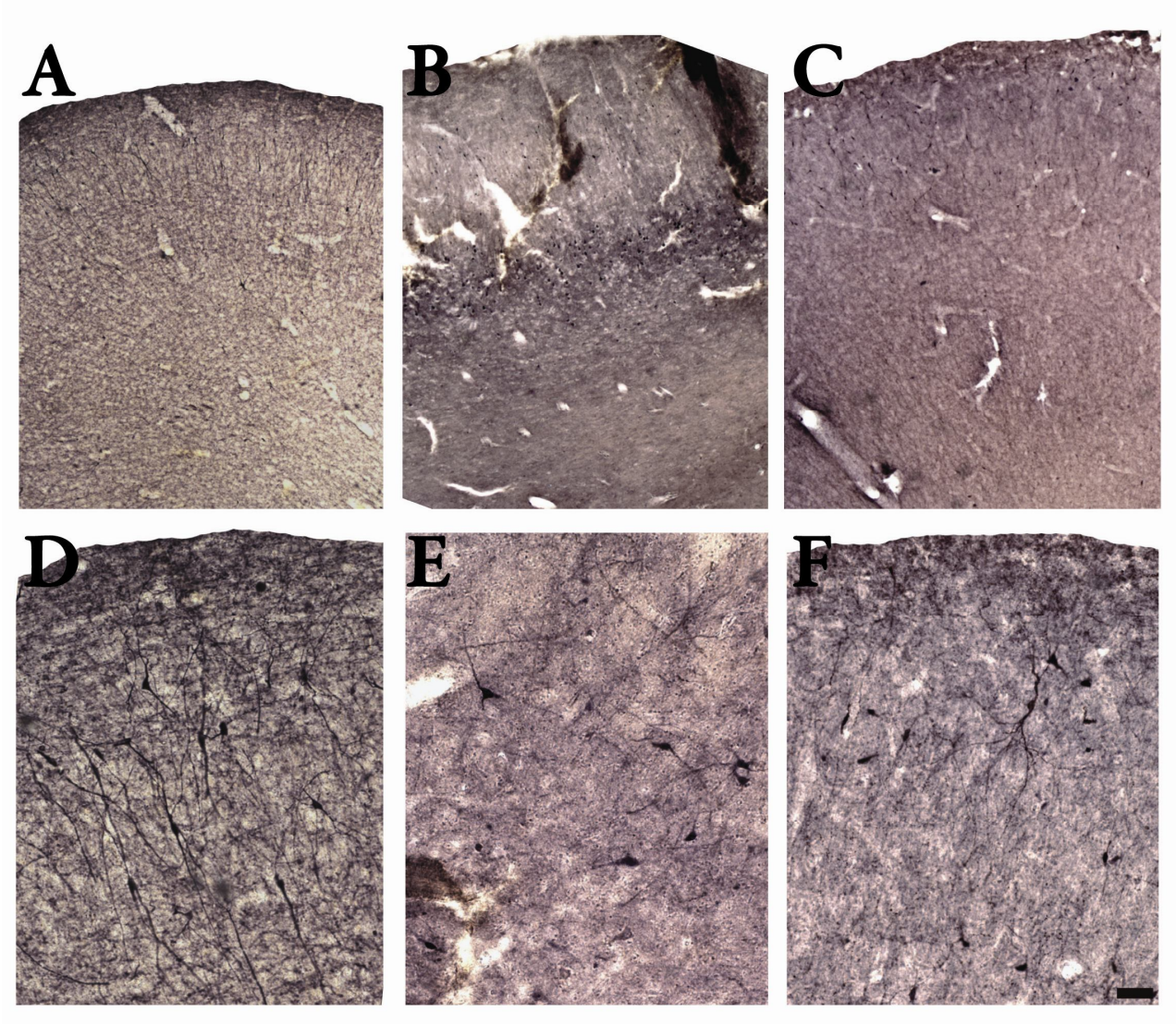

Figure 9. Comparison of the distribution of CR-immunoreactive neurons in the ACC of *H. liberiensis* (A, D), *O. rosmarus rosmarus* (B, E), and *D. bicornis* (C, F). Scale bar= 60 µm (D-F), 240 µm (A-C).

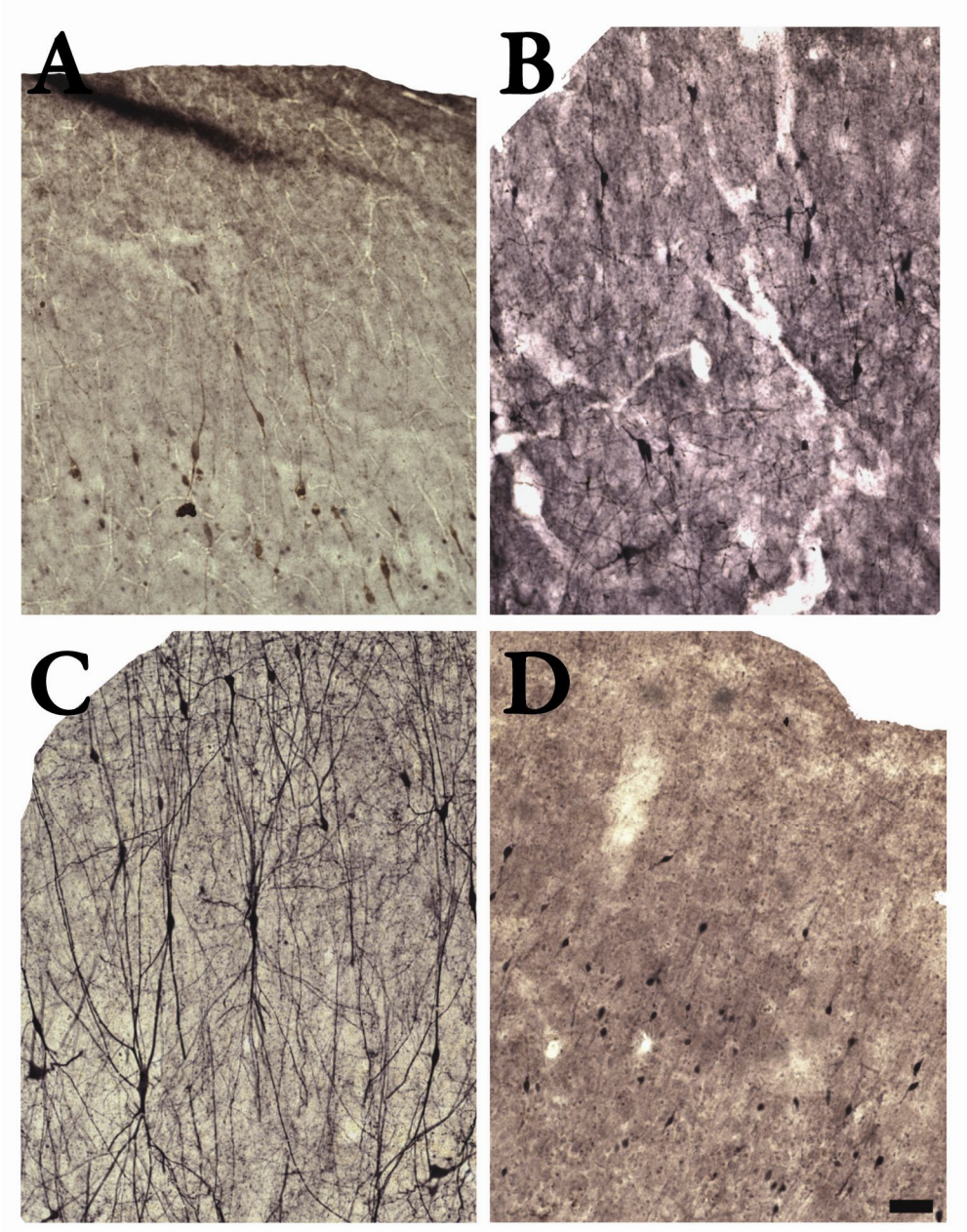

Figure 10. Comparison of CR-immunoreactive neurons in the anterior insula (AI) of *P. phocoena* (A), *B. acutorostrata, H. liberiensis* (C), and *O. rosmarus rosmarus* (D). Scale bar = 60 µm.

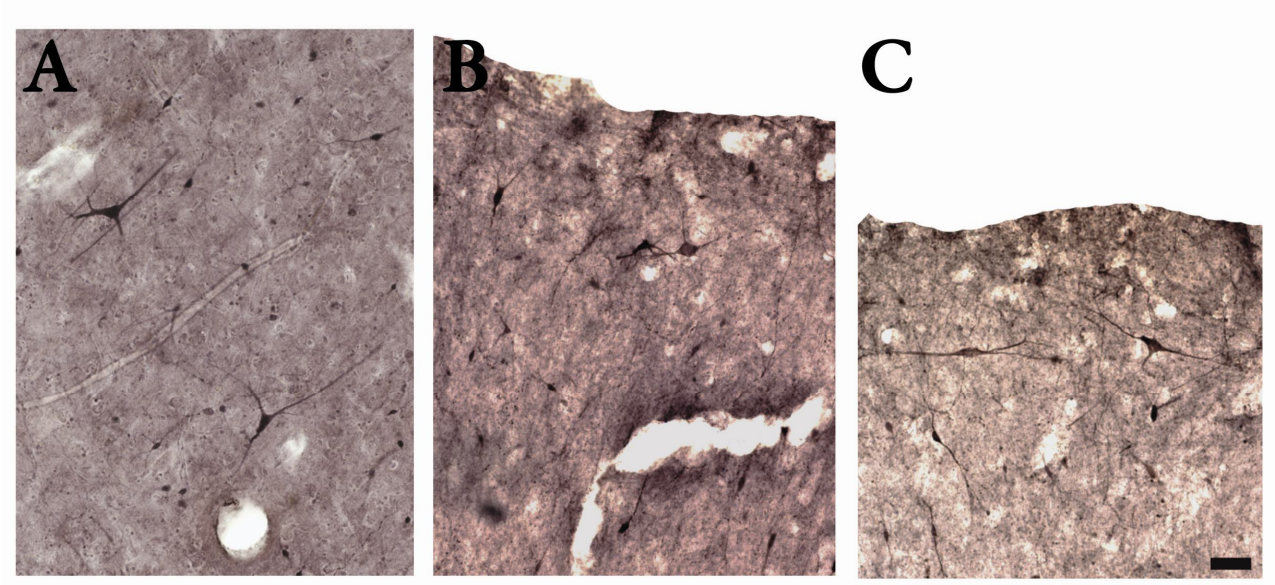

Figure 11. Atypical neuronal types in the neocortex of *O. rosmarus rosmarus* (A) and *D. bicornis* (B, C). Giant CR-immunoreactive pyramidal neurons in layer V of the AI of *O. rosmarus rosmarus* (A); large CR-immunoreactive multipolar neurons (B), and a possible Cajal-Retzius cell (arrowhead) in layer I of the ACC of *D. bicornis* (C). Scale bar = 60 µm.

Table 2. Protocol used for the Nissl staining procedure of all of the samples analyzed in the present thesis.

Solution	Immersion time	Notes
70% EtOH	2 min	
95% EtOH	2 min	
100% EtOH	2 min	
100% EtOH	2 min	
Chloroform 1	5 min	
Chloroform 2	5 min	
100% EtOH	2 min	
100% EtOH	2 min	
95% EtOH	2 min	
70% EtOH	2 min	
50% EtOH	2 min	
30% EtOH	2 min	
dH2O	2 min	
Cresyl violet 0.2%	5 min	
dH_2O	dip twice	
dH_2O	dip twice	
30% EtOH	7-10 s	
50% EtOH	7-10 s	
70% EtOH	7-10 s	
95% EtOH + Acetic acid	between 2.5 and 3 min (or until differentiated)	1 l of 95% EtOH + 500 µl of glacial acetic acid
100% EtOH 1	5 s	
100% EtOH 2	5 s	
Limonene 1	10 min	
Limonene 2	10 min	

Chapter 3

Glia/neuron index in the cetacean brain

Introduction

It is now generally recognized that there exists an inverse relationship between brain size and neuronal density (Tower and Elliott, 1952; Shariff, 1953; Tower, 1954; Haug, 1987; Poth et al., 2005). As such, even if large brains have a higher total number of neurons than small brains, their neuronal density is, as a rule, lower. However, glial cell numbers and densities have not been systematically studied in detail, and in particular the literature on the ratio of glial cell and neuron numbers (the glia/neuron index, GNI) in mammals with large brains, such as cetaceans, is rather sparse (Tower, 1954; Hawkins and Olszewski, 1957; Friede and Van Houten, 1962). Moreover, the analytical approaches used in these studies differ too much to draw meaningful comparative conclusions among these data. Particularly, how the number of glial cells relates to the number of neurons, brain size, and neuronal size remains poorly understood.

In general, when referring to "glial cells" all these studies refer to astrocytes and oligodendrocytes, the two main types of macroglia in the brain. Astrocytes play fundamental roles in many brain processes such as integration of neuronal inputs and modulation of synaptic activity and synaptic strength (Smith, 1994; Araque et al., 1999; LoTurco, 2000; Parpura and Haydon, 2000; Haydon, 2001), regulation of glucose storage and metabolism (Coles and Abbott, 1996; Tsacopoulos and Magistretti, 1996; Wender et al., 2000; Pellerin and Magistretti, 2004; Pellerin et al., 2007; Magistretti, 2009), glutamate uptake and release (Mennerick and Zorumski, 1994; Santello and Volterra, 2009), regulation of synaptic transmission (Smith, 1994; Pfrieger and Barres, 1997; Kang, 1998; Newman and Zahs, 1998; Newman, 2003; Zhang et al., 2003; Piet et al., 2004; Gordon et al., 2005; Pascual et al., 2005; Haydon and Carmignoto, 2006), regulation of blood flow (Parri and Crunelli, 2003) modulation of oligodendrocyte myelination activity (Ishibashi et al., 2006), synaptogenesis (Ullian et al., 2001; Pfrieger, 2009), and neurogenesis (Song et al., 2002; Horner and Palmer, 2003; Nedergaard et al., 2003). Oligodendrocytes are mainly involved in the formation of the myelin sheaths around the axons that ensure the conduction speed and the efficiency of action potential propagation (Baumann and Pham-Dinh, 2001) and they depend upon constant interaction with neurons (specifically the axon) for their survival (Barres et al., 1992; Barres and Raff, 1993, 1999). Dysfunction of both astrocytes and oligodendrocytes has been implicated in neurodegenerative diseases (Maragakis and Rothstein, 2006), and in psychiatric conditions such as schizophrenia (Hakak et al., 2001; Hof et al., 2003; Tkachev et al., 2003; Segal et al., 2007). Moreover, reduction of the number of glial cells in some cortical regions of the human brain has been demonstrated in bipolar disorder (Öngür et al., 1998; Bowley et al., 2002).

Unbiased estimates of glia and neuron numbers using stereologic methods have been obtained in many anthropoid primates (O'Kusky and Colonnier, 1982; Dombrowski et al., 2001; Lidow and Song, 2001; Sherwood et al., 2006; Christensen et al., 2007), but only few reports are available for humans (Pakkenberg et al., 2003; Sherwood et al., 2006). These studies, regardless of the cortical region or layer investigated, report GNI values varying between 0.56 to 1.72 in Old and New World monkeys, 0.98 to 1.22 in hominoids, and 1.55 to 2.99 in humans. Classical studies of the organization of the cetacean brain report a ratio of glial cells to neurons of 5.86 in the fin whale, and values that range between 2 and 3 respectively for the limbic and visual cortices of the

bottlenose dolphin (Hawkins and Olszewski, 1957; Morgane et al., 1982; Garey and Leuba, 1986). The only quantitative study of the number of neurons and glial cells in the brain of cetaceans using an unbiased stereologic approach was performed by (Eriksen and Pakkenberg, 2007) in the whole extent of the minke whale (*B. acutorostrata*) neocortex. These authors did not report a GNI value but provided the total number of glia (98.2×10^9) and neurons (12.8×10^9). However, if these values are used to calculate a ratio of glia to neurons a GNI value of 7.7 is obtained.

The issue of whether cetaceans are outliers for GNI compared to mammals with comparable brain size and complexity represents a matter of debate (Manger, 2006; Marino et al., 2008). To address this issue further we estimated, using unbiased stereology, the GNI in the anterior cingulate cortex (ACC) and in the primary somatosensory cortex (S1) of representative cetacean species featuring a wide range of brain and body sizes. For comparative purposes we analyzed the GNI in the same cortical regions of the Florida manatee (*Trichecus manatus latirostris,* Sirenia, Trichechidae*)*, pigmy hippopotamus, (*Hexaprotodon liberiensis*, Artiodactyla, Hippopotamidae), African elephant (*Loxodonta africana*, Proboscidea, Elephantidae*)*, rock hyrax (*Procavia capensis,* Hyracoidea, Procavidae), lowland streaked tenrec (*Hemicentetes semispinosus,* Afrosoricida, Tenrecidae), and the black and rufous elephant shrew (*Rhynchocyon petersi*, Macroscelidea, Macroscelididae) (see Table 1 for details). The manatee is an aquatic mammal with a brain characterized by a lissencephalic condition (Reep and O'Shea, 1990); elephant and hyrax are the closest terrestrial relatives of the manatee (Kellogg et al., 2007) and have brains of very different sizes; tenrec and elephant shrew are closely related to manatee, elephant, and hyrax but they have much smaller brains. Finally, the hippopotamuses are the closest relatives of cetaceans (Gatesy, 1997; Boisserie et al., 2005; Agnarsson and May-Collado, 2008). Our sample of species is representative of the two major phylogenetic groups Cetartiodactyla (dolphins, whales, porpoises and even-toed ungulates) and Afrotheria (tenrecs, elephant shrews, aardvark, sirenians, hyraxes, and elephants), and will be particularly meaningful to understand if a specific and unique trend of GNI exists in the brain of cetaceans setting them apart from terrestrial mammals.

Materials and methods

Specimens and histological preparation

Nine cetacean brains, including seven odontocetes (Bottlenose dolphin, *Tursiops truncatus*; Risso's dolphin, *Grampus griseus*; harbor porpoise, *Phocoena phocoena*; beluga whale, *Delphinapterus leucas*; dwarf sperm whale, *Kogia simus*; sperm whale, *Physeter macrocephalus*; killer whale, *Orcinus orca*), and two mysticetes (humpback whale, *Megaptera novaeangliae* and minke whale, *Balaenoptera acutorostrata*) were used in the present study. In addition, the brains of the Florida manatee (*Trichecus manatus latirostris*), pigmy hippopotamus (*Hexaprotodon liberiensis*), African elephant (*Loxodonta africana*), rock hyrax (*Procavia capensis*), lowland streaked tenrec (*Hemicentetes semispinosus*), and the black and rufous elephant shrew (*Rhynchocyon petersi*) were used for comparative purposes. The cetacean, pigmy hippopotamus, one manatee, and two elephant brains were obtained from strandings, and marinelands or zoos where the animals died of natural causes and were available for prompt postfixation in 10% buffered formalin or 4% paraformaldehyde. The brain of the African elephant was gravity-perfused with 100 liters of 4% paraformaldehyde 0.1 M following a cull during a 2008 population management strategy in Zimbabwe (Manger et al., 2009). Blocks containing the regions of interest (ROIs) were collected from the right or left hemisphere, cryoprotected by immersion in graded concentrations of sucrose solutions up to 30%, frozen in dry ice, cut with a sliding microtome into

80 or 60 μm-thick sections, mounted on glass slides, and stained for Nissl substance in a solution of 0.2% cresyl violet. Sections were then coverslipped in 100% DPX for examination. The brains of a *T. manatus latirostris*, a *P. capensis*, a *H. semispinosus*, and a *R. petersi* were provided by the Yakovlev collection of the National Museum of Health and Medicine, Washington, DC. The brains of these specimens were dehydrated in alcohol solutions up to 30% and embedded in celloidin. Coronal sections throughout the brain were cut into 35 μm-thick sections, and stained alternatively for Nissl substance with thionin. The sections were then mounted on glass slides and coverslipped in clarite for examination.

Identification of cortical areas, neurons, and glia

The ROIs (ACC and S1) were identified in the cetaceans using landmarks as described in the introduction (see pages 9-10 for details). The ACC was identified in the other species as the comparable topographical domain of cortex surrounding the anterior part of the corpus callosum and the sampling of blocks or the outlining of the ACC in the coronal sections of the whole brains were made always including the most rostral part of cortex around the genu of the corpus callosum and using the latter as a reference structure. The identification of S1 in different species was based on detailed descriptions of the sensory cortical areas by (Krubitzer, 1997) for the lowland streaked tenrec (*H. semispinosus*), and by (Dengler-Crish, 2006) for the black and rufous elephant shrew (*R. petersi*). Given the lack of references in the literature on the location of the primary somatosensory cortex (S1) in the Hippopotamidae and specifically in the pigmy hippopotamus (*H. liberiensis*), S1 was identified based on cytoarchitecture as described in Chapter 2. The regions of interest were investigated upon availability and staining condition and as such, S1 of the brains of *P. capensis*, *L. africana*, and *T. manatus latirostris* could not be investigated. Particularly, S1 of *L. africana* specimens were not available and the poor staining condition of S1 in *T. manatus latirostris* and *P. capensis* did not allow for the identification of the morphology of glial cells (and thus the cell count) with a good degree of precision. Maps showing the location of the regions of interest in the species here examined are showed in Figures 12-14.

In all the species neurons were identified in Nissl-stained sections by the presence of a large nucleus, a darkly stained nucleolus and the presence of Nissl substance in the cytoplasm. Glial cells were recognized by their much smaller size, a nucleus containing much heterochromatin, and the lack of a well defined nucleolus (Figs 15-17). Finally, in order to conform the present study to comparable data available in literature, I limit here the discussion to astrocytes and oligodendrocytes and use thereafter the term “glia” to designate this two cell types.

Stereologic design

Quantitative analyses were performed on a stereology workstation equipped with a Zeiss Axiophot photomicroscope, Plan-Neofluar objectives 2.5x (N.A. = 0.075), 40x (N.A. = 0.75), 40x LD (N.A. = 0.6), 100x (N.A = 1.30) and Plan Apocromat objectives 10x (N.A. = 0.32), 20x (N.A. = 0.8) (Zeiss, Thornwood, NY, USA), a motorized stage (Ludl Electronics, Hawthorne, NY, USA), an Optronics MicroFire digital camera (Optronics, Goleta, CA, USA) and a stereology software (SteroInvestigator, MBF Bioscience, Williston, VT, USA). Starting with a random section number, a systematic sampling (every 30^{th}, 40^{th} or 50^{th} Nissl-stained sections) of 2 to 5 sections throughout the available blocks of the ROIs was performed. An exception is represented by the available tissue for *R. petersi*. Due to the poor quality of the staining, only one section showed enough morphological details to allow the counting, and the GNI for this species and cortical region was therefore estimated on a single section. However, as stressed below, assuming a constant GNI within a given cortical region, the values obtained in this case are not biased given that the GNI is based on a ratio. To increase the sampled area, the stereologic parameters were, in this case, adjusted to obtain a sufficient number of sampling sites within one section. The boundaries of the

ROIs were traced at low magnification (2.5x) on the computer display and cortical layers I-VI were outlined in all the species. An additional outline of layers II-VI was made in the brain of all cetaceans and of *H. liberiensis*.

The ratio of glia and neurons were calculated from the density of cells within unbiased virtual counting spaces representing a known fraction of the section volume, the Optical Disector (Gundersen, 1977; Schmitz, 2000; Schmitz, 2005). The term "relative density" will be used to indicate the density of each cell type within the total volume of the disectors used during the counting and does not reflect the density of the cells within the whole ROI.

Neurons and glia relative densities were estimated within the available blocks of the regions of interest using the Optical Fractionator (West et al., 1991). The software used a systematic-random sampling approach to place a series of unbiased virtual counting spaces within each outlined contour. The sampling grid size was set in each specimen and ROIs to sample approximately 200-300 cells of each type. The disector height was set to sample at least 80% of the tissue measured thickness and guard zones of 1 or 2 μm were placed at the top and at the bottom of each section to avoid any bias in number estimates due to the loss of particles at the upper and lower surface of the section during sectioning (the so-called "lost caps effect", (Andersen and Gundersen, 1999; Schmitz and Hof, 2005). The enumeration of neurons and glial cells was performed at the magnification of 100x (see Tables 4 and 5 for details on stereologic parameters used for the Optical Fractionator).

The relative densities of neurons and glial cells were calculated by multiplying the number of cells counted by the volume of the disector used and by the number of disectors. The glia-neuron ratio was then obtained using these relative density values (Table 3) that refer to the density of each cell type within all the disectors investigated and therefore are not indicative of the average densities for the specific cortical area.

Finally, to define what the influence of a thick layer I is, as it contains only sparse neurons, we estimated the ratio of glial cells to neurons in the species showing a thick molecular layer both including and excluding layer I (Table 3). Data on the density of neurons and glial cells in the entire ROI were not calculated because the available blocks did not represent the whole rostrocaudal extent of the structures and, as a consequence, any cell density estimate would not be reliable. The nature of the block would, however, not affect the estimation of the GNI, because the index is a ratio and is not affected by volume changes in any way. Moreover, we assumed that the ratio of glia to neuron would not change within a specific cortical field and the available block was considered representative of that specific cortical region.

Statistical analysis

Because the GNI values in the Cetartiodactyla were obtained both including and excluding layer I a paired samples *t* test was performed to define if there were significant differences in the GNI values calculated including or excluding layer I. A *t* test for independent samples was used to determine whether the GNI values obtained in ACC and S1, within the same layers group, were statistically comparable.

In order to define the best-fit line for the bivariate relationship between brain weight and GNI these values were first transformed into a logarithmic scale and the Least Squares method was used as a regression model. However, as the *x* variable was measured with potential error, given that n = 1 in most species, the Standard Major Axis (SMA) was used as a second regression model to account for the potential error biasing the *x* values. Finally, the line obtained using the slope and the intercept values of the SMA analysis was used as a general mammalian fitting line to predict expected GNI values from a given brain weight.

Results

GNI values calculated in layers I-VI versus layers II-VI were found to be significantly different among Cetartiodactyla for all comparisons and in both cortical regions in the paired *t* test (ACC: $t_9 = 4.335$, $p = 0.002$; S1: $t_9 = 2.261$, $p = 0.05$) with the values obtained including layer I constantly greater than the values obtained excluding it (Table 3). Specifically, among Cetartiodactyla, GNI values of layers I-VI were 5.72% to 46.8% and 2.3% to 38.6% greater than those in layers II-VI in the ACC and S1, respectively. Two exceptions are S1 of *D. leucas* in which the GNI values are identical for layer I-VI and layers II-VI, and *T. truncatus* in which the GNI value of layers II-VI resulted greater than that of layers I-VI. However, it is important to note that layer I in the sections of these two specimens was particularly damaged given the poor quality of the tissue and the estimates of the GNI values in layers I-VI in these specimens are, therefore, underestimates. Moreover, in the case of *T. truncatus* the blocks available for ACC and S1 came from different specimens raising the possibility that differences between cortical regions in this case are partially due to intraspecific variation.

Differences in GNI values of layers group I-VI between cortical regions of interest within the Cetartiodactyla and within the Afrotheria were found to be not significant in all of the comparisons on a *t* test for independent samples ($t_{22} = 0.574$, $p = 0.572$). GNI values of layers II-VI were not significantly different between the cortical regions in the Cetartiodactyla. The same comparison among Afrotheria was not possible given the lack of the data of GNI in layers II-VI for the latter taxa.

In the Least Squares (LS) method with a critical $p = 0.05$ when the values of GNI in layers I-VI of the ACC of Cetartiodactyla and Afrotheria were plotted against brain weight, a significant relationship was observed between log GNI and log brain weight among Cetartiodactyla and Afrotherians combined ($y = 0.2771x$-0.1394; $r^2 = 0.8297$; $p < 0.0001$), among Afrotherians ($y = 0.2385x$-0.1333, $r^2 = 0.9064$; $p = 0.0125$) but not among Cetartiodactyla ($p = 0.0813$). When plotting values of log GNI in layers 1-6 of the S1 against log brain weight, the only group that showed a significative relationship was the combination of Cetartiodactyla and Afrotheria: ($y = 0.2494x$-0.09610; $r^2 = 0.7754$; $p = 0.0002$). The values of log GNI in layers II-VI of ACC showed a significant relationship against log brain weight in the Cetartiodactyla and Afrotheria combined ($y = 0.2488x$-0.1143; $r^2 = 0.4097$; $p = 0.0339$) and in the Cetartiodactyla alone ($y = 0.2702x$-0.1908; $r^2 = 0.4134$; $p = 0.0449$). The remaining relationships involving GNI of layers I-VI and II-VI in S1 were found to be statistically not significant.

The Reduced Major Axis (RMA) analysis with a critical $p = 0.05$ confirmed the results of the LS. Significant relationships were found when log GNI of ACC layers I-VI was plotted against brain weigh of Cetartiodactyla and Afrotheria combined ($y = 0.3042x$-0.2131; $r^2 = 0.830$; $p < 0.0001$), of Afrotheria ($y = 0.2505x$-0.1530; $r^2 = 0.906$; $p = 0.013$) but not Cetartiodactyla ($p = 0.081$). Values of log GNI in layers I-VI of S1 showed a significant relationship against log brain weight only in the Cetartiodactyla and Afrotheria combined ($y = 0.2832x$-01897; $r^2 = 0.775$; $p < 0.0001$). The values of log GNI in layers II-VI of ACC showed a significant relationship against log brain weight in the Cetartiodactyla and Afrotheria combined ($y = 0.3887x$-0.5615; $r^2 = 0.410$; $p = 0.034$), but an extremely weak relationship when considering the Cetartiodactyla alone ($y = 0.4203x$-0.6796; $r^2 = 0.413$; $p = 0.045$).

Even if several relationships of GNI values against brain weight turned to be significant, the strongest one including both taxa was that of log GNI of layers I-VI of ACC against log brain weight. In this case, GNI values showed a common scaling against brain mass if plotted as logarithmic values using either LS or SMA (ACC: SMA slope = 0.30, lower confidence interval (Lower CI) = 0.24, upper confidence interval (Upper CI) = 0.39, $p < 0.0001$; LS slope = 0.2771, $r^2 = 0.8297$, $p < 0.0001$; S1: SMA slope = 0.28, Lower CI = 0.20, Upper CI = 0.39, $p < 0.0001$; LS slope = 0.25 $r^2 = 0.78$, $p = 0.0002$). As such, the fitting line resulting from this relationship was used as a predictive line to establish the expected GNI values of a given brain weight (Fig. 18).

Discussion

This is the first study of the GNI of a large sample of cetaceans using unbiased stereologic methods. The use of this approach is important to obtain rigorous data that can be compared among taxa. Although investigations on glia and neuron numbers in several groups of mammals are available from the literature (Hawkins and Olszewski, 1957; Blinkov and Glezer, 1968; Gihr and Pilleri, 1969; Kraus and Pilleri, 1969; Garey and Leuba, 1986; Reichenbach, 1989; Stolzenburg et al., 1989; Ren et al., 1992), here I used as comparison only data obtained with unbiased stereologic methods (O'Kusky and Colonnier, 1982; Dombrowski et al., 2001; Lidow and Song, 2001; Sherwood et al., 2006; Christensen et al., 2007; Eriksen and Pakkenberg, 2007).

The first analysis pointed to the potential influence of layer I in the values of GNI in the cetartiodactyls. Results show that layer I has a variable but substantial influence on the cortical GNI value in both cortical regions investigated and that ACC and S1 are equally representative of the GNI of a given species among the taxa examined, yielding statistically comparable values. As mentioned above, the influence of layer I on the overall GNI values was biased by the poor conditions of the tissue in *T. truncatus* and *D. leucas* and did not allow for an extensive sampling of layer I in these two specimens. As a general observation, the GNI values in the cetacean species, regardless of cortical area or layer, vary between 2.6 in *D. leucas* to 13.2 in *P. macrocephalus* (see Table 3 for details). These values are extremely high compared to GNI values ranging between 0.56 and 1.65 reported in different cortical regions of primate species (O'Kusky and Colonnier, 1982; Dombrowski et al., 2001; Lidow and Song, 2001; Sherwood et al., 2006; Christensen et al., 2007). However, an increased number of glia per neuron in large brains was demonstrated in a limited number of species (Friede, 1954; Hawkins and Olszewski, 1957; Tower and Young, 1973). When choosing the strongest RMA regression within our sample as a predictive relationship between log brain weight and log GNI, the apparently high GNI of the brains of cetaceans is very close to the values expected for their brain size. It is important to note that this allometric relationship is based on the values of the cetacean GNI including layer I and, as such, these values are directly comparable to the values obtained in layers I-VI of the afrotherians and they are representative of the "real" GNI. Our results are in contrast with the view of an approximately constant GNI across species proposed by Herculano-Houzel and Lent (2005) and are in support of the hypothesis that the GNI values are not constant among mammals with different brain sizes and that such values show scaling against brain weight (Hawkins and Olszewski, 1957; Sherwood et al., 2006).

A limit of the present study was the small sample of species, if considering the whole mammalian phylogeny, and as such these results cannot be extrapolated to taxa beyond those investigated. The regression presented here is based on the values of two taxa (namely, Cetartiodactyla and Afrotheria) that differ greatly in respect to brain size and, as such, the regression line lacks points representative of species with an intermediate brain weight.

It is interesting to note that Sherwood et al., (2006) in an investigation of the primate GNI found a slope of 0.26 for the LS regression of log GNI against log brain weight based on a wide sample of anthropoid primate species and that Tower and Young (1973) reported a LS slope of 0.23 for the same regression in a heterogeneous sample of mammals including rat, rabbit, cat, cow, fin whale, and sperm whale. These values are very close to the slope of the LS and SMA regression in our sample (0.28 and 0.30, respectively). This is an indication of a similar trend of scaling of the GNI against brain weight in a wide sample of mammals. However, the intercept of the SMA regression reported above (Fig. 18) differs from the intercept found by Sherwood et al. (2006) providing evidence for differences in the two trajectories position and elevation. The present study, given the rarity of most of the species analyzed, was limited by the number of specimens available for a given species. Every GNI value was in fact the measurement of a single specimen for a given species (except in the case of the African elephant in which n = 3).

It is also worth noting that given the great variety of brain sizes that characterizes cetaceans, it is impossible to choose a group representative of the whole order. This is evident also in the high variance around the best-fit line in the SMA plot (Fig. 18). A larger sample size and independent contrast analysis to account for phylogenetic influences of the data presented here, will help elucidating the nature of the difference between the correlation here showed for Cetartiodactyla and Afrotheria and the correlation reported by (Sherwood et al., 2006) for primates.

Altogether our results indicate that the GNI values show a common scaling to brain mass among Cetartiodactyla and Afrotheria and that cetacean brains are characterized by the values of GNI that would be expected for their brain size. An important exception in the scaling pattern is represented by the pigmy hippopotamus (*H. liberiensis*) that shows a GNI higher than expected for its brain size (log GNI expected based on the SMA regression = 0.52; log GNI measured = 0.89). However, it is worth noting that *H. liberiensis* is the results of a process of dwarfism (Weston and Lister, 2009) that resulted in a body mass six to eight times smaller than the common hippopotamus (*Hippopotamus amphibius*) (Eltringham, 1999). The process of body size reduction in mammals is accompanied by a more limited reduction in brain size (Shea, 1983) that could have led to a smaller brain that retained some anatomical features (such as the GNI) of the larger brain it derived from. However, this remains a speculation and the evidence for *H. liberiensis* having a GNI much higher than what predicted is based on the measurement on a single specimen. A wider sample including more specimens and the possible comparison with other hippopotamidae, such as the larger *H. amphibius*, will help resolving the uncertainty around the value of GNI of *H. liberiensis*.

Another interesting fact is that the values of GNI in the three *L. africana* specimens in comparison to cetaceans with similar brain weight such as *O. orca* and *P. macrocephalus* are very similar and constantly lower than in *O. orca* and *P. macrocephalus*. This finding is however difficult to interpret because our GNI values are based on a single measurement and *L. africana* is the only terrestrial mammal with a brain size comparable to the cetaceans included in the present study, and the only other terrestrial mammal with a relatively large brain size (*H. liberiensis*) seems to be an outlier in the regression. Besides these exceptions, the observed regression suggests a general mammalian trend of scaling of GNI against brain weight that includes at least the species of cetaceans here analyzed. Cetaceans, as a group, do not appear to be outliers in GNI as previously proposed (Manger, 2006).

Several hypotheses have been formulated to explain the increase in glial cells number per neuron as the brain increases in size and this includes the phylogenetic position of the species analyzed (Friede, 1954), the size of the brain (Hawkins and Olszewski, 1957), the necessity to limit eat loss during Eocene-Oligocene ocean temperatures decrease (Manger, 2006), and the axonal length (Friede and Van Houten, 1962; Friede, 1963). This latter hypothesis is supported by evidence that the added glial volume in a large brain is proportionate to the added length of the axons that is necessary to maintain efficient connections at greater distances (Jehee and Murre, 2008), and by the evidence that the volume of white matter increases proportionally faster than the volume of gray matter as the brain size increases (Zhang and Sejnowski, 2000), as seen by imaging techniques in the human brain (Schoenemann et al., 2005). Thus the increase in neuron size, axonal length and witdth in larger brains is the necessary “adaptation” to reduce metabolic firing costs and increase the efficiency of action potential transmission (Wang et al., 2008). Moreover, neuronal energy metabolism depends heavily upon astrocytes. Astrocytes play a key role in “feeding” neurons, responding to neuronal activity mediated by the neurotransmitter glutamate with an increase in the consumption of glucose and production of lactate, the preferential oxidative substrate of neurons (Pellerin and Magistretti., 2004; Aubert et al., 2005; Magistretti, 2006; Magistretti and Allaman, 2007; Pellerin et al., 2007). As such, larger neurons would be energetically more expensive and longer axons would require more myelin to maintain an efficient action potential transmission, and this is consistent with the number of both astrocytes and oligodendrocytes per neuron increasing as the brain size (and thus the neuron size and the axonal lenght) increases.

However, it remains to be determined whether the increase in GNI value with brain weight observed in the analyzed sample of species , and more generally within the mammalian brain, is mostly due to the increase of a specific glial cell type or to an equal increase in the number of both astrocytes and oligodendrocytes. In the present study it was not possible to distinguish between astrocytes and oligodendrocytes given that the Nissl-stain in our materials did not allow for reliable distinction of the morphological features of the two cell types with a sufficient degree of precision.

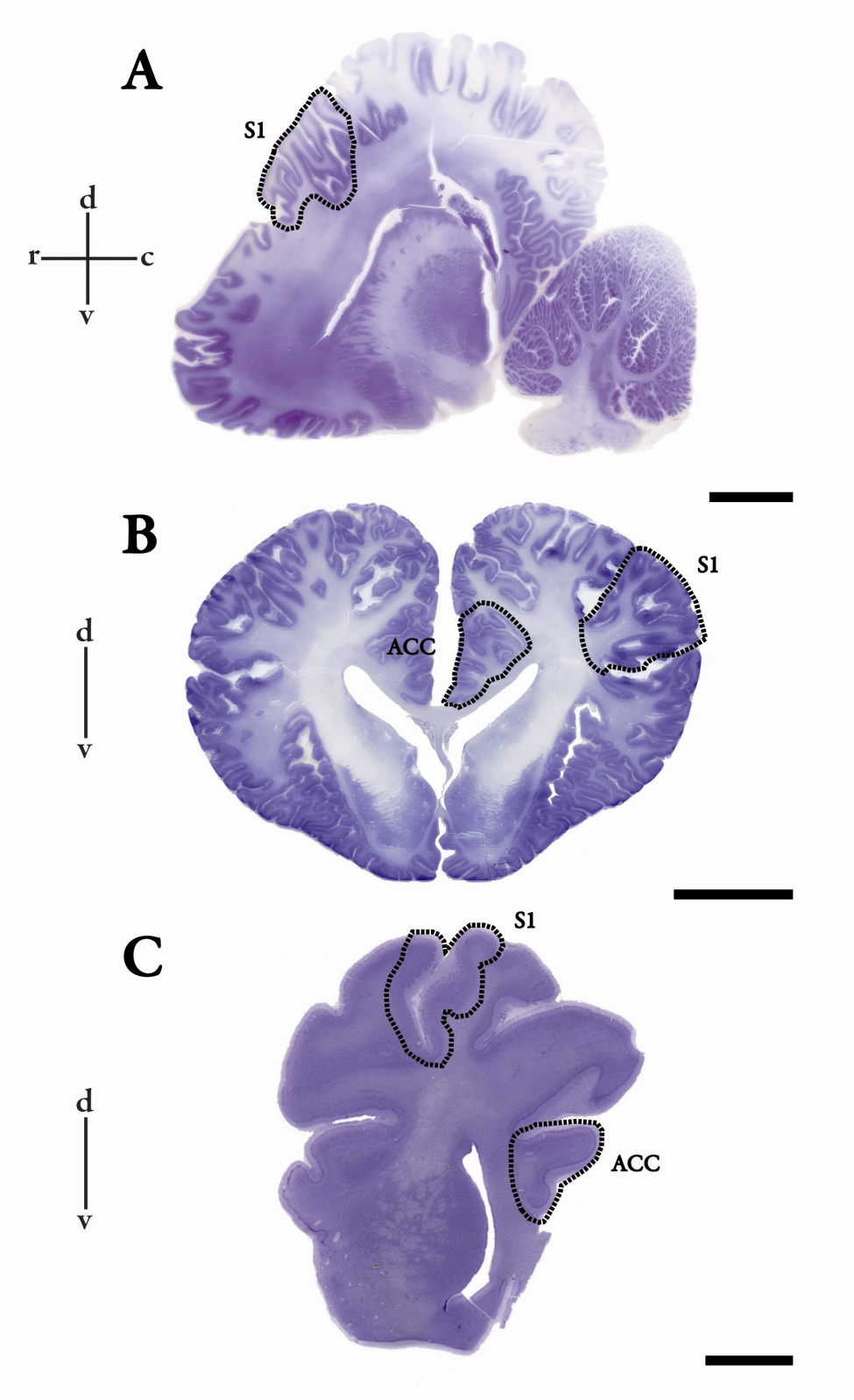

Figure 12. Maps showing the *location of the ROIs in sagittal (A) and coronal (B and C) sections of the brain of M. novaeangliae (A),* T. truncatus (B), *H. liberiensis* (C). The ROIs are outlined by a dotted line. ACC, anterior cingulate cortex; S1, primary somatosensory cortex. Scale bars =1 cm.

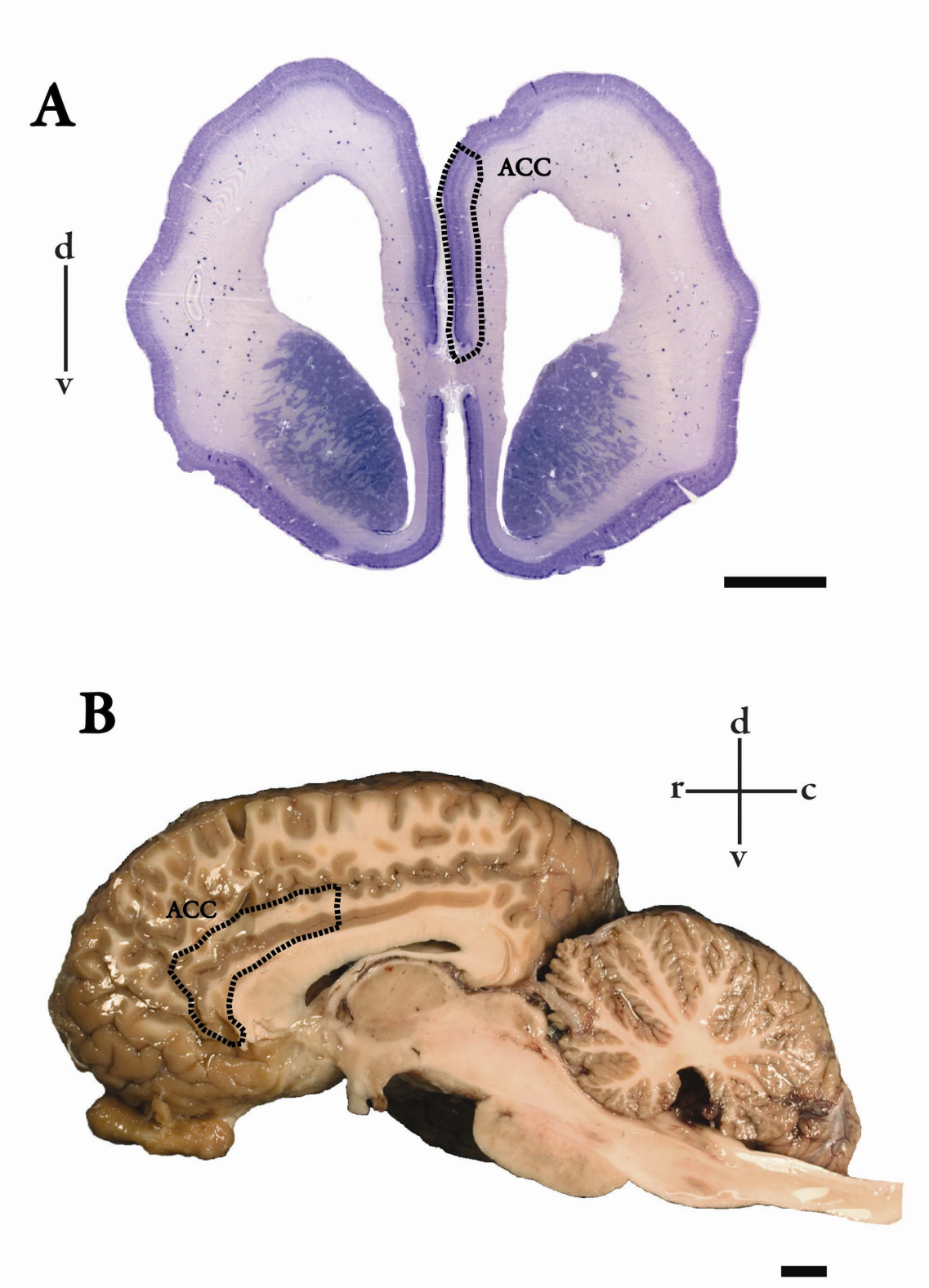

Figure 13. Maps showing the location of the ROIs in coronal (A) and sagittal (B) sections of the brain of *T. manatus latirostris* (A) and *L. africana* (B). The ROIs are outlined by a dotted line. ACC, anterior cingulate cortex; S1, primary somatosensory cortex. Scale bars=1 cm.

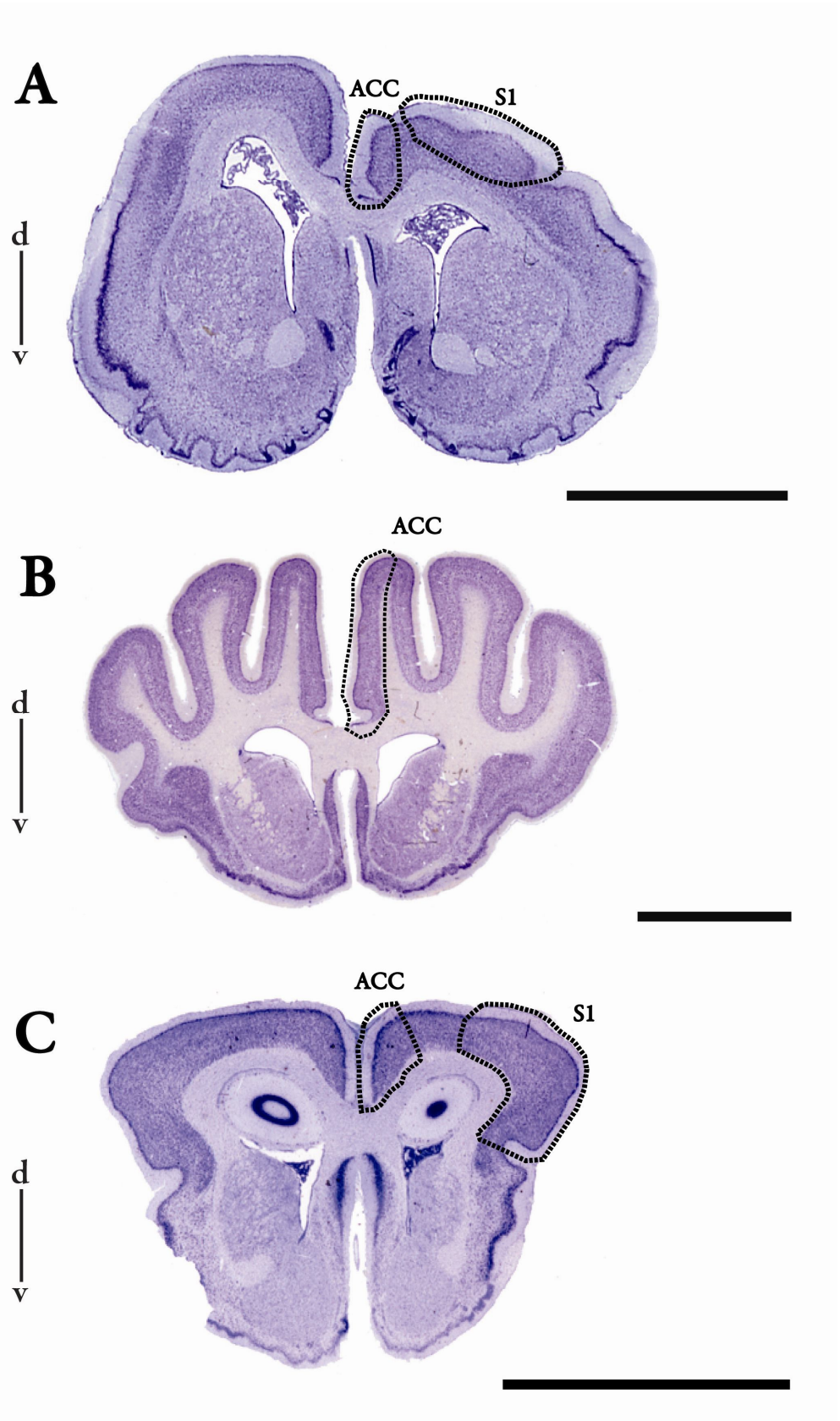

Figure 14. Maps showing the location of the ROIs in coronal sections of the brain of *H. semispinosus* (A), *P. capensis* (B), and *R. petersi* (C). The ROIs are outlined by a dotted line. ACC, anterior cingulate cortex; S1, primary somatosensory cortex. Scale bars=5 mm.

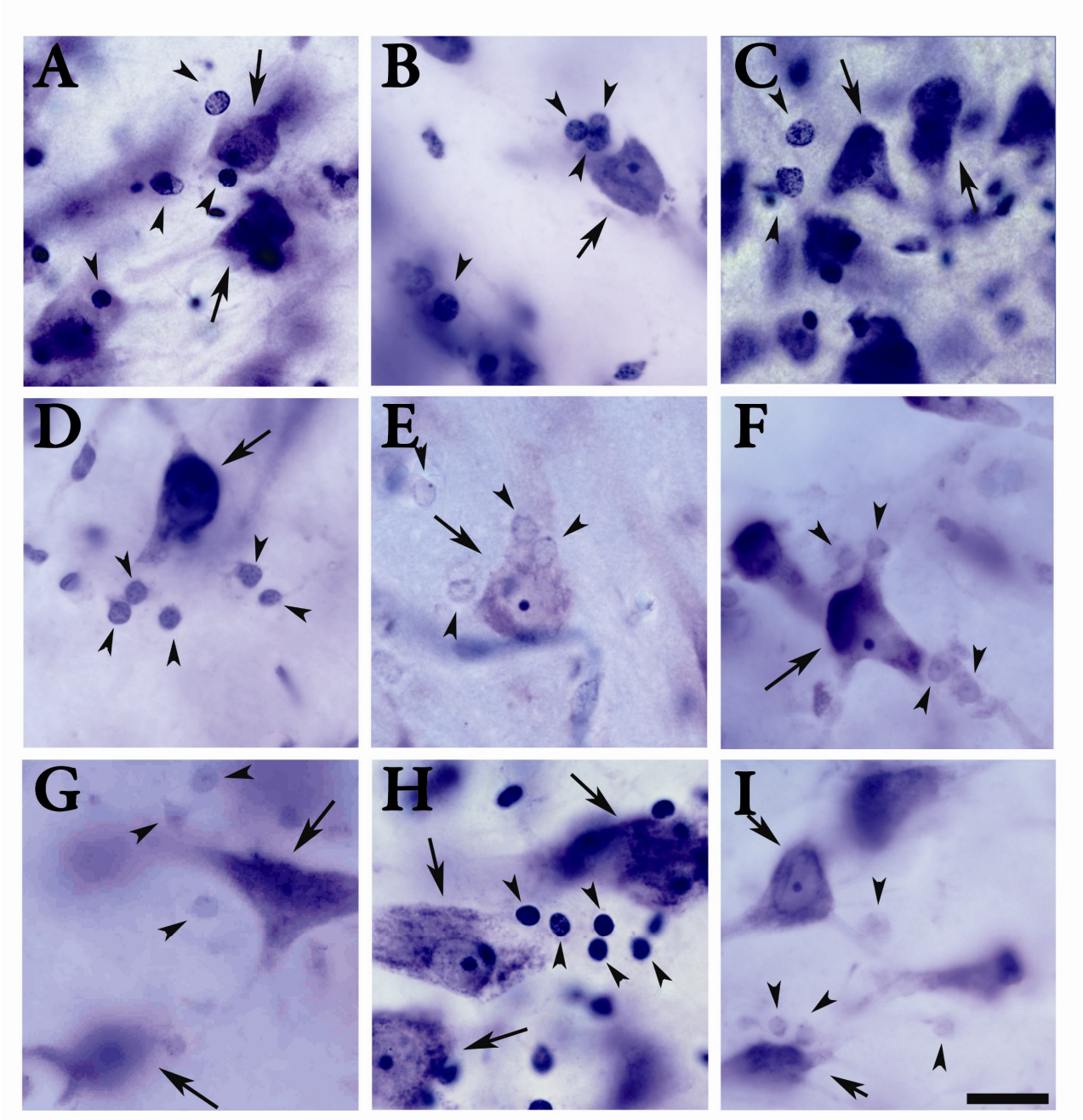

Figure 15. Microphotographs of Nissl-stained neurons and glia in the ACC of the cetaceans species examined in the present study. *T. truncatus* (A), *G. griseus* (B), *P. phocoena* (C), *K. simus* (D), *D. leucas* (E), *O. orca* (F), *P. macrocephalus* (G), *B. acutorostrata* (H), *M. novaeangliae* (I). Arrows indicate examples of neurons and arrowheads indicate examples of glial cells. Scale bar = 20 μm.

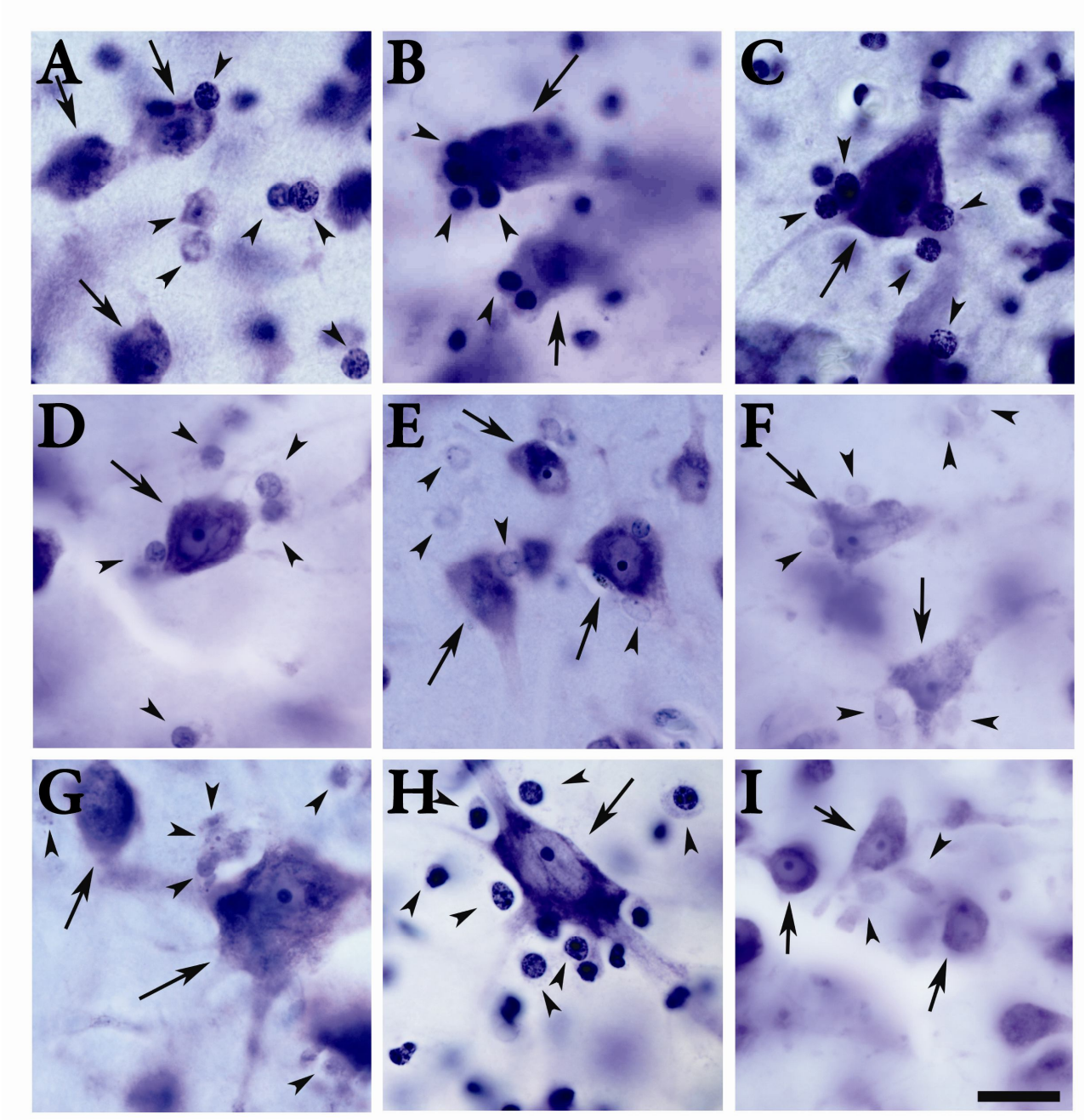

Figure 16. Microphotographs of Nissl-stained neurons and glia in the S1 of the cetaceans species examined in the present study. *T. truncatus* (A), *G. griseus* (B), *P. phocoena* (C), *K. simus* (D), *D. leucas* (E), *O. orca* (F), *P. macrocephalus* (G), *B. acutorostrata* (H), and *M. novaeangliae* (I). Scale bar = 20 μm.

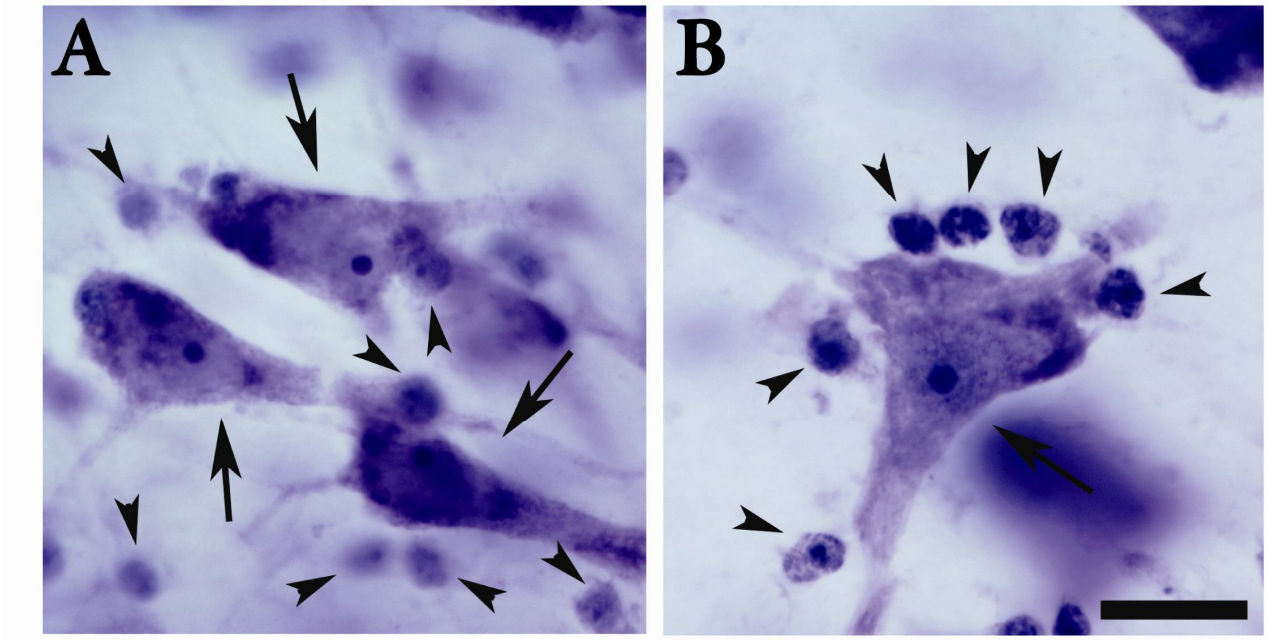

Figure 17. Microphotographs of Nissl-stained neurons and glia in the ACC of two of the Afrotherian species examined in the present study, *T. manatus latirostris* (A) and *L. africana* (B). Arrows indicate examples of neurons and arrowheads indicate examples of glial cells. Scale bar = 20 μm.

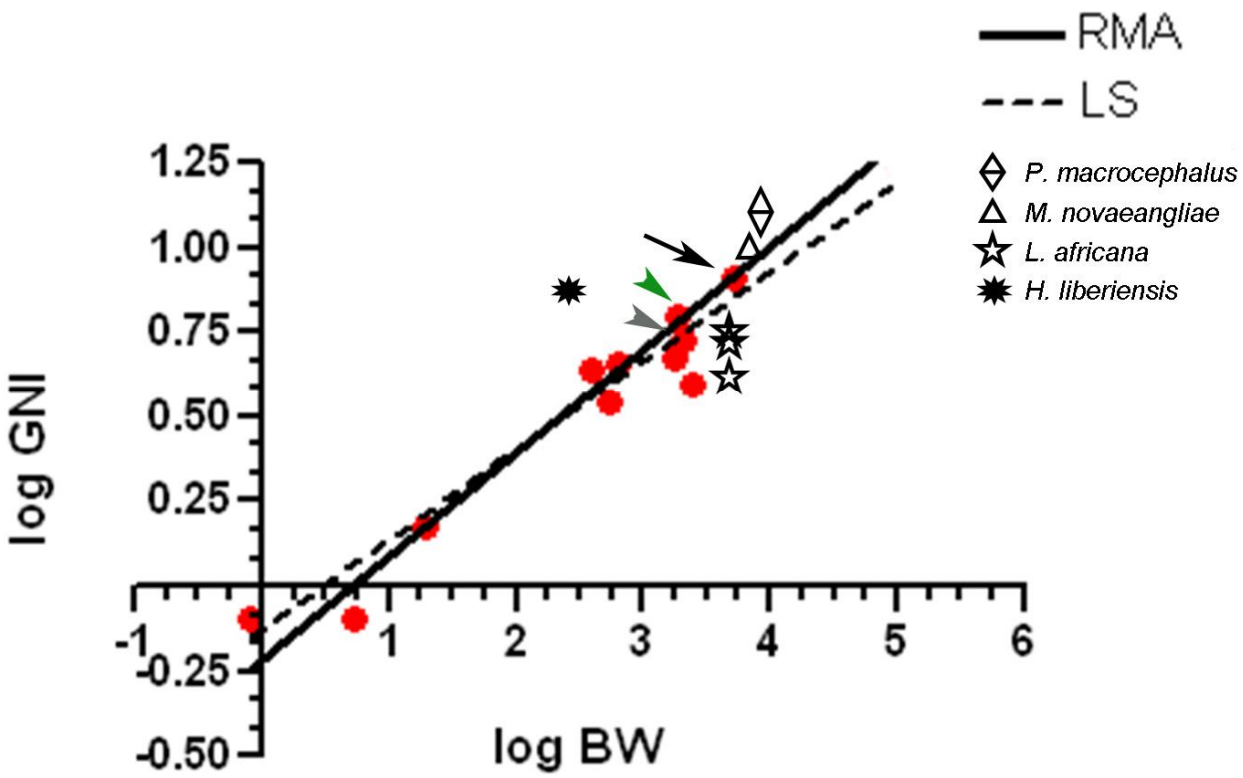

Figure 18. The allometric scaling of the glia-neuron index against brain weight in layers I-VI of the ACC in Cetartiodactyla and Afrotheria. A solid line represent the RMA regression (y = 0.3042x- 0.2131; r 2 = 0.830; p < 0.0001) and a dotted line represent the LS regression (y = 0.2771x – 0.139; r 2 = 0.8297; p < 0.0001) that are the best fit to the cetartiodactyl and afrotherian data. Note that because n = 1 in every species except for *L. africana* (n = 3) every data point in the graph represent the GNI measured in one specimen. The data point indicated by an arrow is *O. orca*, the cetacean with the brain weight closer to that of the elephant. Two arrowheads point to the value for *T. truncatus* (green) and *D. leucas* (gray).

Table 3. Brain weights and glia/neuron indexes for layers I-VI and II-VI in the ACC and S1. Brain weights are the average value for the species and taken from Marino et al. (2004a), Hof et al. (2005), and Eriksen and Pakkenberg (2007) for the cetaceans; from Manger (2009) for *L. africana*; from Bauchot and Stephan (1966) for *H. semispinosus*. The brain weight values of *H. liberiensis*, *T. manatus latirostris*, *P. capensis*, and *R. petersi* are measurements of our specimens (n = 1 for each species). The values of GNI of the 2 groups are the average values.

Species	n	Brain weight (g)	GNI ACC		GNI S1	
			Layers I-VI	Layers II-VI	Layers I-VI	Layers II-VI
T. truncatus	1	1,824	6.2	3.3	4.2	4.4
G. griseus	1	2,387	3.9	3	4.5	4.3
P. phocoena	1	540	3.5	3.3	5.6	5.3
D. leucas	1	2,083	5.3	4.3	2.6	2.6
K. simus	1	622	4.5	3.7	4.2	3.1
P. macrocephalus	1	8,028	13.2	12.1	11.4	7
O. orca	1	5,059	8.1	6.1	6.4	5.1
M. novaeangliae	1	6,411	10.6	9.7	9.8	8.1
B. acutorostrata	1	1,810	4.7	4.3	4.7	3.9
H. liberiensis	1	262	7.7	4.9	4.5	4.4
L. africana	3	5,000	4.65	-	-	-
T. manatus latirostris	2	384	4.35	3.95	-	-
P. capensis	1	19	1.5	-	-	-
H. semispinosus	1	0.8	0.8	-	1.1	-
R. petersi	1	5.4	0.8	-	0.7	-

Table 4. Summary of parameters used in the Optical Fractionator for the analysis of neuron and glia density in the ACC. If the parameters used in layers I-VI differ from the ones used in layers II-VI, the latter are reported in bold.

Parameters	Number of sections	Area of the unbiased counting frame (μm^2)		Sampling grid size (μm)	Guard zones (μm)	Disector height (μm)	CE (Schmitz-Hof) 2nd	
		N	G				N	G
T. truncatus	3	3600	400 **1225**	4000 x 2400	1	28	0.056 **0.057**	0.07 **0.051**
G. griseus #1	3	3600	400	1900 x 1300	1	36	0.026 **0.027**	0.041 **0.048**
P. phocoena	3	3600	1225	800 x 1300	1	28	0.057 **0.054**	0.046 **0.052**
D. leucas	4	4225	1225	1000 x 1400	1	20	0.072 **0.061**	0.078 **0.104**
K. simus	3	3600	400	600 x 800	1	32	0.037 **0.040**	0.053 **0.063**
P. macrocephalus	4	3600	400	1300 x 1200	1	36	0.067 **0.071**	0.057 **0.066**
O. orca	3	3600	400	1100 x 1200	1	34	0.051 **0.053**	0.054 **0.065**
M. novaeangliae	4	3600	400	1000 x 1200	1	30	0.045 **0.045**	0.041 **0.045**
B. acutorostrata	3	4225	1225	2500 x 1400	1	28	0.077 **0.069**	0.061 **0.063**
H. liberiensis	3	3600	400 **1225**	1300 x 800	1	32	0.057 **0.057**	0.064 **0.045**
L. africana#1	4	4225	1225	1600 x 1500	1	12	0.061 **0.064**	0.055 **0.062**
L. africana#2	2	10000	1600	920 x 920	2	8	0.097	0.11
L. africana#3	2	10000	1600	920 x 920	2	8	0.088	0.11
T. manatus latirostris #1	4	3600	400	600 x 1100	1	20	0.049 **0.050**	0.062 **0.062**
T. manatus latirostris #2	3	2500	1600	400x600	2	8	0.058 **0.059**	0.045 **0.053**
P. capensis	3	2500	1600	200x200	2	8	0.047	0.048
H. semispinosus	4	400	400	75x75	2	8	0.057	0.065
R. petersi	1	2500	1600	150x250	2	8	0.045	0.064

Table 5. Summary of parameters used in the Optical Fractionator for the analysis of neuron and glia density in the S1. If the parameters used in layers I-VI differ from the ones used in layers II-VI, the latter are reported in bold.

Parameters	Number of sections	Area of the unbiased counting frame (μm^2)		Sampling grid size (μm)	Guard zones (μm)	Disector height (μm)	CE (Schmitz-Hof) 2st	
		N	G				N	G
T. truncatus	3	3600	400	1700 x 700	1	28	0.043 **0.045**	0.064 **0.068**
G. griseus #2	4	3600	400	900 x 800	1	18	0.043 **0.043**	0.062 **0.064**
P. phocoena	3	3600	400	700 x 500	1	27	0.041 **0.045**	0.053 **0.060**
D. leucas	3	4225	1225	1600 x 1400	1	22	0.046 **0.046**	0.056 **0.055**
K. simus	3	3600	400	500 x 800	1	34	0.029 **0.031**	0.044 **0.053**
P. macrocephalus	3	4225	1225	1800 x 2200	1	30	0.063 **0.064**	0.038 **0.045**
O. orca	3	3600	1225	800x 1400	1	28	0.057 **0.058**	0.039 **0.044**
M. novaeangliae	3	4225	1225	2300 x 2000	1	28	0.062 **0.065**	0.039 **0.045**
B. acutorostrata	3	4225	1225	1200 x 2000	1	30	0.061 **0.065**	0.052 **0.062**
H. liberiensis	3	3600	400	1000 x 1100	1	34	0.046 **0.048**	0.065 **0.068**
H. semispinosus	5	400	400	100x100	2	8	0.060	0.058
R. petersi	3	2500	1600	500x300	2	8	0.049	0.074

Chapter 4

Von Economo neurons in the cetacean brain

Introduction

Von Economo neurons (VENs) have been proposed to subserve certain aspects of higher cognitive abilities in humans such as social and emotional cognition, awareness, and intuition (Allman et al., 2005). However, their specific morphology, uneven distribution, low numbers, and the fact that they send an axon subcortically suggests that they represent a neuronal specialization comparable to the Meynert or Betz cells of the visual and motor cortex.

VENs are large bipolar projection neurons located in layer V of the anterior cingulate cortex (ACC) and frontoinsular cortex (FI) that were observed in a few early classical human neuroanatomical studies (Betz, 1881; Ramón y Cajal, 1899), but their first detailed descriptions is attributable to Constantin Von Economo (1926). Recently, VENs have been discovered in great apes (Nimchinsky et al., 1995; Nimchinsky et al., 1999) where they are less abundant than in humans (Allman et al., 2005), and are larger than neighboring pyramidal neurons and fusiform cells (Nimchinsky et al., 1999). VENs are absent in monkeys and lesser apes, and besides hominids, they have been recently observed with a similar regional distribution in the humpback whale (*Megaptera novaeangliae*), the fin whale (*Balaenoptera physalus*), the sperm whale (*Physeter macrocephalus*), and the killer whale (*Orcinus orca*) (Hof and Van der Gucht, 2007). VEN-like large spindle neurons occur in the neocortex of the harbor porpoise (*Phocoena phocoena*; Behrmann, 1993) and were considered a variant of the largest pyramidal cells. VENs have also been observed in the homolog regions of the elephant brain (Hakeem et al., 2008).

Quantitative data on VENs in cetaceans, to complement studies in hominids and elephants, are lacking. Here I report the results of the examination of the brain of smaller odontocetes including the bottlenose dolphin (*Tursiops truncatus*), the Risso's dolphin (*Grampus griseus*), and the beluga whale (*Delphinapterus leucas*), as well as two humpback whales (*M. novaeangliae*) as a representative of the suborder Mysticeti, for comparative purposes, in view of a recent observation in the bottlenose dolphin showing that, contrary to a previous report (Hof and Van der Gucht, 2007), VENs appear to be also present in the ACC, FI, and frontopolar cortex (FPC) of small odontocetes (Hakeem et al., 2008). In these species and regions, I performed a quantitative study of the total number of VENs, their somatic volume in comparison to that of the neighboring layer V pyramidal neurons and layer VI fusiform neurons.

Materials and methods

Brain specimens and tissue processing

Five cetacean brains from specimens belonging to both toothed whales (Odontoceti, Delphinoidea: bottlenose dolphin, *T. truncatus*; Risso's dolphin, *G. griseus*; beluga whale, *D. leucas*) and baleen whales (Mysticeti, Balaenopteridae: humpback whale, *M. novaeangliae*) were examined in the present study (Fig. 19). In addition, the brain of a zebra (*Equus burchelli*), of a pigmy hippopotamus (*H. liberiensis*) and of a Florida manatee (*T. manatus latirostris*) were investigated for comparative purposes. The brains of *H. liberiensis* and *T. manatus latirostris* were also used in the cytoarchitectural study, and details on these specimens are reported in Chapter 2. The brain of *E. burchelli* belonged to the Yakovlev collection of the National Museum of Health and Medicine of Washington and was processed as described for *M. novaeangliae*. The brains of a captive juvenile male bottlenose dolphin (1.90 m beak-to-fluke notch length, 3 years old), and of a stranded adult female Risso's dolphin (2.90 m beak-to-fluke notch length, 18 years old) were collected at necropsy within 24 hours from death, postfixed and stored in 10% formalin for about 3 years at the Marine Mammals Tissue Bank of the University of Padova, Italy. Blocks of ACC from the left hemisphere and the right hemisphere, respectively, were collected, cryoprotected in graded sucrose solutions up to 30%, frozen in dry ice and cut into 80 µm-thick coronal sections with a sliding microtome (Leica Biosystems, Nussloch, Germany). The sections were then mounted on glass slides, Nissl-stained in a 0.2% cresyl violet solution and coverslipped in 70% DPX in xylene for examination. The brain of a female humpback whale (13.7 m beak-to-fluke notch length) was collected after stranding and postfixed in 10% formalin. Blocks containing the left ACC and the left anterior insula were collected and cut into serials 3 cm-thick slabs. These slabs were then processed as for the bottlenose dolphin's blocks. Blocks from the right ACC and AI of a beluga whale and the whole right hemisphere of the brain of a stranded adult female humpback whale (13.8 m beak-to-fluke notch length) were dehydrated in graded alcohol solutions up to 30%, embedded in celloidin and processed serially at 35 µm on a modified large specimen microtome (Jacobs et al., 1971, 1979, 1984). The hemisphere of the humpback whale was cut in the sagittal plane relative to the beak-fluke axis while the blocks from the beluga brain were cut into the coronal plane and series of adjacent sections were selected for the quantitative analysis. Sections were stained alternatively for Nissl substance with the Bielchowsky-Plien cresyl violet method or for myelin with the Loyez-Weigert method (Bertrand, 1930). The sections were then mounted on glass slides and coverslipped in clarite for examination. The brains of the two humpbacks and of the beluga whale were collected in the 1960s and kept in fixative for an unknown amount of time. Information on the postmortem interval was also not available for these three specimens. Unfortunately, we were not able to examine all the regions of interest (ROIs) in every species owing to the availability of the materials. In some cases, part of, or a whole ROI were not collected or had been used by other investigators and thus were not available for the present study. Finally, because the brains of the specimens investigated in the present study were collected from different sources and information on the specific brain and body weight were not available, average values from the literature for each of these species are provided in Table 6.

Stereologic design

For stereologic quantification we selected every 10^{th} section from the bottlenose dolphin, Risso's dolphin and the beluga whale and every 20^{th} section from the humpback whale, in view of the larger size of the humpback whale brain compared to the smaller odontocetes. Moreover, in the four examined species, VENs were found to be distributed beyond the FI into the whole anterior

part of the insula (Hof and Van der Gucht, 2007). Thus, when referring to VENs distribution in the cetacean insula, we use the term “anterior insula” (AI) instead of “frontoinsular cortex” (FI).

All the quantitative analysis were performed on a stereology workstation equipped with a Zeiss Axiophot photomicroscope, Plan-Neofluar objectives 2.5x (N.A. = 0.075), 40x (N.A. = 0.75), 40x LD (N.A. = 0.6) and Plan Apochromat objectives 10x (N.A. = 0.32), 20x (N.A. = 0.8) (Zeiss, Thornwood, NY, USA), a motorized stage (Ludl Electronics, Hawthorne, NY, USA), an Optronics MicroFire digital camera (Optronics, Goleta, CA, USA) and a stereology software (StereoInvestigator, MBF Bioscience, Williston, VT, USA). Starting with a random section number, a systematic sampling (every 10^{th} or 20^{th} Nissl-stained sections depending on the specimen) throughout the ROIs was performed. The boundaries of the ROIs in each section were traced at low magnification (2.5x) on the computer display. The whole cortical thickness was included in the traced area. Within the cortical ROIs, additional subregions, including exclusively layers III and V were traced separately.

Total VENs numbers were estimated, within each subregion’s contour, using the Optical Fractionator (West et al., 1991). However, the relatively small number of VENs and their peculiar distribution in clusters required that to ensure every VEN to have an equal probability of being counted we perform an exhaustive count. To achieve this, the dimension of the sampling grid was set equal to the dimension of the counting frame. To prevent bias due to an uneven surface of the section or to the loss of nucleoli during the cutting procedure, guard zones at the top and at the bottom of the section were established. The size of the guard zones was set to allow the disector height to sample at least 80% of the tissue thickness as measured after processing. All stereologic parameters were set after taking into account the degree of shrinkage caused by histological processing (approximately 60% in our specimens, see below). Details on the stereologic parameters used for Optical Fractionator analyses of VENs number are summarized in Table 7.

The typical VEN morphology is showed in comparison to that of pyramidal and fusiform neurons in Figure 20. Neurons were identified as VENs in Nissl-stained sections if they were present either in deep layer III or in layer V of the ACC, AI, and FP and displayed the morphological features presented in Figure 21. The nucleolus was used as the counting reference and VENs were counted when the nucleolus came into focus inside the counting frame within the disector height. Only the VENs that had their nucleolus totally or partially inside the counting frame and not crossing the exclusion lines of the frame were counted.

The total number of neurons of the available areas containing VENs was assessed in each species using the Optical Fractionator for estimation of the VENs fraction of the total neuronal population. The software defined a systematic-random sampling sequence of frames within the outlines of the ROIs, in which neurons were quantified. Due to differences in the processing protocols and in the size of the regions of interest between specimens the parameters set for the total neurons quantification changed between animals, as every animal was considered separately. The dimensions of the sampling grid were set to sample at least 200-300 neurons per specimen and the disector height was selected to sample at least 80% of the section thickness. Guard zones of 1 μm were used on the top and on the bottom of every section. Details on the stereologic parameters used for the Optical Fractionator in estimating total neuron numbers are summarized in Table 8. Neurons (including pyramidal cells and interneurons) were counted using the same inclusion criteria as described above for VENs if they had pale nuclei, dark and recognizable nucleoli, and a relatively large soma size.

Changes in tissue volume due to histological processing are a potential source of bias for estimates of the cell volume which depend on the fixation and embedding protocol used (Schmitz and Hof, 2005). When studying cetacean brains, the use of standardized protocols is difficult owing to the nature and rarity of the specimens. In fact, several brain specimens came from histological collections established decades ago, others from captive animals, and others from stranding events, making it nearly impossible to obtain brains processed under identical conditions.

In the present study I attended to such potential sources of bias as follows. The shrinkage in the z-direction was compensated for all the specimens examined by measuring systematically the thickness of the sections at selected intervals. Although I could minimize the shrinkage in the x-y direction in the brain of one of the humpback whales, the bottlenose dolphin, and the Risso's dolphin by ensuring that the sections were mounted soon after cutting and before staining (Schmitz et al., 2002), I had no control on the processing of the brain tissue of the beluga whale and of the second humpback whale, that were embedded in celloidin, an embedding medium that considerably increases the shrinkage of the tissue. However, Schmitz et al. (2000) showed that the total number of pyramidal cells obtained in methacrylate-embedded sections versus cryostat sections in the mouse hippocampus were comparable. It should also be noted that the Optical Fractionator does not rely on the calculation of an estimate of an actual volume of reference, and as such our number estimates are not affected by differential shrinkage.

The volume of every counted VEN was assessed using the Optical Rotator (Tandrup et al., 1997), a stereologic three-dimensional local estimator of volume that samples focal planes through the central region of a cell thereby avoiding problems with the identification of its top and bottom borders. For limitations due to the nature of the preparations, the volume of VENs in one of the humpback whale could not be measured with a sufficient degree of precision using the Optical Rotator. The brain sections of this specimen were coverslipped with thick coverglass and did not allowed a sharp image of each focal plane throughout the thickness of the section as required by the Optical Rotator. Assuming that intraspecific differences in the volume of VENs would not to be found, we investigated sections from only one humpback whale to assess the average volume of VENs in this species. The thin coverslips used on the histological sections of the brain of this specimen allowed the measurement of the VENs volume using the Optical Rotator. Details on the stereologic parameters used for the Optical Rotator are summarized in Table 9.

Moreover, as the major histological collections of human, apes and cetacean tissue are embedded in celloidin and coverslipped with thick coverglass, I considered it important to define the degree of over- or underestimation of the VENs volume caused by a probe that can be used in such materials, such as the Nucleator (Gundersen, 1988). The Nucleator is a two dimensional local probe that measures the cross-sectional area of a particle in only one focal plane and assumes uniformity in all directions. However, VENs are not isotropic and any estimate obtained using the Nucleator will inevitably be inaccurate. I investigated sections from the celloidin-embedded humpback whale brain using a six-rays Nucleator and compared the VENs volume estimates with the values obtained for the other humpback whale using the Optical Rotator. Again, I assumed that there are no differences in VENs volume within the same specie. The average VENs body volume assessed with the Optical Rotator was 6,188 ± 948 μm^3, and the average value assessed with the Nucleator in the other specimen was 5,870 ± 1,311 μm^3, yielding an overall underestimation of about 5% using the Nucleator in these celloidin-embedded sections. However, this difference also reflects the possible degree of shrinkage that different histological protocols (in this case dehydration and celloidin-embedding versus freezing of formalin postfixed materials) may cause. The difference in cell volume estimates being rather small, based on my results, the use of one probe or the other should not significantly bias the average measured volume. However, to address the potential bias when comparing volume estimates obtained in specimens prepared using different histological protocols I decided to express the VEN volume as a "VEN volume index" given by the ratio of the average VEN volume to the average pyramidal cell volume in each specimen. In this way, volume estimates provide values unaffected by shrinkage artifacts. Using the same stereological procedures, I estimated the individual volumes of a smaller sample of pyramidal neurons in layer V and of smaller fusiform neurons in layer VI (approximately 100 for each cell type in every specimen, for comparison with VEN volumes). Details on the stereologic parameters used for the Optical Rotator in each cell type are summarized in Table 9. Quantitative and volumetric estimates of VENs, pyramidal, and fusiform neurons were made using the 40x

(N.A. = 0.75) or the 40x LD (N.A. = 0.6) objectives, depending on the quality of the histological preparations. VENs densities were not calculated given their uneven and clustered distribution in all regions, which prevents the elaboration of meaningful and reliable density estimates.

Photomicrographs were edited for brightness and contrast using Adobe Photoshop. Maps of VENs distribution were imported and graphically adjusted in Adobe Illustrator.

Statistical analysis

Total VEN numbers were obtained in only one specimen per species and, as a consequence, statistical analysis was not possible to perform. The Levene test was used to define whether the variances were homogeneous within the volumetric measurements. Because the volume of every counted VEN was measured but volumetric data of the pyramidal and fusiform cells was based on a sample of 100 neurons, I had to normalize group sizes. To achieve this, the interquartile range was calculated within every neuron type dataset and the measurements falling outside this range were excluded from the analysis. Within the sets of data falling between the first quartile (Q1) and the third quartile (Q3) I randomly chose a sample of 50 measurements (lists were randomized by random.org and the first 50 values from the lists were chosen) that was used for further analysis. I used the non-parametric Kruskal-Wallis analysis of variance and Dunn's post-hoc tests to determine whether there were significant differences in volume among VENs, pyramidal, and fusiform neurons among and within species. To investigate possible correlation between the VENs volume, brain weight, body weight, and EQ, I used the non-parametric Spearman's correlation test. EQ data were obtained from Marino (1998), Marino et al. (2004), and Hof et al. (2005).

Results

Quantitative analysis

VENs were observed in all of the examined species and regions. Their morphology was easily distinguishable and they were present in layer V and deep layer III (Fig. 22). As previously reported in the humpback whale (Hof and Van der Gucht, 2007), VENs predominantly assemble in small clusters, generally of 3 to 5 cells, near the crown of the gyri in the ACC, AI, and FPC, whereas more scattered VENs are observed along sulcal banks (Figs 22-28). The majority of the VENs had a stout cell body with straight and long apical and basal dendrites departing from the soma (Fig. 21D-F, I-L). However, a few VENs were extremely slender with very long apical and basal dendrites almost as thick as the cell body (Fig. 21B, C, H). Others had an elongate cell body with thin and curly basal and apical dendrites (Fig. 21A). Occasionally, I observed cells with the basal dendrite divided into two branches (Fig. 21G). These morphologies were observed in all of the investigated species and cortical regions.

The number of VENs in the regions of interest was expressed as a percent of VENs from the estimated total number of neurons in that region and species (Table 10). Unfortunately, due to the availability of the materials, not all of the ROIs could be investigated in every species and the comparison of VENs quantitative data are based only on the available regions. Also, it should be noted that the number of sampled neurons, and thus the estimated total numbers, do not represent exhaustive counts for the entire ROIs considered except in the case of *M. novaeangliae*.

A comparison of VENs number among species was possible only on the basis of my findings in the ACC, the only region available for all the four species examined. Within the ACC the highest number of VENs was observed in the humpback whale, while the quantitative data of bottlenose dolphin, Risso's dolphin and beluga whale were fairly comparable and yielded lower values (Fig. 31B). Comparisons among ROIs were possible only for the humpback whale for which all the three regions were available (Table 10). The numbers of VENs in the ROIs were in this case comparable among the three regions (Fig. 31C). Overall the percent of VENs from the

estimated total neuron numbers was consistently low across species and varied from 0.01 to 0.06% depending on the region. Interestingly, among all the regions and species the insular cortex of the beluga whale showed the highest percent of VENs from the total neuronal population estimated for the species in this specific region of interest (Table 10). However, the observed higher percent of VENs is not due to a major increase in total VENs number in this species but rather to a lower total number of neurons.

Volumetric estimates show that similarly to humans and great apes (Nimchinsky et al., 1999), the volume of VENs in cetaceans is larger than that of layer V pyramidal neurons and considerably larger than layer VI fusiform neurons (Table 11). Specifically, within the present specimens, VENs were found to be 8-43% larger than pyramidal neurons of layer V, and 54-73% larger than fusiform neurons of layer VI, depending on the species. Volume estimates, expressed as "VEN index" (ratio between the average volume of VEN and the average volume of pyramidal neurons for each species), indicate that, within the studied species, the largest index was found in the humpback whale followed by the bottlenose dolphin, the beluga whale, and the Risso's dolphin with very close indices (Fig. 31A). Because the average variation in pyramidal cell somatic size among species is only 14% we consider the variation in indices to reflect differences in the volume of VENs. In this view, as expected, my results show that the larger VENs belong to the humpback whale while the volume estimates of VENs of the three odontocete species are fairly comparable. The somatic volume of VENs was found to be significantly different among species for all comparisons ($p < 0.001$), except for the Risso's dolphin and beluga whale. Moreover all differences in volume among neuron types within any of the species were found to be significant ($p < 0.001$), except for between VENs and pyramidal cell volumes in the Risso's dolphin which had smaller VENs compared to other species (Table 11). In contrast to what had been reported in great apes (Nimchinsky et al, 1999), the raw VENs volumes did not, in the present sample, show any significant correlation with the brain weight, body weight, or EQ (see Table 6; Spearman's rank order correlation: $r = 0.20$, $P = 0.91$; $r = 0.40$, $P = 0.75$; $r = -0.40$, $P = 0.75$, respectively).

VENs in other species

In the attempt to understand the selective pressures that may have driven the convergent evolution of VENs in phylogenetically distantly related taxa, such as primates, cetaceans, and elephants and to shed some light on the possible significance of the restricted and specific cortical distribution of VENs in the cetacean cerebral cortex, I carefully examined the brain of species either phylogenetically related to cetaceans, such as the pigmy hippopotamus, *Hexaprotodon liberiensis* (Cetartiodactyla: Hippopotamidae); possessing a large brain such as the zebra, *Equus burchelli* (Perissodactyla: Equidae) or sharing the adaptation to the aquatic environment with cetacans such as the Florida manatee, *Trichecus manatus latirostris*, (Sirenia, Trichechidae).

Interestingly the cerebral cortex of these three mammals is characterized by the presence of VEN-like cells but with a distribution that differs extremely from the selective presence in the ACC, FI and FPC (or dlPFC) in great apes, elephants and cetaceans. Particularly, in the cerebral cortex of the pigmy hippopotamus and of the zebra, VEN-like cells are sparse and abundant throughout the cortex with a laminar distribution that is still restricted to layer V. The cerebral cortex of the Florida manatee, on the other hand, is characterized by extremely rare and sparse VEN-like cells.

This phylogenetical distribution suggests that, as previously hypothesized by Hof and Van der Gucht (2007), VENs evolved several times in evolution in brains of a certain size and complexity, possibly to rely fast processing of information between distant cortical regions. However, the presence of VEN-like cells and their pattern of distribution in the closest relative of cetaceans, the pigmy hippopotamus, indicates that a process of refinement of distribution (which translate into a refinement of projection) of the VENs took place during the evolution of the cetaceans from the common ancestor that they share with the hippopotamuses. Even though there

is no direct evidence of the significance of this process, I can infer some explanation considering the functions related to the cortical areas where the VENs are concentrated. It looks like the VENs pattern of distribution changed from a general distribution in every sensory area of the cortex whithout prioritizing any particular function, to a distribution in which the priority is given to the functions underlined by the ACC, FI, and FPC (or dlPFC). Table 12 shows the list of the species (from the present study and literature) in which VENs were observed up to date and their distribution and frequency.

Discussion

The occurrence of VENs in all of the cetacean species analyzed is striking. The predominant distribution of VENs in clusters and their regional distribution pattern comparable to that seen in humans and great apes makes their presence in the cetacean brain a particularly interesting neuroanatomical feature from an evolutionary perspective. In light of the phylogenetic distance between hominids and cetaceans and the absence of VENs in the other species analyzed so far, VENs can be considered to be the product of a process of convergent evolution rather than the product of postnatal mechanical factors that would have affected the morphology and distribution of relatively few neurons in a restricted cortical domains, particularly in locations subject to bending stresses such as the crown of gyri.

Taken together with the finding of the presence of VENs in three small odontocetes, the recent discovery of VENs in both the African elephant (*Loxodonta africana*) and the Indian elephant (*Elephas maximus*) (Hakeem et al., 2008), provide support to the concept that VENs may represent a possible obligatory neuronal adaptation in very large brains permitting fast information processing and transfer along highly specific projections and that evolved in relation to emerging social behaviors in select groups of mammals. Cetaceans form complex societies in which individuals relate to each other depending on their hierarchical position, they have been reported to create nested alliances, to use tools, to be able to learn symbolic artificial languages, and, like elephants, to show self-awareness as demonstrated by tests of mirror self- recognition (Reiss and Marino, 2001).

VENs have been proposed to play a key role in the organization of the connectivity in cognition-related networks in large brains (Allman et al., 2002, 2005). The presence of VENs in the ACC, AI, and FP of the cetacean brain is not a direct demonstration of high-level cognition, but it is consistent with the existence in these species of complex cognitive abilities, and hints at a neuronal specialization that may underlie their expression. It is interesting, in this light, to point out that cetaceans and primates possess the highest levels of encephalization among vertebrates with EQ values of 7.0 for modern humans, between 1.5 and 3.0 for great apes, and of 4.5 for some odontocetes species, placing cetaceans second to humans with EQs considerably higher than any other mammal (Marino, 1998; Marino et al., 2004a). In great apes, the somatic volume of VENs was shown to be highly correlated with brain volume residuals (Nimchinsky et al., 1999). The present data show that VENs volume is not correlated with brain weight, body weight, or EQ. This lack of correlation may reflect not only the small sample size of four species, three of which being very close in terms of brain size, to which our study was limited to, but also the fact that mysticetes are not particularly encephalized owing to their large body size (Marino et al., 2004). If a correlation of VENs volume with any of these parameters were observed, it would be more likely among the smaller odontocetes, assuming that VENs occur in all or most of these species. Moreover, the fact that in the humpback whale, VENs, but not pyramidal nor fusiform cells, are considerably larger than the same cell types in the examined odontocetes, supports the possibility that a relationship between body size and VENs size exists. The present study was limited in this respect to three delphinoid taxa and a more extensive sample of cetacean species to allow for a more complete representation of brain size variability, especially among the smaller bodied

odontocetes, will be necessary to determine whether VEN volume is correlated with any of these parameters.

VENs are 42-79% larger than pyramidal neurons of layer V and 75-92% larger than fusiform cells of layer VI in great apes, depending on the species (Nimchinsky et al., 1999). The present results show that, even if the difference in somatic volume among neuronal types is statistically significant within a given species, the magnitude of this difference is less pronounced in cetaceans than in primates. Neuron size (and thus axon length and width) increases as a consequence of brain size increase. There is in fact evidence showing that in large brains the need to reduce metabolic firing costs and transmissions delays is prioritized over limiting an increase in neuronal size (Wang et al., 2008). However, there may be rules acting on the optimization of the conduction that constrain the maximum size and length axons can achieve thus inevitably influencing the somatic size of a particular neuron. It could be that in the case of cetaceans, the increase in brain size could not be followed by the expected increase in VENs volume in order to keep the optimal efficiency of VENs conduction thus explaining the less pronounced difference in somatic volume among neuronal types observed in these species compared to hominids.

Considering that for the three odontocetes, the blocks I analyzed included only a portion of the ROI, and therefore doubtless represent underestimates, whereas for the humpback whale we had access to the entire structure, I can use the latter to make comparison of absolute numbers of VENs between cetaceans and data available for humans, great apes, and elephants. The present results show that the absolute number of VENs in the humpback whale, at least in the AI, is fairly comparable to other species in which the FI was analyzed (for data on hominids and elephants VENs, see Hakeem et al., 2008, Kaufman et al., 2008, and Allman et al., in preparation). In fact, there are overall twice as many VENs in the humpback whale FI/AI than in the Western lowland gorilla and elephant, comparable numbers as in newborn humans and chimpanzees, but 2.5 times fewer than in human adults (Hakeem et al., 2008; Kaufman et al., 2008; Allman et al., in press). It should be however kept in mind that VENs are present not only in the FI but also in the AI in the humpback whale, in contrast to hominids and elephants where they are mostly concentrated within FI, revealing a notable variant in the distribution of VENs among these three mammalian groups. The low percent of VENs in the humpback whale compared to hominids and elephants is thus mainly due to the much higher number of total neurons, and much larger AI in the whale.

VENs send an axon out of the cerebral cortex, based on observations in postmortem human brain after DiI labeling (Nimchinsky et al., 1995), but there is no direct evidence about their functional role due to the fact that the species in which they occur make it impossible to use invasive approaches. The ACC and FI (and more generally the AI) are connected to the prefrontal and orbitofrontal cortices in macaque monkeys (Cavada et al., 2000; Öngür and Price, 2000). The evidence that VENs send axons in the subcortical white matter in humans (Nimchinsky et al., 1999; Allman et al., 2005; Watson et al., 2006) and their selective presence in these reciprocally linked region of the cortex suggest that they may connect ACC and FI/AI (Craig, 2008). Also, as shown by human fMRI studies, the regions containing VENs are involved in high-level cognitive processing such as feelings of empathy (Singer et al., 2004), guilt (Shin et al., 2000), embarrassment (Berthoz et al., 2002), pain (Craig et al., 1996; Rainville et al., 1997), as well as judgement, social knowledge and consciousness of visceral feelings (Craig, 2003; 2004). Interestingly in this context, neuropathological investigations in brains from patients with frontotemporal dementia, a disorder that disrupts several aspects of social functioning and self-awareness, have revealed a 74% reduction in VENs number. In these cases, many of the remaining VENs displayed severe morphologic alterations and abnormal accumulation of pathologic proteins (Seeley et al., 2006, 2007). In addition, their localization in layer V is suggestive of projections to subcortical regions such as the amygdala, hypothalamus, and periaqueductal grey to which the ACC and FI/AI are known to project in primates (Nimchinsky et al., 1999; Barbas et al., 2003; Hof and Van der Gucht, 2007). Altogether, VENs may be involved in the integration of emotions,

vocalization control, facial expression, or social conduct as well as regulation of autonomic visceral, olfactory, and gustatory functions. Moreover, the evidence that VENs do project subcortically, even though their final targets are still unknown, their uneven and specifical regional and laminar distribution, as well as their large size, reminds of other two specialized cell model, the Meynert and Betz cells in the visual and motor cortex, respectively (Hof et al., 2000b; Rivara et al., 2003). The interconnection of ACC, AI and FPC and the selective presence of VENs in these three regions could be the anatomical substrate for the transmission of fast informations along networks implicated in the emotional response to external stimuli and generation of goal-directed behaviors in large mammals. In conclusion, the specific distribution of VENs in the ACC, AI, and dlPFC (FPC in the case of cetaceans) of all of the species in which VENs have been described to date, suggests that, in large brains, these regions of the cortex (and their specific networks) were shaped by comparable selective pressures of which the VENs may be the evolutionary outcome. In the specific case of cetaceans, the presence of VENs in selected areas of the brain in both cetacean suborders may be the anatomical basis for the observed behavioral cognitive convergences that, despite a long phylogenetic divergence, are widely recognized to be shared by primates and cetaceans. Moreover, given their selective vulnerability, the study of the evolution of VENs, of their functional role and connectivity is necessary to further our understanding of the evolution of neocortical circuits that, when disrupted in human-specific neuropsychiatric illnesses, are responsible for the impairment of social and cognitive skills.

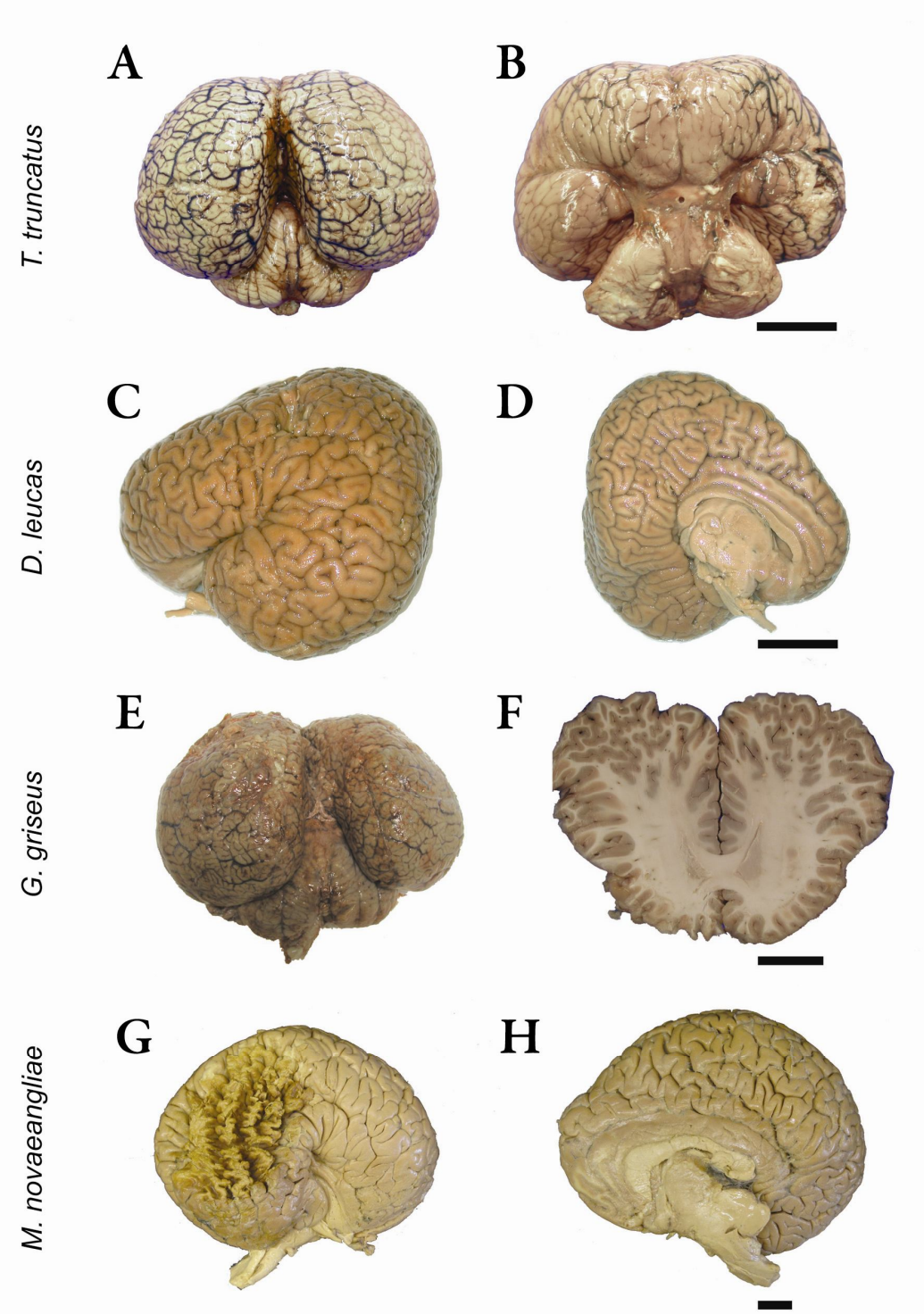

Figure 19. Macroscopic views of the brains of the cetacean species analyzed in the present study. Dorsal (A) and ventral (B) views of the brain of a bottlenose dolphin; lateral (C) and midline (D) views of the right hemisphere of the brain of a beluga whale; dorsal view (E) and coronal slab at the level of the genu of the corpus callosum (F) of the brain of a Risso's dolphin; lateral (G) and midline view (H) of the right hemisphere of the brain of a humpback whale. Note the large size of the brains and the complex gyral pattern. The lateral aspect of the parietal lobe of the humpback whale brain sustained damage at the time the specimen was removed from the skull (G). This however did not affect the present study. The brains are not shown to scale. Scale bars = 3 cm.

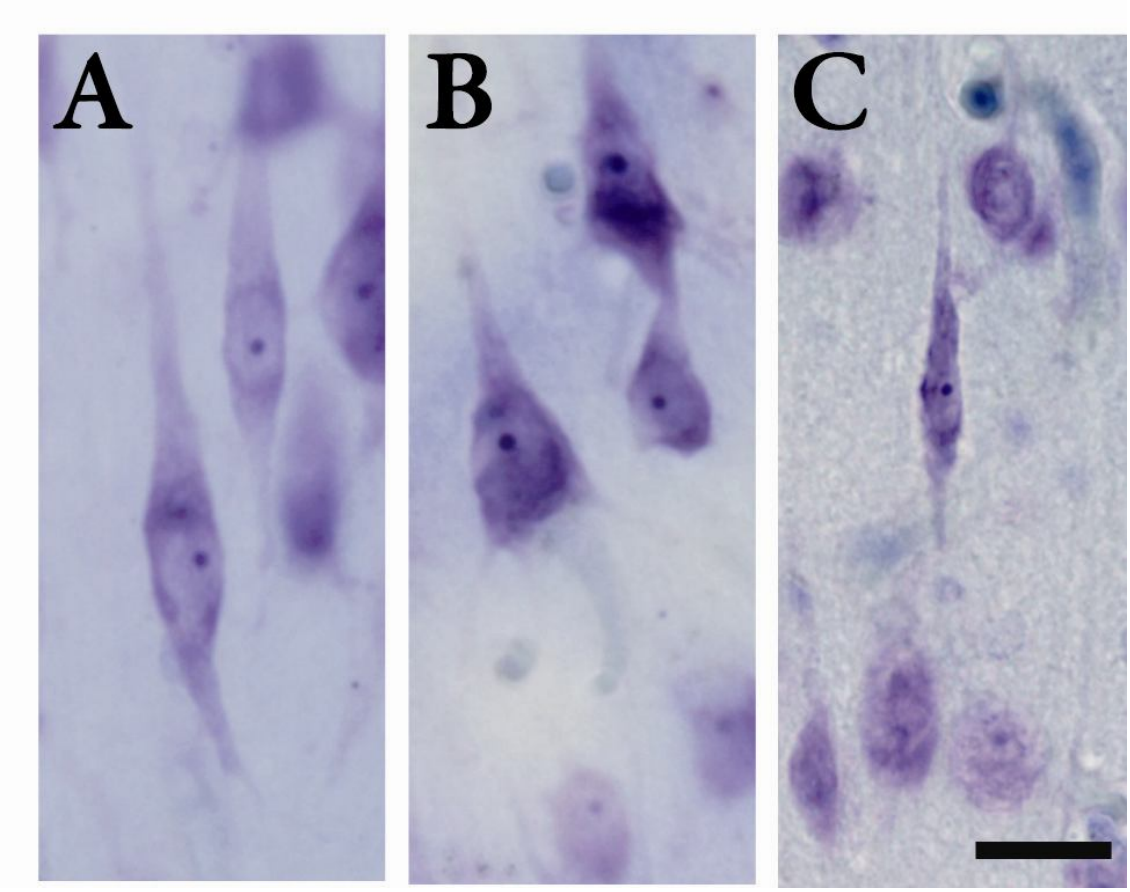

Figure 20. Comparison of the typical morphology of a VEN (A) with a pyramidal neuron of layer V (B), and a fusiform cell of layer VI in the AI of the beluga whale (C). Note the large difference in size between VENs and the layer VI fusiform neuron. Scale bar = 40 μm.

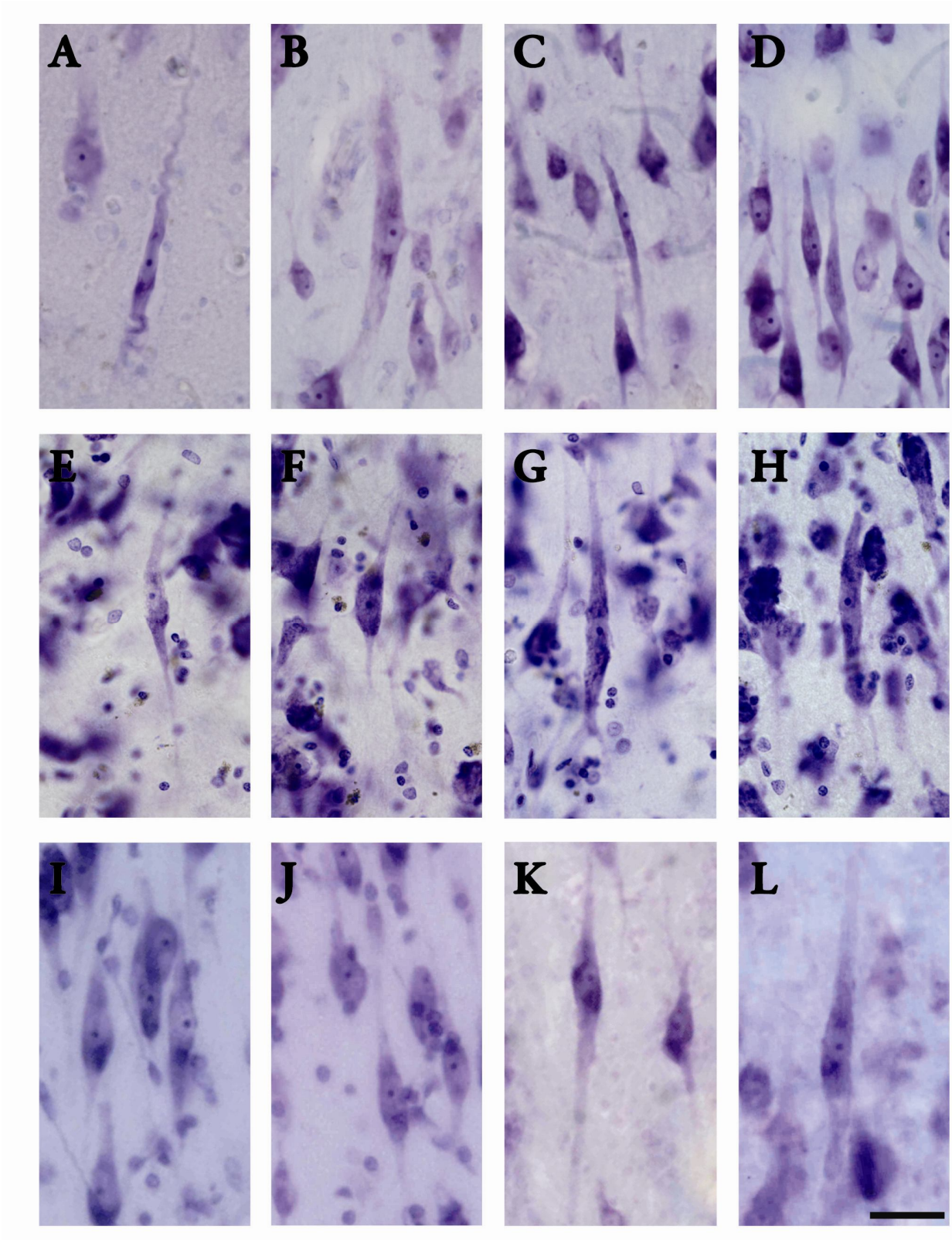

Figure 21. Morphology of VENs. Anterior cingulate cortex (A-B) and anterior insular cortex (C-E) of the beluga whale; anterior cingulate cortex of the Risso's dolphin (F-H); anterior cingulate cortex of the bottlenose dolphin (I, J) and frontopolar cortex of the humpback whale (K, L). Scale bar = 40 μm.

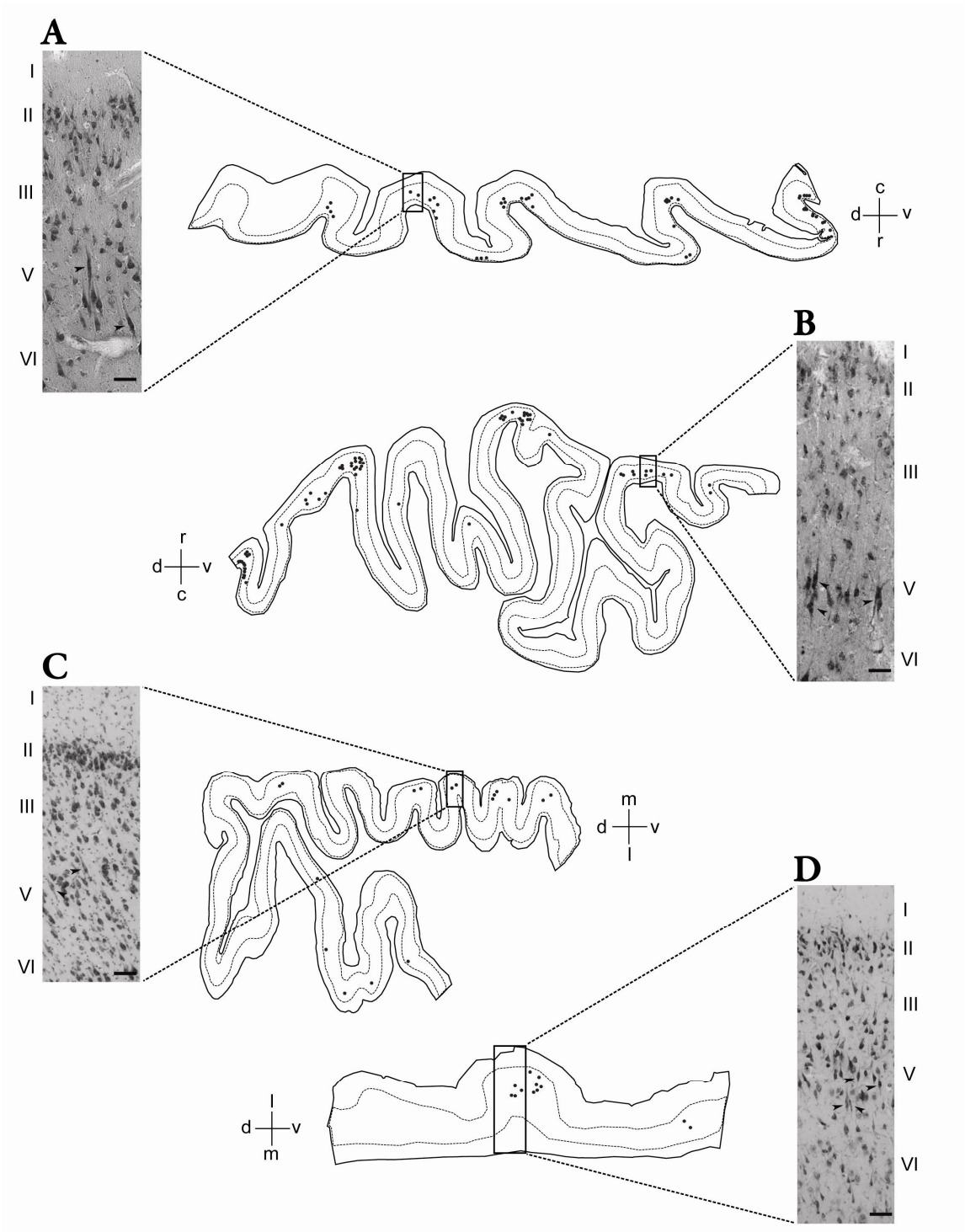

Figure 22. Maps of neocortical distribution of VENs. Anterior insular cortex (A) and frontopolar cortex (B) of the humpback whale; anterior cingulate cortex of the bottlenose dolphin (C) and anterior insular cortex of the beluga whale (D). The ROI (whole cortex) is outlined by a continuous line and layers III and V are outlined by a dashed line. Every dot corresponds to one VEN (see corresponding arrowheads on the microphotographs). VENs are located in deep layer III and layer V, clustered at the crown of the gyri and only scattered cells are present along the banks of the sulci. Cortical layers are indicated by Roman numerals. Scale bars = 100 μm.

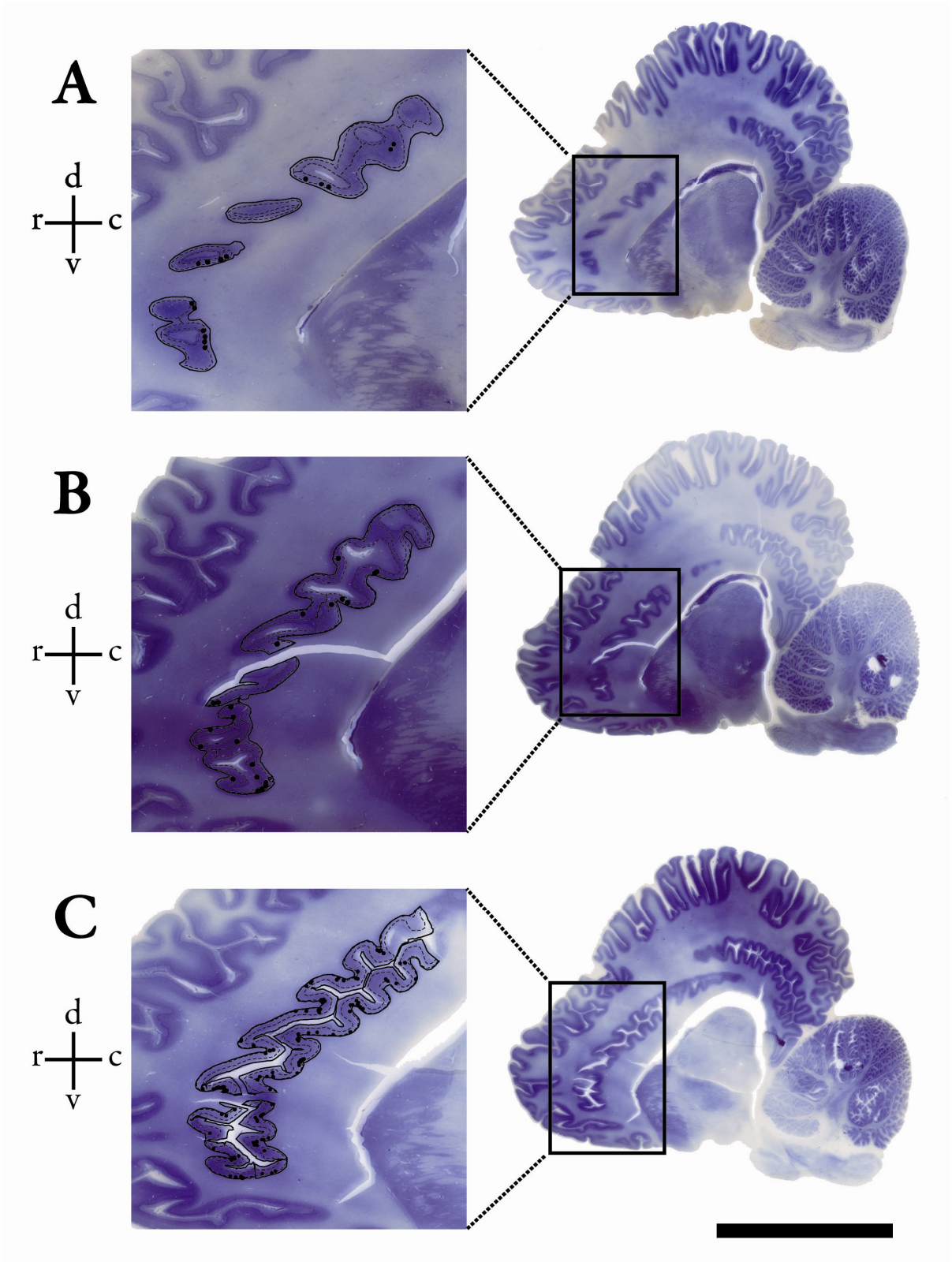

Figure 23. Maps showing the landmarks of the anterior cingulate cortex (ACC) and the pattern of distribution of VENs in the humpback whale. The ROI (whole cortex) is outlined by a continuous line and layers III and V are outlined by a dashed line. Every dot corresponds to one VEN. VENs are clustered at the crown of the gyri and fewer are present along the banks of the sulci. Scale bar = 6 cm.

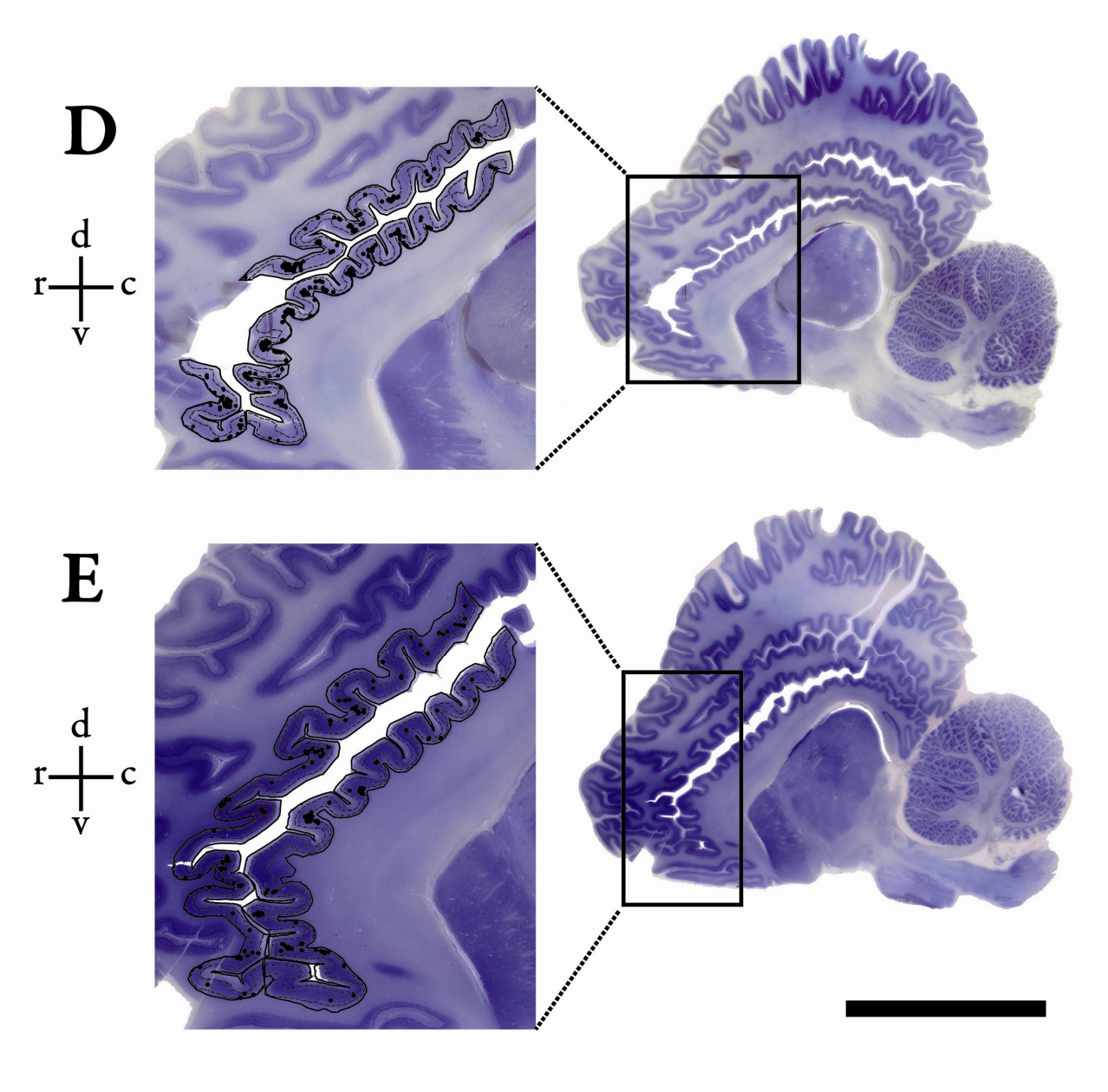

Figure 24. Maps showing the landmarks of the anterior cingulate cortex (ACC) and the pattern of distribution of VENs in the humpback whale. The ROI (whole cortex) is outlined by a continuous line and layers III and V are outlined by a dashed line. Every dot corresponds to one VEN. VENs are clustered at the crown of the gyri and fewer are present along the banks of the sulci. Scale bar = 6 cm.

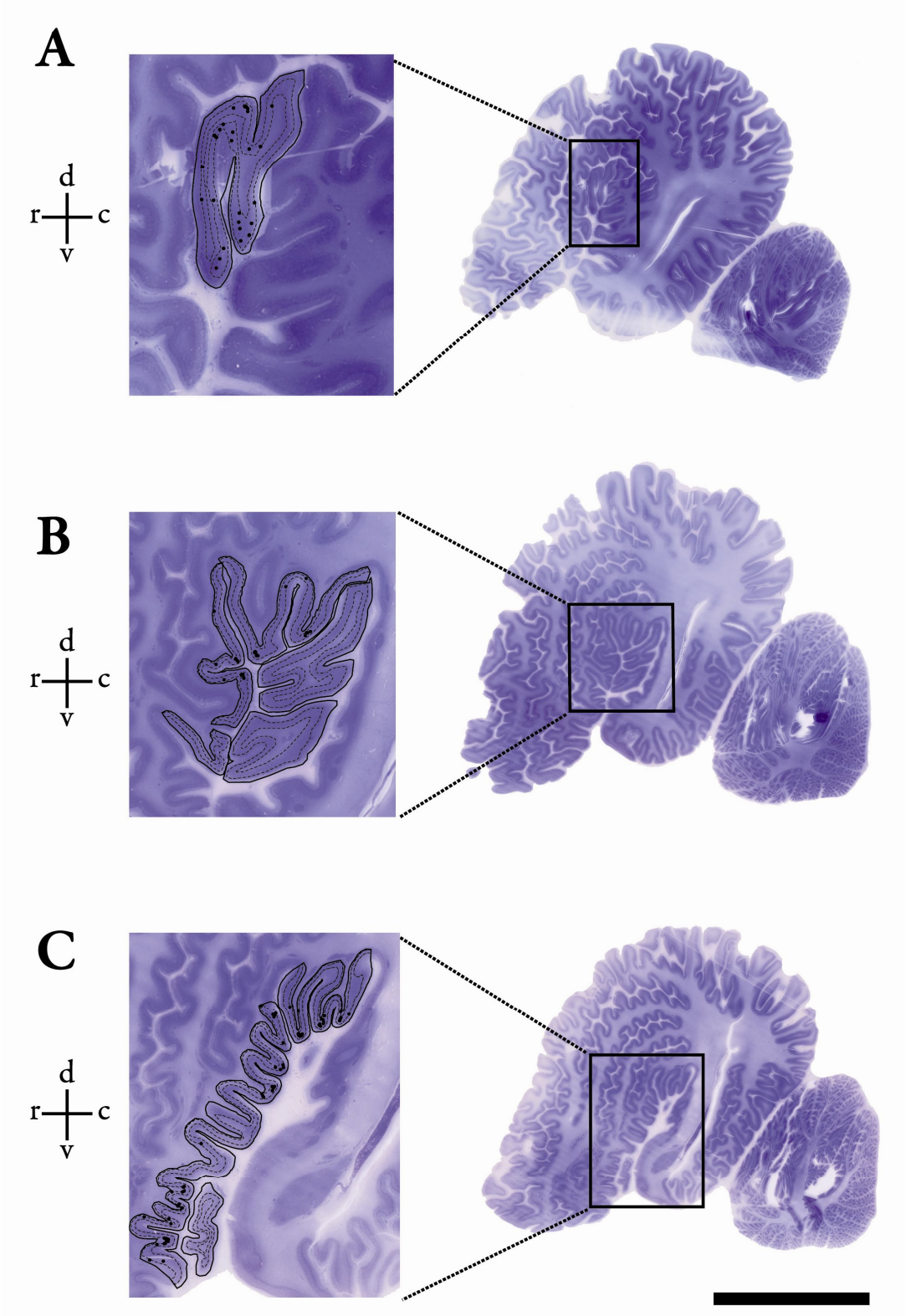

Figure 25. Maps showing the landmarks of the anterior cingulate cortex (ACC) and the pattern of distribution of VENs in the humpback whale. The ROI (whole cortex) is outlined by a continuous line and layers III and V are outlined by a dashed line. Every dot corresponds to one VEN. VENs are clustered at the crown of the gyri and fewer are present along the banks of the sulci. Scale bar = 6 cm.

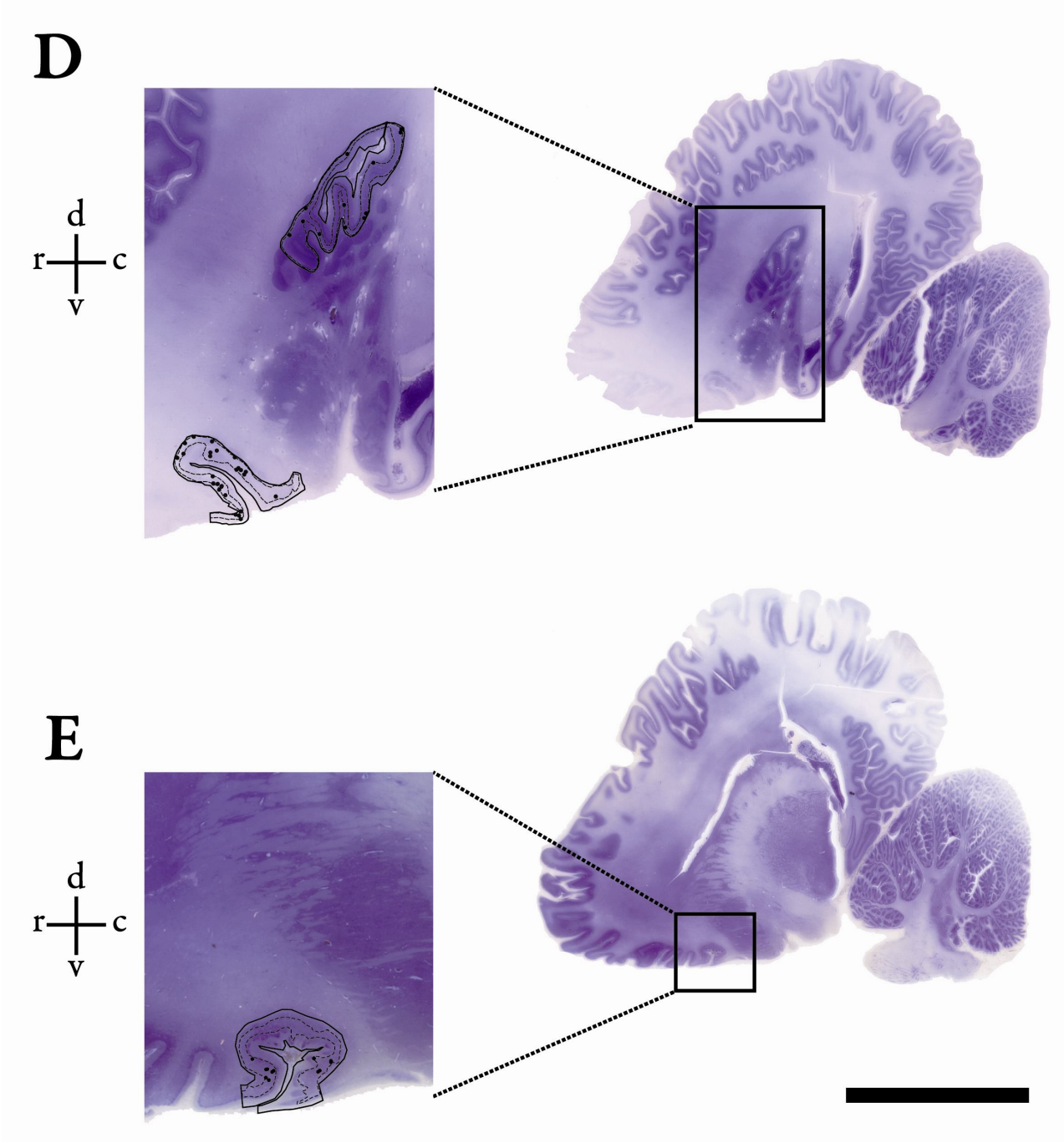

Figure 26. Maps showing the landmarks of the anterior insula (AI) and the pattern of distribution of VENs in the humpback whale. The ROI (whole cortex) is outlined by a continuous line and layers III and V are outlined by a dashed line. Every dot corresponds to one VEN. Scale bar = 6 cm.

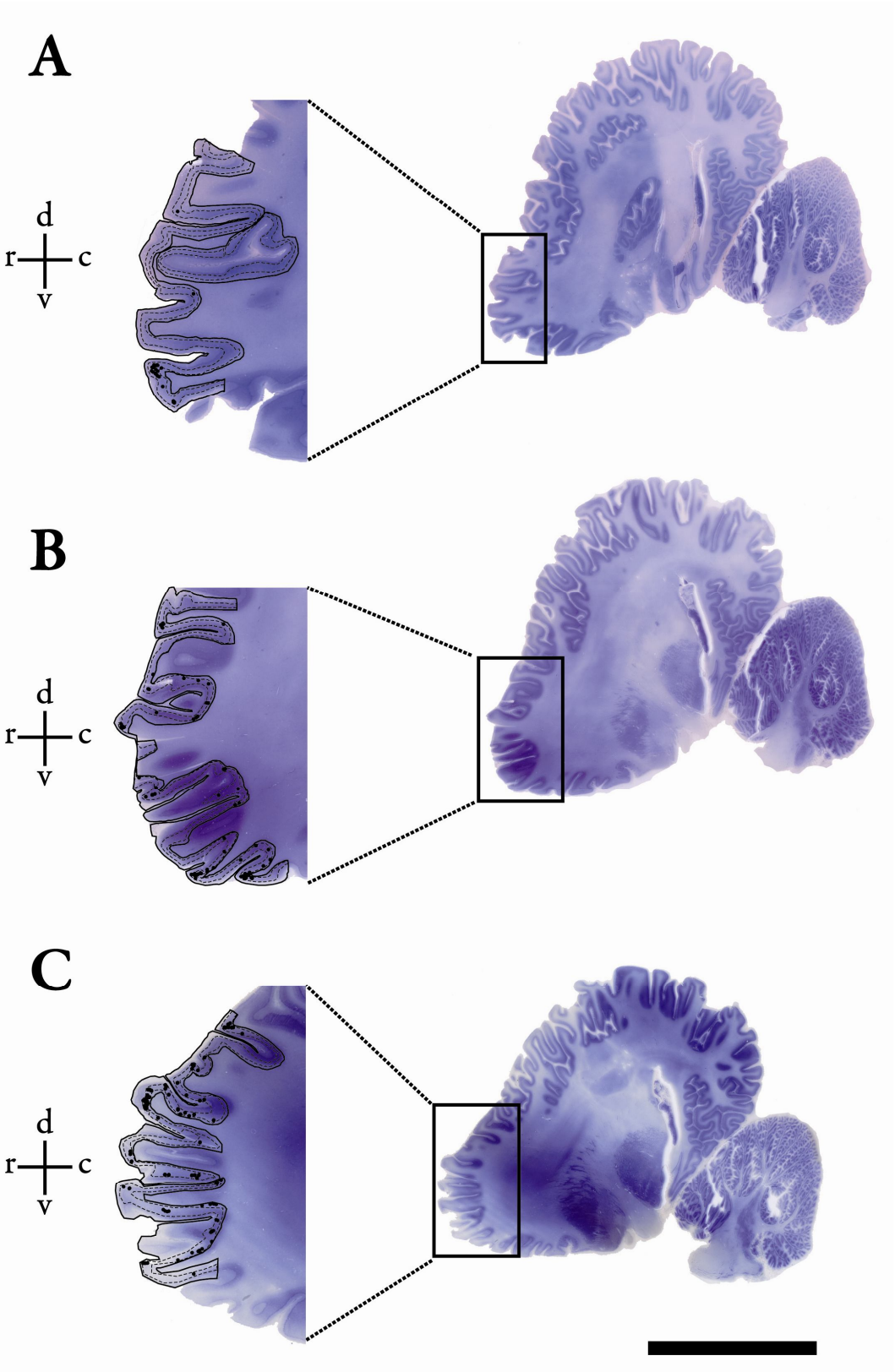

Figure 27. Maps showing the landmarks of the anterior frontopolar cortex (FP) and the pattern of distribution of VENs in the humpback whale. The ROI (whole cortex) is outlined by a continuous line and layers III and V are outlined by a dashed line. Every dot corresponds to one VEN. Scale bar = 6 cm.

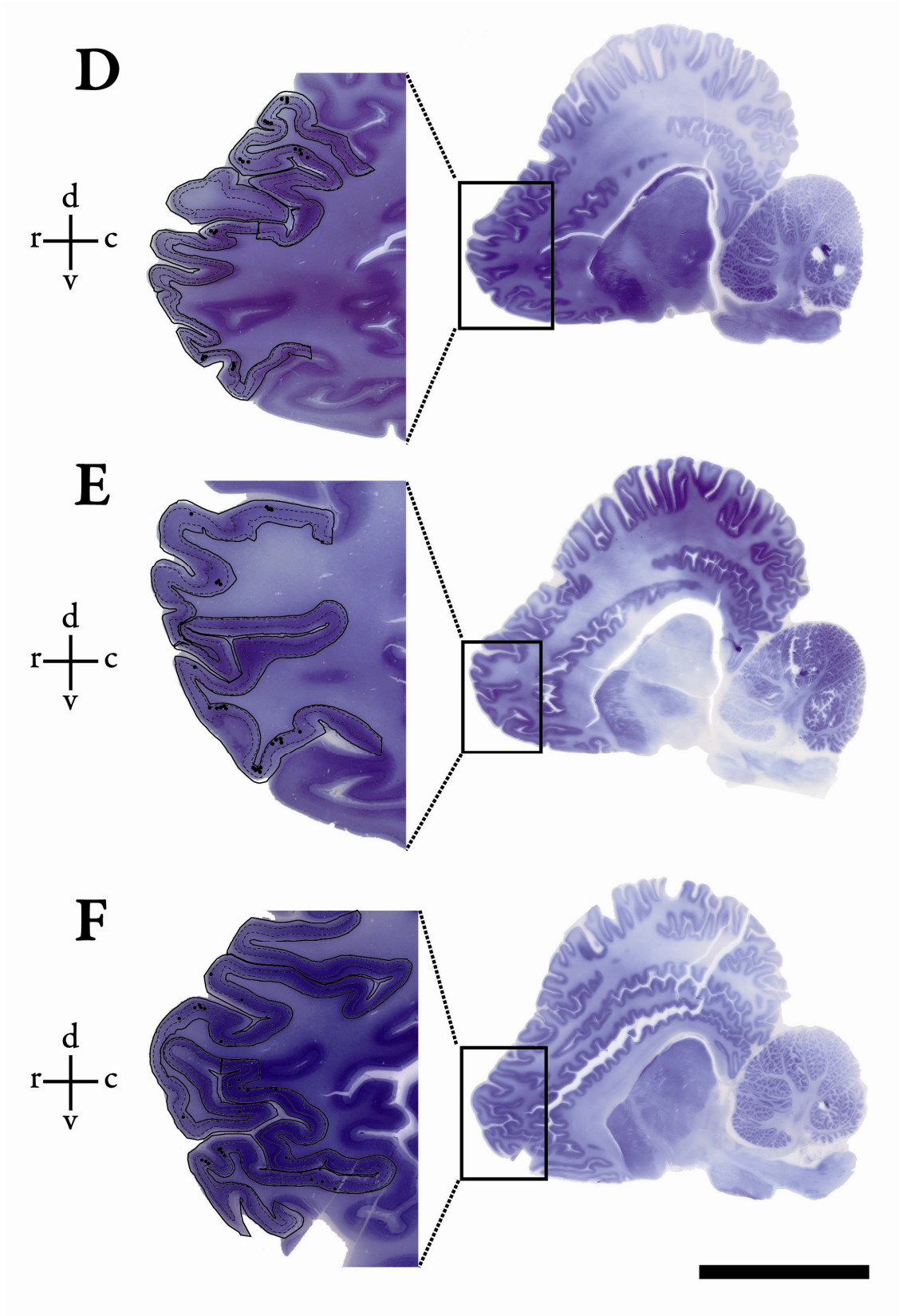

Figure 28. Maps showing the landmarks of the anterior frontopolar cortex (FP) and the pattern of distribution of VENs in the humpback whale. The ROI (whole cortex) is outlined by a continuous line and layers III and V are outlined by a dashed line. Every dot corresponds to one VEN. Scale bar = 6 cm.

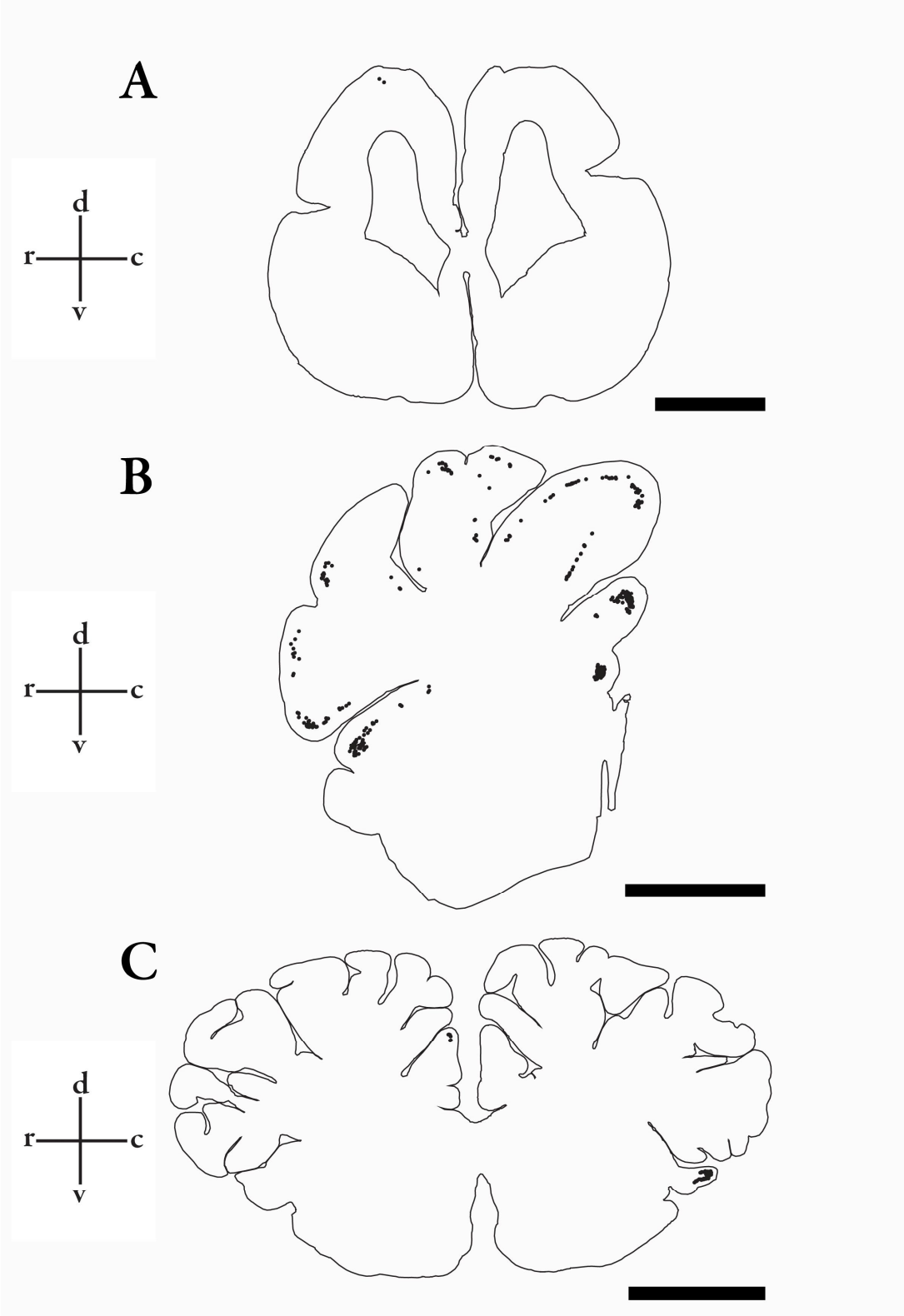

Figure 29. Maps of distribution of VEN-like neurons in the cortex of the Florida manatee (*T. manatus latirostris*) (A), the pigmy hippopotamus (*H. liberiensis*) and the common zebra (*E. burchelli*) (C). Scale bars = 1 cm.

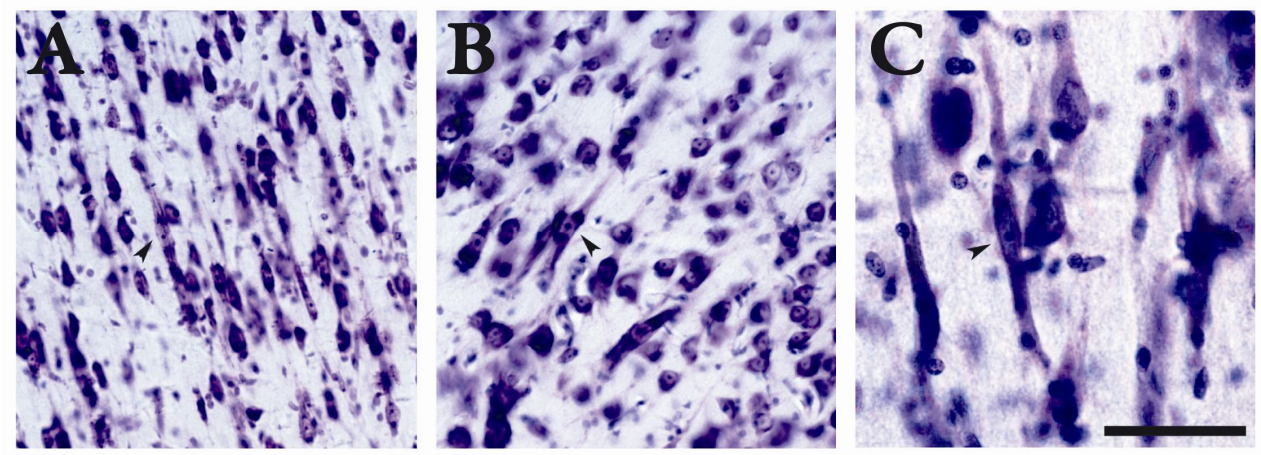

Figure 30. VEN-like neurons in layers V of the cortex of the Florida manatee (*T. manatus latirostris*) (A), the common zebra (*E. burchelli*) and the pigmy hippopotamus (*H. liberiensis*). Scale bar = 40 μm (C) and 90 μm (A, B).

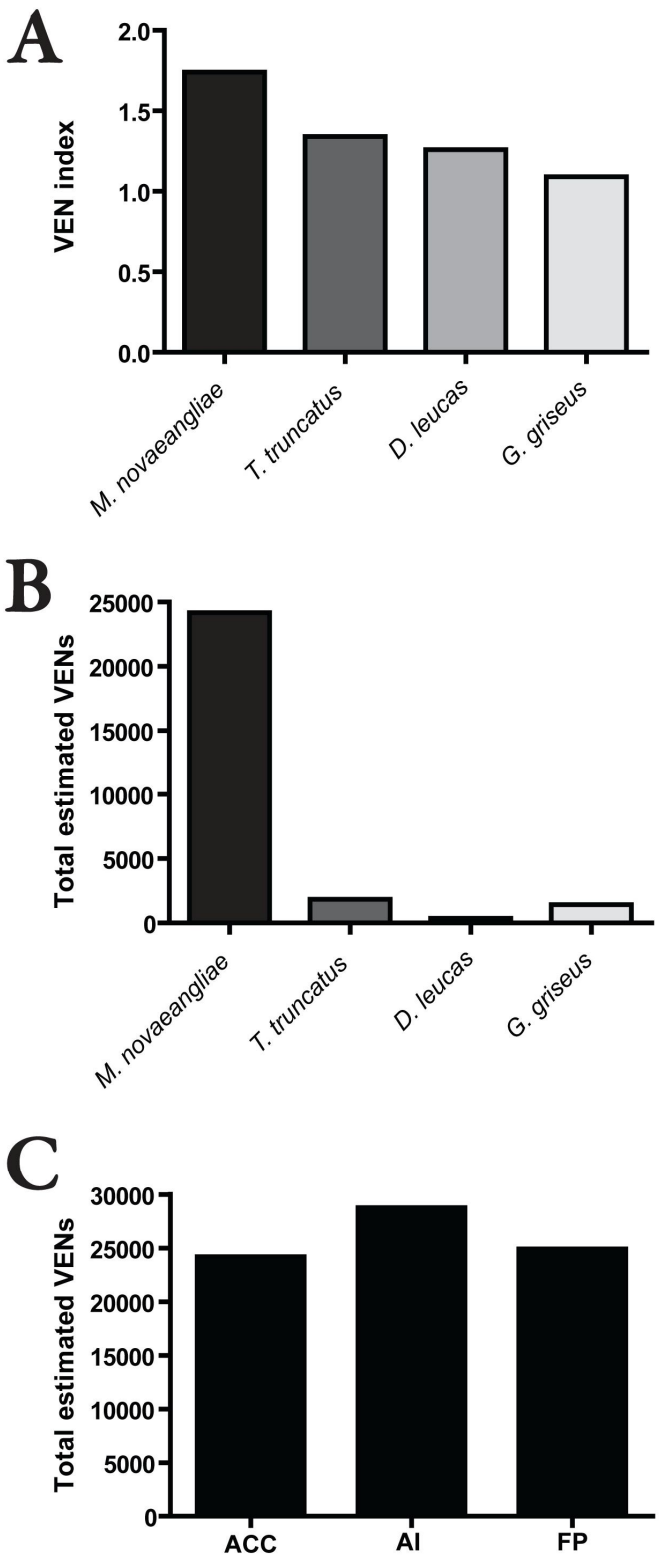

Figure 31. Ratio of the average VEN volume to the average pyramidal cell volume "VEN index", (A), and total estimated numbers of VENs in the four examined species (B), and in the three regions of interest of the humpback whale (C).

Table 6. Average values of brain weight, body weight, and EQ for the analyzed species Brain weight and body weight were unavailable for most of the specimens in this study. The values in the table were taken from Marino et al. (2004) and Hof et al. (2005).

Species	Brain weight (g)	Body weight (g)	EQ
T. truncatus	1,824	209,530	4.14
G. griseus	2,387	328,000	4.01
D. leucas	2,083	636,000	2.24
M. novaeangliae	6,411	39,295,000	0.44

Table 7. Summary of parameters used for the Optical Fractionator in the analysis of VEN numbers. ACC, anterior cingulate cortex; AI, anterior insula; FPC, frontopolar cortex; ROI, region of interest.

Parameter	ROI	*T. truncatus*	*G. griseus*	*D. leucas*	*M. novaeangliae*
Number of sections	ACC	17	24	16	5
	AI			26	24
	FPC				13
Number of microscopic fields	ACC	11,375	17,845	1,382	29,718
	AI			1,520	54,540
	FPC				58,267
Mean section thickness after processing (μm)		30	30	14	14
Area of the unbiased counting frame (μm^2)		20,900	20,900	20,900	42,500
Disector height (μm)		28	28	12	12
Guard zones (μm)		1	1	1	1

Table 8. Summary of parameters used for the Optical Fractionator in the analysis of total neuron numbers. ACC, anterior cingulate cortex; AI, anterior insula; ROI, region of interest.

Parameter	ROI	*T. truncatus*	*G. griseus*	*D. leucas*	*M. novaeangliae*
Number of sections	ACC	7	12	16	
	AI			26	26
Number of microscopic fields	ACC	183	500	478	
	AI			499	226
Area of the unbiased counting frame (μm^2)		3600	3600	3600	3600
Sampling grid size (μm)		2,000x2,000	2,000x2,000	1,000x1,400	5,000x5,000

Table 9. Summary of parameters used for the Optical Rotator analysis of each neuronal type.

Parameter	VENs	Pyramidal cells	Fusiform cells
Focal plane separation (μm)	2	3	2
Grid line separation (μm)	9	6	6
Optical slab thickness (μm)	7	7	4
Number of grid lines	4	4	4
Slab type	isotropic	isotropic	isotropic

Table 10. Results of stereologic estimates of total VEN numbers in the investigated species and cortical regions VENs numbers in the odontocetes represent only the available blocks from the ROI and are therefore underestimates. Moreover, the estimates were obtained in the only available hemisphere in each specimen. The right hemisphere of *T. truncatus* and the left hemispheres of *G. griseus*, *D. leucas*, and *M. novaeangliae*, as well as the FP in the odontocetes, were not available as they had been used previously or were distributed to other investigators. ACC, anterior cingulate cortex; AI, anterior insula; FP, frontopolar cortex; SUBG, subgenual cortex; LH, Left hemisphere; RH, Right hemisphere; ROI, region of interest; VENs %, percent of VENs calculated from the total number of neurons in the cortical area of interest; CE, Coefficient of error (calculated as the inverse of the square root of the number of cells counted). The CE measures the accuracy of the estimates and takes into account the distribution of the counted particles in the tissue and the total number of particles sampled (Schmitz and Hof, 2005). Due to the uneven and clustered distribution of VENs and their low number of cells, CE values are sometimes higher than desirable (> 0.1) and are not optimal indicators of the accuracy of the estimates, which in these cases resulted from exhaustive enumerations.

Species	ROI	Estimated VENs RH	Estimated VENs LH	VENs %	CE
T. truncatus	ACC		1,850		0.07
	SUBG		600	0.009	0.13
G. griseus	ACC	1,430			0.08
	SUBG	580		0.004	0.13
D. leucas	ACC	370		0.012	0.16
	AI	1,910		0.061	0.07
M. novaeangliae	ACC	24,180			0.04
	AI	28,770		0.027	0.03
	FP	24,900			0.03

Table 11. Volume of layer V VENs and pyramidal cell and fusiform cells of layer VI. Volumes are expressed as mean (μm^3) ± SD. The VEN index is the ratio between the average volume of VEN and the average volume of pyramidal neurons.

Species	VENs	Pyramidal neurons	Fusiform	VEN index

			neurons	
T. truncatus	4,449 ± 524	3,323 ± 310	1,436 ± 175	1.34
G. griseus	3,186 ± 479	2,923 ± 298	1,460 ± 158	1.09
D. leucas	3,406 ± 468	2,710 ± 347	1,248 ± 150	1.26
M. novaeangliae	6,189 ± 948	3,558 ± 393	1,662 ± 231	1.74

Table 12. List of species, cortical regions and frequency of distribution of VENs.

Species	VENs distribution	VENs frequency	Source
Cetartiodactyla			
M. novaeangliae	ACC, AI, FPC	Abundant/clusters	Hof and Van der Gucht, 2007; Butti et al., 2009
B. physalus	ACC, AI, FPC	Abundant/clusters	Hof and Van der Gucht, 2007
B. acutorostrata	ACC, AI, FPC	Abundant/clusters	Hof and Van der Gucht, 2007
P. macrocephalus	ACC, AI, FPC	Abundant/clusters	Hof and Van der Gucht, 2007
O. orca	ACC, AI, FPC	Abundant/clusters	Hof and Van der Gucht, 2007
T. truncatus	ACC, AI, FPC	Abundant/clusters	Butti et al., 2009
G. griseus	ACC, AI, FPC	Abundant/clusters	Butti et al., 2009
D. leucas	ACC, AI, FPC	Abundant/clusters	Butti et al., 2009
S. coeruleoalba	ACC, AI, FPC	Abundant/clusters	present thesis
H. liberiensis	Throughout the cortex	Abundant	present thesis
Afrotheria			
T. manatus latirostris	ACC	rare	present thesis
L. africana	ACC, AI, FPC, dlPFC	Abundant/clusters	Hakeem et al., 2008
E. maximus	As above	Abundant/clusters	Hakeem et al., 2008
Perissodactyla			
E. burchelli	ACC , AI	Abundant/clusters	present thesis

Chapter 5

General discussion

Comparison of cortical organization in cetaceans and terrestrial mammals

Definition of the prefrontal cortex in cetaceans in a phylogenetic perspective

The prefrontal cortex (PFC) of primates is the cortical region extending from the frontal pole to the premotor cortex that includes cortical fields located on the medial wall of the hemisphere such the ACC, and specifically area 24, 25 and 32. It is characterized by a highly heterogeneous structure composed of several architectonic areas, a granular organization, owing to the presence of a generally well-developed internal granular layer (layer IV), and a dense afferentation from the mediodorsal nucleus of the thalamus (MD) (Rose and Woolsey, 1948; Barbas and Pandya, 1989; Goldman-Rakic and Porrino, 1985; Giguère and Goldman-Rakic, 1988; Schwartz et al., 1991; Preuss and Goldman-Rakic, 1991). The PFC is involved in cognitive processes, attention, working memory and recall, and executive functions such as planning of complex behaviors and judgment (reviewed in Barbas, 2000). The PFC is selectively vulnerable to normal aging processes (Morrison and Hof, 1997, 2007; Raz et al., 1997; Duan et al., 2003; Hof and Morrison, 2004) as well as to devastating neurodegenerative diseases such as Alzheimer disease (AD) (Bussière et al., 2003a,b), frontotemporal dementia (FTD) (Ishii et al.,1999; Seeley et al., 2008), and schizophrenia (Casanova, 1997;Goldman-Rakic and Selemon, 1997; Hof et al., 2003; Driesen et al., 2008; Hamilton et al., 2009). Given its involvement in aspects of behavior considered broadly to be human-specific, the presence of a homologous[5] cortical region in other mammalian species has been a topic of debate. However, the identification of homologous structures (or areas in the case of the neocortex) in comparative neuroananatomical studies is challenging. In fact, the original ancestral structures from which homologous traits originate in different species undergo different evolutionary processes that can shape differently the original structure, and as such, anatomical similarity is not a necessary condition for homology.

In neuroanatomy, the principle commonly used to define if cortical regions in different species represent homologues is to define their connections, and thus, their potential functions. Specifically, the mediodorsal nucleus (MD) represents the main source of thalamic afferents to the PFC in primates (Rose and Woolsey, 1948; Akert, 1964; Goldman-Rakic and Porrino, 1985; Giguère and Goldman-Rakic, 1988; Siwek and Pandya, 1991), and even though this view has been questioned (Markowitsch and Pritzel, 1979; Preuss, 1995), it still represents the main criterion to identify possible homologues of the PFC in the frontal cortex of non-primate species. The possibility of using invasive methods to trace neuronal connections in the large majority of laboratory animals, provides evidence for the presence of a region of the frontal cortex receiving dense afferents from the MD, which can thus be considered homologous to the primate PFC in a series of mammals (Krettek and Price, 1977; Divac et al., 1978; Cavada and Reinoso-Suárez,

[5] Homologous structures are traits possessed by two or more species and that are derived from a common structure in an ancestral organism.

1985). However, these studies report that, in different species, the regions densely innervated by the MD exhibit a somewhat different topographic distribution than they do in the frontal lobe in primates providing evidence for a variable organization of the areas of the frontal lobe among mammals.

Some authors provided evidence that the MD, in primates, does not project uniquely to the granular frontal cortex but also to the cingulate, medial frontal and insular cortices (Mufson and Mesulam, 1984; Vogt et al., 1987), and as a consequence it was argued that the connection of a given cortical areas with the MD in non-primate mammals is not *per se* sufficient to identify PFC and that instead the interpretation of homology should be based on a larger number of anatomical features rather than on just few (reviewed in Preuss, 1995). In this context it is worth citing the work of Dombrowski et al. (2001) who used a quantitative approach to assess the structural differences among PFC regions in primates. This study shows that a distinct pattern of neuronal density, cortical thickness, and distribution of PV-immunoreactive neurons characterizes distinct areas and that these parameters can be used as indicators of different architectonic profiles.

In the specific case of cetaceans, the task is made even more challenging by the fact that the cetacean cortex is completely agranular and the brain underwent extreme modifications during evolution with a topographical location of the main sensory areas that is very different from that of primates (see the Introduction for details). Moreover, invasive approaches such as lesion or connectivity studies are impossible to perform and direct evidence of any kind of afferent innervation to the frontal region of the cetacean brain would be extremely difficult to accomplish. However, if the classic architectonic approach is used to define cortical fields in the cetacean frontal cortex, a large and highly gyrified domain, the so-called frontopolar cortex (FPC), can be identified cytoarchitecturally and is very distinct compared to adjacent fields (Hof and Van der Gucht, 2007; Chapter 2 of the present thesis). The additional presence in layer V of the cetacean FPC of the Von Economo neurons, similarly to observations in the human dlPFC (area 46), (Hof and Van der Gucht, 2007; Fajardo et al., 2008; Butti et al., 2009) suggests that this area is, as in hominids, endowed with high-level cognitive functions and that this likely cortical homologue of the primate dlPFC is very well developed and specialized in cetaceans. Moreover, it is important to stress the enlargement and the histological complexity of the ACC and AI in cetaceans (Jacobs et al., 1979; Hof and Van der Gucht, 2007) and their connections with the prefrontal and orbitofrontal cortices in primates (Cavada et al., 2000; Ongür and Price, 2000; Barbas et al., 2003; Höistad and Barbas, 2008).

Additional quantitative analyses of the FPC and its related structures such as the ACC and AI could be useful to reveal other aspects of the organization of the frontal cortex in cetaceans, such as neuronal densities, cortical thickness and distribution of molecular markers, that may help further establish it as the homologue of the primate dlPFC.

Finally, the involvement of the primate PFC in several memory-related processes (Goldman-Rakic, 1988, 1995; Barbas, 2000; Chafee and Goldman-Rakic, 2000; Constantinidis et al., 2001; Compte et al., 2003;Wang et al., 2004) is intriguing in a comparative perspective. In the brain of cetaceans, in fact, the structure classically involved in memory processes, the hippocampus, is remarkably diminutive compared to that of primates and of large-brained terrestrial mammals such as the elephant (Breathnach and Golby, 1954; Hakeem et al., 2005; Hof et al., 2005; Hof and Van der Gucht, 2007). Both odontocetes and mysticetes possess a very well developed entorhinal cortex in contrast with the dramatically reduced size of its main projection area, the dentate gyrus (Zola-Morgan and Squire, 1993). Given this contrasting features of the hippocampal formation the issue of how the cortical networks underlying memory processing are organized in the cetaceans remains wholly unknown. There is documented behavioral evidence of learning and memory in cetaceans (reviewed in Marino et al., 2008) and the idea that, even if purely a speculation, the wide and cytoarchitecturally specific domain of the FPC, as well as a comparatively broadly expanded cingulate and insular cortices in cetaceans may play a key role in

memory processes is intriguing. Although extensive studies are needed to understand better the organization of the cortex of cetaceans, the present knowledge on their behavior and complex cortical organization does not argue against the possibility that a cortical homologue of the primate dlPFC is present in the cetacean brain. Moreover, cytoarchitectural evidence gives reason to think that, if such homologue exists, it could be represented by the FPC and be very well developed.

Conclusions

Given that it is now widely accepted that the enlargement of the cetacean brain was driven by evolutionary selective pressures acting on complex cognitive abilities (reviewed in Marino et al., 2007), the study of the cortical regions that are known to be involved in judgment, attention, intuition, and social awareness in primates (Allman et al., 2005) are of special interest in a comparative perspective. In the research described in this thesis, I used different approaches to investigate the complexity of the brain of cetaceans and, in particular, of cortical regions such as the ACC, AI, and FPC, classically related to high-level cognitive functions. In Chapter 2, I gave a description of qualitative features, with emphasis on the cyto- and chemoarchitecture of these three cortical regions in a wide series of cetacean species and used select terrestrial and aquatic mammals as comparative taxa. In Chapter 3, I focused on quantitative aspects of the cortical organization of the cetacean brain by investigating the ratio of glial cells to neurons (GNI) in the ACC and the primary somatosensory cortex (S1, as a control region), in species representative of the major cetacean families together with terrestrial and aquatic mammals selected for comparison. In Chapter 4, I discussed the presence in the three cortical regions of interest of a neuronal specialization thought to be involved in high-level cognitive processes, the Von Economo neurons. Altogether, these data contributed to the overall goal of this thesis to identify traits of complexity of the cetacean cerebral cortex as well as specific patterns of cortical organization that are either shared with other mammals or uniquely derived in the cetacean brain. Below I address and discuss the main findings of each chapter in a general perspective. Technical limitations and the adopted approaches are considered whenever relevant.

Findings reported in Chapter 2 are consistent with previous descriptions of the general organization of the cetacean cortex but includes new insights. The three regions of interest have been investigated in the present thesis in a wide range of cetacean species never described before, and the results show that even if the cortical organization among cetaceans follows a common *Bauplan*, specific differences are present between the three cortical regions and more generally between odontocetes and mysticetes. Particularly, clustering of layers II and V, differences in the thickness of the cortical layers and in the density and size of neurons within one layer, as well as different degrees of modularity distinguish the cortical regions of interest (see chapter 2 for details). Moreover, overall differences in neuron size and neuronal density are observed between small and large cetaceans, the largest species such as *M. novaeangliae*, *P. macrocephalus* and *O. orca*, having larger neurons and lower densities than small delphinids and balenopterids. Differences in neuronal size and density among small and large cetaceans have been reported previously (Hof and Van der Gucht, 2007; Poth et al., 2005) and they are consistent with the proposed inverse relationship between brain size and neuronal density (Tower, 1954).

The similarity in the structural and chemical organization of the cetacean neocortex and that of the pigmy hippopotamus, is in agreement with the fact that brain organization and neurochemical specializations can be interpreted as reflection of phylogenetic relatedness among mammals (Hof et al., 2005) given that a sister-taxon relationship has been recognized between cetaceans and hippopotamuses (Gatesy, 1997; Boisserie et al., 2005; Agnarsson and May-Collado, 2008).

Observations in Chapter 3 challenge a previous report that suggested that cetaceans have a very high GNI and that they should be considered outliers among mammals in the relationship

brain size/GNI (Manger, 2006). Results reported in Chapter 3 indeed show a very high GNI in the brain of cetaceans, especially in large-brained species, independent of their belonging to mysticetes or odontocetes, but this value is correlated with brain size showing that the high GNI reported in the cetacean brain is that expected for their brain size. However, different types of glial cells (e.g., astrocytes and oligodendrocytes) subserve different functions and it would be interesting to define whether the increase in the ratio of glia to neurons, in small versus large brains, is due mainly to one type of glial cell and whether species with similar brain sizes and GNI values possess a different ratio of glial cells types. The present study used Afrotheria as a comparison group, including species with a large variation in brain size such as the elephant and the rock hyrax. However, a limitation of the present study is in fact the availability for this analysis of only two groups. Plots of groups each containing only phylogenetically related species may result in bias given that closely related species are not evolutionarily independent. As such, an analysis of the GNI that includes other, not directly related, taxa at the ordinal or superordinal level and that controls directly for phylogeny effects, (using independent contrasts), needs to be performed to confirm these results.

Chapter 4 provides evidence for the presence of a neuronal specialization, the Von Economo neurons, in the brain of several cetacean species and of a laminar and regional distribution of these neurons similar to that described in great apes. The identification of these neurons is based on morphological criteria, and it could be argued that these neurons are an artifact of preparation in the cetacean brains anlyzed. This is an issue that was originally addressed by Von Economo (1926) in his original paper. He described the process of "spindling" of the cortical elements as a process he considered common to all cell types in the neocortex and that he saw as responsible for the enhancement of the sharp contrast in morphology between "VENs" and surrounding pyramidal cells. As in previous studies of VENs in humans and great apes, the VENs were observed mainly at the crown of the gyri, but were sparse along the banks of sulci, confirming that they represent a cellular specialization rather than an artifact of preparation.

In regard to the specimens available for analysis, and considering that I could not exhaustively sample all relevant regions in all of the odontocetes, the total number of VENs in this group is significantly lower than in hominids, elephants, and the humpback whale (in spite of the high EQ of the small odontocetes). This may reflect the fact that although VENs appeared early in the evolutionary history of modern whales, being present in both mysticetes and in the oldest family of toothed whales, the physeterids (Fordyce and Barnes, 1994), their distribution and numbers continued to evolve in the recent history of cetaceans, perhaps representing a certain degree of refinement in the projections they may subserve. In this context, it will be interesting to investigate VENs in the brains of small physeterids like the pygmy sperm whale (*Kogia breviceps*), and a small balaenopterid like the minke whale (*B. acutorostrata* which incidentally possesses VENs in a seemingly comparable distribution as in *M. novaeangliae* [Butti and Hof, unpublished observations]). Moreover, the uneven distribution and overall low numbers of VENs (varying from less than 1% to about 3% of the total number of neurons depending on the species and region) in the cortex of hominids, cetaceans, and elephants, recalls the distribution and density of other highly specialized neuronal populations such as the Betz and Meynert cells which are found only in layer Vb of the primary motor and in layer VI of the primary visual cortex, respectively, in primates (Hof et al., 2000; Rivara et al., 2003), and exhibit species-dependent morphologic and functional specialization (Sherwood et al., 2003). Even though the total numbers of VENs in great apes, cetaceans and elephants are rather variable, the presence of this peculiar cell type within the same regional and laminar pattern across divergent species indicates that the projections that VENs may provide are perhaps as specific as those furnished by neurons like Betz and Meynert cells. What their specific function might be remains, however, to be elucidated.

In conclusion, this thesis investigated the qualitative and quantitative aspects of the ACC, AI, and FPC in cetaceans in a comparative perspective. The data can be used as future comparative reference for the study of cytoarchitecture of other regions of the cetacean brain and more generally in the broader context of the organization of the mammalian brain. The understanding of the organization of a complex and large brain such as that of cetaceans is fundamental for elucidating the more general rules that drove the evolution of the mammalian. The sharing among cetaceans and hominids of a morphological cellular specialization with the same laminar and regional pattern such as the VENs make the cetaceans an interesting link in the study of the evolution of a neuronal type that is selectively disrupted in neurodegenerative disease occurring uniquely in humans.

Future directions

Use of the Grey Level Index (GLI) to map the parcellation of the cetacean frontal cortex

Most of the studies on parcellation of the cerebral cortex are based on the visual inspection of histological slides. This method, however, is classically affected in observer-dependent differences between maps and boundaries of cortical area (Brodmann, 1909; von Economo and Koskinas, 1925). Particularly, in species in which the parcellation of the cortex is more difficult to perform, given the presence of large transitional areas between adjacent cortical fields, such as cetaceans and great apes, the use of an observer-independent method could provide extremely reliable information on the parcellation of cortical regions. The Grey Level Index (GLI) is an automated method that defines boundaries between adjacent cortical regions. It is defined as the ratio of the area covered by Nissl-stained elements to the unstained area. The automated system measures alterations in the vertical column organization extending from the cortical surface to the white matter, the so-called profile. The vertical laminar pattern of each profile is represented by a curve and curves belonging to neighboring profiles are compared in sequence using vectors. Curves that differ more than the set level of acceptance will be considered representative of different profiles, meaning different cortical areas. The GLI have been successfully used in several studies of the human cortex (Schleicher et al., 1986, 1990, 1999; Amunts et al., 2003; Eickhoff et al., 2006; Rottschy et al., 2007; Schenker et al., 2008), and has been applied only to the study of the cetacean auditory cortex (Fung et al., 2005). In the context of the study of the cetacean frontal cortex, this method could finally resolve the controversy on its parcellation.

The role of different classes of glial cells in the determination of the glia-neuron index (GNI) through the use of specific markers such as GFAP (Glial Fibrillary Acidic Protein) and MOSP (Myelin/Oligodendrocyte Specific Protein)

The most of the studies of the GNI use stereologic methods based on Nissl-stained sections (see Introduction of Chapter 3 for specific references), and do not differentiate between different glial types since this staining does not allow for identification of morphological details of astrocytes and oligodendrocytes with a sufficient degree of precision. As a consequence, as discussed in the present thesis, the GNI is a quantitative parameter indicative of the ratio of glial cells to neurons, but does not give any information on the potential evolutionary pressures that defined the increase of one glial cell type over the other (or the equal amount of the two cell types). Another approach used recently in the study of the GNI is the Isotropic Fractionator (Herculano-Houzel and Lent, 2005), that consists on a chemo-mechanical dissociation of tissue and on the detection of the neuronal nuclear antigen NeuN using a specific antibody, followed by the calculation of the non-

neural (considered as “glial”) nuclei by subtraction. However, this method too does not permit to obtain information on the different types of glial cells.

The use of markers specific for each glial cell type, such as GFAP (Glial Fibrillary Acidic Protein) for astrocytes and MOSP (Myelin/Oligodendrocyte Specific Protein) (Dyer et al., 1991) for oligodendrocytes, could help in obtaining a GNI value that includes the ratio of the two glial types. However, while GFAP has been proven to be highly stable among vertebrates (Dahl and Bignami, 1973), and has been previously used to study the cetacean cortex (Pritz-Hohmeier et al., 1994), MOSP has mostly been used in the mouse (Dyer et al., 1991; Dyer and Matthieu, 1994) but the evidence to be a good marker for oligodendrocytes in other species is lacking. As a consequence, its usefulness as a marker of the cetacean oligodendrocytes has to be tested. Moreover, in quantitative studies, a major possible bias is due to the use of markers that are not fully ubiquitous within a cell population. If the percent of GFAP-immunoreactive astrocytes and MOSP-immunoreactive oligodendrocytes calculated from the total population of each cell type does not match, any ratio would be biased because not reflecting the real ratio of the two cell types. The use of this kind of markers will have to be anticipated by a pilot study, possibly using Nissl-counterstained sections, to determine which percent of each cell population is immunoreactive to the marker and allow, thus, the calculation of the appropriate correction factor for the final GNI values.

Determination of the presence/absence of Von Economo neurons (VENs) and map their distribution in species representative of the whole mammalian phylogeny

An important result of the present thesis is the finding that other species, including ungulates and elephants, other than hominids and cetaceans, possess VEN-like neurons, and of particular interest is their pattern of distribution. As described in Chapter 4, VENs are found in the neocortex of humans, great apes, cetaceans, and elephant with a comparable distribution in three cortical areas, ACC, AI, and FPC (or dlPFC in humans). In other species in which VENs have been described (see Chapter 4) their distribution is uniform throughout most of the cortical mantle, suggesting an evolutionary process of refinement of the VENs projections towards specific cortical and subcortical structures in the cetaceans, comparble to what might have taken place in the case of hominids and elephants. However, the species in which VEN-like neurons have been described in the present thesis are representative only of the ungulates. A more extensive analysis, including a wider range of species and mapping at least the main families of the mammalian phylogeny, will help in elucidating the selective pressures involved in the evolution of this neuronal specialization.

Determination of changes in neuronal morphology during aging in cetaceans

Several studies report age-related changes in neuronal morphology during normal aging in primates (Page et al., 2002; Duan et al., 2003; Hao et al., 2006, 2007). Subtle alterations in the morphological integrity of neurons have been proposed to play a key role in the functional impaiment of network responsible for the cognitive decline associated with aging (Duan et al., 2003; Kabaso et al., 2009). In the context of the study of aging and brain evolution, the brain of cetaceans assumes a particular interest given its large size and the longevity of this group of mammals that make them a potential good model to study, in a non-primate, neuronal types affected in normal-aging and human-specific neurodegenerative diseases. It would be interesting to use techniques such as dye-loading of different neuronal types in postmortem materials followed by neuronal tracing and three-dimensional imaging of traced neurons (Duan et al., 2003; Dickstein et al., 2007; Radley et al., 2008) to assess possible qualitative and quantitative changes related to aging in the brain of these large marine mammals. This type of anatomical studies, coupled with

information from the increasingly more numerous long-term behavioral studies in marineland and zoos could give precious insights into the neurobiology of aging in cetaceans, as well as the evolution and development of common neurodegenerative diseases.

Acknowledgements

This research project has been carried out at the Department of Experimental Veterinary Science of the University of Padova, Italy, and at the Department of Neuroscience of the Mount Sinai School of Medicine in New York, USA. The present thesis has been possible thanks to the effort of a large number of people and I wish to express my most sincere thanks to:

My supervisor, *Professor Bruno Cozzi*, for welcoming me in his lab as a PhD student and giving me the freedom of pursuing my research interests studying the cetacean neuroanatomy. For the inspirational discussions we had on different scientific topics and for his crucial contribution in shaping my determination to face new important challenges in the United States.

My co-supervisor, *Professor Patrick R. Hof* for his constant support and impact on my understanding of comparative neuroanatomy, for being not only a brilliant mentor but also a friend with a profound influence on my professional and personal growth, for letting me have independence in my research projects though being always available for discussions and advice, for feeding day by day my motivation and passion for science, and for all the good laughs we had when I needed it most. You are an inspiration for whom I want to become and I am extremely grateful to have had the chance of working with you.

All the members of the Department of Experimental Veterinary Science of the University of Padova in my first year of PhD:
*Prof.Gianfranco Gabai, Prof. Massimo Morgante, Prof. Francesco Mascarello, Prof. Claudia Simontacchi, Prof. Giuseppe Radaelli, Prof. Mario Pietrobelli, and Prof.Gabriele Bono; Dr. Cristina Ballarin, Dr. Antonio Frangipane di Regalbono, Dr. Simona Normando,*and *Dr.Marco Vincenzo Patruno* for being always available for advice and support.
Antonella, Maristella, Marta, Lisa, Roberta, Susanna, Daniela, Eugenia, Mariacristina, Francesca, Claudia, Tiziana, Carlo, Paolo, Elena, Daniela, Tommaso, Laura, Giovanni, Federica, Cinzia, and Rudi for making every day enjoyable.
A special thank goes to *Sandro* for his crucial help and support (other than for being so funny) during endless roadtrips (with the slowest truck ever!) to retrieve stranded specimens and during necropsies that on a couple of occasions lasted the whole night. Finally, I wish to thank *Emanuele* for being always available for any necropsy-related need.

All the members of the Hof lab in the past three years:
Bridget Wicinski, for being "the" head tech (other than "the yachtwoman"). For her enthusiasm in following me everywhere I wanted to go to get more brains and for being my right hand-man when the freshest sperm whale ever decided to get stranded on the worst possible winter day.
Dara Dickstein for being a good friend when I needed it most and for teaching me that working hard is absolutely necessary to achieve our aspirations and success.
Malin Hoistad for her contagious passion on any comparative topic, for the amount of weekend hours spent discussing papers and projects, and for her availability whenever I needed it. I've learned so much from you!
Devorah Segal, for bringing positivity into the lab and making me smile no matter what mood I was in. Your ability to cope with everything the way you do will be always an unresolved mystery to me. I have no doubts you will make an excellent doctor.
Steve Stockton for his craziness and for being always willing to help. You are a character very much needed in any lab!
Jessica Walsh, for all the wild fun time we had together and for dealing with my moody days.

Hannah Brautigam, Yazmeen Afzal, Danae Papapetrou, Sandy Harry, and *Alex Kern* for making the everyday lab life fun.
Farid Hamzei- Sichami, for being a great companion late nights in the lab, and for being the most devoted fan of Camillo Golgi I will ever meet (Italians included)!
And last, but not least, *Bill Janssen* for being absolutely irreplaceable in every day troubleshooting and for introducing me to Napa Valley wine.

All the members of the Morrison lab in the past three years:
Prof. J.H. Morrison, Erik, Kim, Athena, Becca, Shannon, Dan O., Carine, Megan, Dani, Jiandong, Charles, Jeff, Dan C., Deena and the whole Department of Neuroscience of the Mount Sinai School of Medicine for making an incredibly vibrant atmosphere that inspired me to give my best every single day.

I wish to thank every collaborator that had a profound influence on my research:
Prof. Chet C. Sherwood at The George Washington University, for the discussions and critics that improved so much the VENs paper and for being constantly present, taking the time to reply promptly to as many scientific questions as one can barely cope with, even from the African continent.
Prof. John Allman at California Institute of Technology, for the long and helpful discussions on the evolution of the VENs during my stays at Caltech.
Dr. Christoph Smitz for his priceless inputs on my understanding of stereology.
Dr. Mary Ann Raghanti at Kent State University, and *Dr. Christopher J. Bonar* at Cleveland Zoo, for the donation of the pigmy hippo brain and of a series of other priceless specimens.
Prof. Joy Reidenberg for providing her amazing expertise in the necropsies of whale specimens and *Prof. Jeffrey Laitman* for his boundless knowledge of everything anatomical.
Prof. Paul Manger in South Africa, for kindly providing rare samples that added so much information to my projects and for being always available to play the devil's advocate, helping me to have a critical (and very different) perspective on my research.
Prof. Lori Marino at Emory University, for allowing me to take part as a co-author at the writing process of my first "neuroanatomy" paper and for being always present whenever I needed help.
And finally, *Dr. Joseph Erwin* for having an important impact on my understanding of the great apes research and comparative biology. Thank you for sharing your knowledge with me.

I also want to express my gratitude to The James S. McDonnell Foundation for making this research possible and every member of the McDonnell collaborative network meeting. Your constructive critics and your contagious enthusiasm meant so much to me!

I wish to thank *Amy* and *Spoc*, for being great collaborators and for working crazy hours (and endless frustrations) in the effort of trying to meet difficult deadlines for the GNI project.

A special thank to all my friends in the United States and around the world:
Athena, the sister I never had. Your strength and devotion mean so much to me. Thank you for sharing joy and sadness and for being absolutely irreplaceble (other than a perfect roommate) when I couldn't have managed to cope with everything otherwise. Thanks for sticking around when you knew I needed you and never had to ask for it. You have been my strongest supporter (sushi apart, of course!) in these last few weeks; *Giuliano*, my personal (and free of charge) guide to the Met and Moma. I didn't expect to find such a good Italian friend in NYC. Who knew that at that party at 230 5th Ave I would have found one of the people I love most?; *Megan and Christine*, two brilliant neuroscientists and among the most caring people in the world. Your incredibly open mind and your cultural background are an inspiration to me; *Sania* and *Sonia* for being always

present in my life even if on the other side of the country (Facebook is not that bad after all!); *Pallavi, Hsiu-Yu, and Elizabeth* for sharing emotions and for our future trips together; *Jake* for endless talks on our future careers and dreams; *Amir*, my coffee man. Thanks for helping me keep my caffeine level optimal in this last few weeks; *Simona,* a random roommate that became an unexpected good friend and the perfect ski buddy!; *Virginie* and *Nicole,* for making me laugh to the edge of crying innumerable times; *Katja, Nike, Najmi, Sara, Lisa, and Lodo, Christian and Suzanne* for being always present in my life, no matter what; *Valeria,* for following me in our Nepalese adventure; *Marco, and Cristiano,* for telling me at least once that they are proud of me; and finally *Angelika*, my roommate, for coping with a very stressed Cami in the past few months.

I wish to thank my parents, Guido and Enrica, for always supporting me no matter what I wanted to do and where, and my grandparents, Giuliana, Armida and Guido for surprising me in their open minded attitude when I told them I was moving to the States. Dad, thanks for always showing me your strong positivism, for trusting me and for making me believe that nothing is impossible to achieve. Mom, thanks for being always there for me and for always supporting my choices of doing what makes me happy.

Finally, my gratitude goes to New York and Ilovik, the two greatest place in the world.

Bibliography

Aggleton JP, Burton MJ, Passingham RE. 1980. Cortical and subcortical afferents to the amygdala of the rhesus monkey (*Macaca mulatta*). Brain Res 190:347-368.

Agnarsson I, May-Collado LJ. 2008. The phylogeny of Cetartiodactyla: The importance of dense taxon sampling, missing data, and the remarkable promise of cytochrome b to provide reliable species-level phylogenies. Mol Phylogenet Evol 48:964-985.

Akert K. 1948. Comparative anatomy of frontal cortex and thalamocortical connections. In: NMcGraw-Hill, editor. The Frontal Granular Cortex and Behavior. New York. p 372-396.

Alexander GE, DeLong MR, Strick PL. 1986. Parallel organization of functionally segregated circuits linking basal ganglia and cortex. Annu Rev Neurosci 9:357-381.

Allman J, Hakeem A, Watson K. 2002. Two phylogenetic specializations in the human brain. Neuroscientist 8:335-346.

Allman JM, Hakeem A, Erwin JM, Nimchinsky EA, Hof PR. 2001. The anterior cingulate cortex. The evolution of an interface between emotion and cognition. Ann NY Acad Sci 935:107-117.

Allman JM, Tetreault NA, Hakeem AY, Kaufman JA, Manaye KF, Griffith H, Semendeferi K, Erwin JM, Goubert V, Hof P. The von Economo neurons in frontoinsular and anterior cingulated cortex in great apes and humans. In preparation.

Allman JM, Watson KK, Tetreault NA, Hakeem AY. 2005. Intuition and autism: a possible role for Von Economo neurons. Trends Cogn Sci 9:367-373.

Amaral DG, Price JL. 1984. Amygdalo-cortical projections in the monkey (*Macaca fascicularis*). J Comp Neurol 230:465-496.

Amunts K, Schleicher A, Ditterich A, Zilles K. 2003. Broca's region: cytoarchitectonic asymmetry and developmental changes. J Comp Neurol 465:72-89.

Andersen BB, Gundersen HJ. 1999. Pronounced loss of cell nuclei and anisotropic deformation of thick sections. J Microsc 196:69-73.

Andressen C, Blümcke I, Celio MR. 1993. Calcium-binding proteins: Selective markers of nerve cells. Cell Tissue Res 271:181-208.

Araque A, Parpura V, Sanzgiri RP, Haydon PG. 1999. Tripartite synapses: Glia, the unacknowledged partner. Trends Neurosci 22:208-215.

Arikuni T, Watanabe K, Kubota K. 1988. Connections of area 8 with area 6 in the brain of the macaque monkey. J Comp Neurol 277:21-40.

Aubert A, Costalat R, Magistretti PJ, Pellerin L. 2005. Brain lactate kinetics: Modeling evidence for neuronal lactate uptake upon activation. Proc Natl Acad Sci USA 102:16448-16453.

Augustine JR. 1996. Circuitry and functional aspects of the insular lobe in primates including humans. Brain Res Rev 22:229-244.

Baimbridge KG, Celio MR, Rogers JH. 1992. Calcium-binding proteins in the nervous system. Trends Neurosci 15:303-308.

Baleydier C, Mauguière F. 1980. The duality of the cingulate gyrus in monkey. Neuroanatomical study and functional hypothesis. Brain 103):525-554.

Balfour D, Balfour S. 1997. African Elephants: Abbeville Press, New York, NY.

Bamiou DE, Musiek FE, Luxon LM. 2003. The insula (Island of Reil) and its role in auditory processing. Literature review. Brain Res Rev 42:143-154.

Barbas H. 1988. Anatomic organization of basoventral and mediodorsal visual recipient prefrontal regions in the rhesus monkey. J Comp Neurol 276:313-342.

Barbas H. 1995. Anatomic basis of cognitive-emotional interactions in the primate prefrontal cortex. Neurosci Biobehav Rev 19:499-510.

Barbas H. 2000. Complementary roles of prefrontal cortical regions in cognition, memory, and emotion in primates. Adv Neurol 84:87-110.
Barbas H, Blatt GJ. 1995. Topographically specific hippocampal projections target functionally distinct prefrontal areas in the rhesus monkey. Hippocampus 5:511-533.
Barbas H, De Olmos J. 1990. Projections from the amygdala to basoventral and mediodorsal prefrontal regions in the rhesus monkey. J Comp Neurol 300:549-571.
Barbas H, Ghashghaei H, Dombrowski SM, Rempel-Clower NL. 1999. Medial prefrontal cortices are unified by common connections with superior temporal cortices and distinguished by input from memory-related areas in the rhesus monkey. J Comp Neurol 410:343-367.
Barbas H, Henion TH, Dermon CR. 1991. Diverse thalamic projections to the prefrontal cortex in the rhesus monkey. J Comp Neurol 313:65-94.
Barbas H, Mesulam MM. 1981. Organization of afferent input to subdivisions of area 8 in the rhesus monkey. J Comp Neurol 200:407-431.
Barbas H, Mesulam MM. 1985. Cortical afferent input to the principalis region of the rhesus monkey. Neuroscience 15):619-637.
Barbas H, Pandya DN. 1987. Architecture and frontal cortical connections of the premotor cortex (area 6) in the rhesus monkey. J Comp Neurol 256:211-228.
Barbas H, Pandya DN. 1989. Architecture and intrinsic connections of the prefrontal cortex in the rhesus monkey. J Comp Neurol 286:353-375.
Barbas H, Saha S, Rempel-Clower N, Ghashghaei T. 2003. Serial pathways from primate prefrontal cortex to autonomic areas may influence emotional expression. BMC Neurosci 4:25.
Barres BA, Hart IK, Coles HS, Burne JF, Voyvodic JT, Richardson WD, Raff MC. 1992. Cell death and control of cell survival in the oligodendrocyte lineage. Cell 70:31-46.
Barres BA, Raff MC. 1993. Proliferation of oligodendrocyte precursor cells depends on electrical activity in axons. Nature 361:258-260.
Barres BA, Raff MC. 1999. Axonal control of oligodendrocyte development. J Cell Biol 147:1123-1128.
Bates JF, Goldman-Rakic PS. 1993. Prefrontal connections of medial motor areas in the rhesus monkey. J Comp Neurol 336:211-228.
Baumann N, Pham-Dinh D. 2001. Biology of oligodendrocyte and myelin in the mammalian central nervous system. Physiol Rev 81:871-927.
Beckmann M, Johansen-Berg H, Rushworth MF. 2009. Connectivity-based parcellation of human cingulate cortex and its relation to functional specialization. J Neurosci 29:1175-1190.
Behrmann G. 1993. Cytoarchitectonic studies of the cerebral cortex of the harbour porpoise, *Phocoena phocoena* (Linné, 1758). Invest Cetacea 24:261-285.
Belichenko PV, Vogt Weisenhorn DM, Myklossy J, Celio MR. 1995. Calretinin-positive Cajal-Retzius cells persist in the adult human neocortex. NeuroReport 6:1869-1874.
Berger B, Alvarez C. 1996. Neurochemical development of the hippocampal region in the fetal rhesus monkey. III: Calbindin-D28K, calretinin and parvalbumin with special mention of cajal-retzius cells and the retrosplenial cortex. J Comp Neurol 366:674-699.
Berthoz S, Armony JL, Blair RJ, Dolan RJ. 2002. An fMRI study of intentional and unintentional (embarrassing) violations of social norms. Brain 125:1696-1708.
Bertrand I. 1930. Techniques histologiques de neuropathologie. Paris: Masson.
Bianucci G, Landini, W. 2006. Killer sperm whale: A new basal physeteroid (Mammalia: Cetacea) from the late Miocene of Italy. Zool J Linn Soc 148:103-131.
Biber MP, Kneisley LW, LaVail JH. 1978. Cortical neurons projecting to the cervical and lumbar enlargements of the spinal cord in young and adult rhesus monkeys. Exp Neurol 59:492-508.

Blinkov S, Glezer, II. 1968. The Human Brain in Figures and Tables. A Quantitative Handbook. New York: Plenum Press.
Boisserie JR, Lihoreau F, Brunet M. 2005. The position of Hippopotamidae within Cetartiodactyla. Proc Natl Acad Sci USA 102:1537-1541.
Bowley MP, Drevets WC, Öngür D, Price JL. 2002. Low glial numbers in the amygdala in major depressive disorder. Biol Psychiatry 52:404-412.
Breathnach AS. 1960. The cetacean central nervous system. Biol Rev 35:187-230.
Breathnach AS, Goldby F. 1954. The amygdaloid nuclei, hippocampus and other parts of the rhinencephalon in the porpoise (*Phocaena phocaena*). J Anat 88:267-291.
Broca P. 1878. Anatomie comparée des circonvolutions cérébrales: Le grande lobe limbique et la scissure limbique dans la série des mammifères. Rev Antropol Ser 21:384-498.
Brodmann K. 1905. Beitrage zur histologischen Lokalisation der Grosshirnrinde. III. Mitteilung: Die Rindenfelder der niederen Affen. J Psychol Neurol 4:177-266.
Brodmann K. 1909. Vergleichende Lokalisationslehre der Grosshirnrhinde. Leipzig: Barth.
Bromham L, Phillips MJ, Penny D. 1999. Growing up with dinosaurs: Molecular dates and the mammalian radiation. Trends Ecol Evol 14:113-118.
Bunney WE, Bunney BG. 2000. Evidence for a compromised dorsolateral prefrontal cortical parallel circuit in schizophrenia. Brain Res Rev 31:138-146.
Bush G, Frazier JA, Rauch SL, Seidman LJ, Whalen PJ, Jenike MA, Rosen BR, Biederman J. 1999. Anterior cingulate cortex dysfunction in attention-deficit/hyperactivity disorder revealed by fMRI and the counting Stroop. Biol Psychiatry 45:1542-1552.
Bush G, Luu P, Posner MI. 2000. Cognitive and emotional influences in anterior cingulate cortex. Trends Cogn Sci 4:215-222.
Bush G, Whalen PJ, Rosen BR, Jenike MA, McInerney SC, Rauch SL. 1998. The counting Stroop: an interference task specialized for functional neuroimaging — validation study with functional MRI. Hum Brain Mapp 6:270-282.
Bussière T, Giannakopoulos P, Bouras C, Perl DP, Morrison JH, Hof PR. 2003. Progressive degeneration of nonphosphorylated neurofilament protein-enriched pyramidal neurons predicts cognitive impairment in Alzheimer's disease: Stereologic analysis of prefrontal cortex area 9. J Comp Neurol 463(3):281-302.
Bussière T, Gold G, Kövari E, Giannakopoulos P, Bouras C, Perl DP, Morrison JH, Hof PR. 2003. Stereologic analysis of neurofibrillary tangle formation in prefrontal cortex area 9 in aging and Alzheimer's disease. Neurosci 117(3):577-592.
Butti C, Sherwood CC, Hakeem AY, Allman JM, Hof PR. 2009. Total number and volume of Von Economo neurons in the cerebral cortex of cetaceans. J Comp Neurol 515:243-259.
Calhoun S, Thompson, RL. 1988. Long-term retention of self-recognition by chimpanzees. Am J Primatol 15:361-365.
Carmichael ST, Price JL. 1995. Limbic connections of the orbital and medial prefrontal cortex in macaque monkeys. J Comp Neurol 363:615-641.
Carmichael ST, Price JL. 1995. Sensory and premotor connections of the orbital and medial prefrontal cortex of macaque monkeys. J Comp Neurol 363:642-664.
Carmichael ST, Price JL. 1996. Connectional networks within the orbital and medial prefrontal cortex of macaque monkeys. J Comp Neurol 371:179-207.
Casanova MF. 1997. Functional and anatomical aspects of prefrontal pathology in schizophrenia. Schizophr Bull 23:517-519.
Cavada C, Company T, Tejedor J, Cruz-Rizzolo RJ, Reinoso-Suarez F. 2000. The anatomical connections of the macaque monkey orbitofrontal cortex. A review. Cereb Cortex 10:220-242.

Cavada C, Goldman-Rakic PS. 1989. Posterior parietal cortex in rhesus monkey: I. Parcellation of areas based on distinctive limbic and sensory corticocortical connections. J Comp Neurol 287:393-421.

Cavada C, Reinoso-Suarez F. 1985. Topographical organization of the cortical afferent connections of the prefrontal cortex in the cat. J Comp Neurol 242:293-324.

Christensen JR, Larsen KB, Lisanby SH, Scalia J, Arango V, Dwork AJ, Pakkenberg B. 2007. Neocortical and hippocampal neuron and glial cell numbers in the rhesus monkey. Anat Rec 290:330-340.

Clementz M, Goswami A, Gingerich PD, Coch PL. 2006. Isotopic records from early whales and sea cows: Contrasting patterns of ecological transition. J Verteb Paleontol 26:355-370.

Coles JA, Abbott NJ. 1996. Signalling from neurones to glial cells in invertebrates. Trends Neurosci 19:358-362.

Condé F, Lund JS, Jacobowitz DM, Baimbridge KG, Lewis DA. 1994. Local circuit neurons immunoreactive for calretinin, calbindin D-28k or parvalbumin in monkey prefrontal cortex: Distribution and morphology. J Comp Neurol 341:95-116.

Connor R, Smolker, RA. 1996. "Pop" goes the dolphin: A vocalization male bottlenose dolphins produce during consortships. Behavior 133:643-662.

Connor R, Wells, RS, Mann, J, Read AJ. 2000. The Bottlenose dolphin. Social relationships in a fission-fusion society. In: Mann J, Connor, RC, Tyack, PL, Whitehead H, editor. Cetacean Societies. Chicago: University of Chicago Press.

Connor RC. 2007. Dolphin social intelligence: Complex alliance relationships in bottlenose dolphins and a consideration of selective environments for extreme brain size evolution in mammals. Philos Trans R Soc Lond 362:587-602.

Connor RC, Norris K. 1982. Are dolphins reciprocal altruists? Am Nat 119:358-374.

Connor RC, Smolker R. 1985. Habituated dolphins (*Tursiops spp*) in Western Australia. J Mammal 66:398-400.

Connor RC, Smolker RA, Richards AF. 1992. Two levels of alliance formation among male bottlenose dolphins (*Tursiops sp.*). Proc Natl Acad Sci USA 89:987-990.

Corbetta M, Miezin FM, Dobmeyer S, Shulman GL, Petersen SE. 1991. Selective and divided attention during visual discriminations of shape, color, and speed: Functional anatomy by positron emission tomography. J Neurosci 11:2383-2402.

Craig AD. 2002. How do you feel? Interoception: The sense of the physiological condition of the body. Nat Rev Neurosci 3:655-666.

Craig AD. 2003. Interoception: The sense of the physiological condition of the body. Curr Opin Neurobiol 13:500-505.

Craig AD. 2004. Human feelings: Why are some more aware than others? Trends Cogn Sci 8:239-241.

Craig AD. 2008. Retrograde analyses of spinothalamic projections in the macaque monkey: input to the ventral lateral nucleus. J Comp Neurol 508:315-328.

Craig AD. 2009. How do you feel — now? The anterior insula and human awareness. Nat Rev Neurosci 10:59-70.

Craig AD, Reiman EM, Evans A, Bushnell MC. 1996. Functional imaging of an illusion of pain. Nature 384:258-260.

Critchley HD. 2005. Neural mechanisms of autonomic, affective, and cognitive integration. J Comp Neurol 493:154-166.

Critchley HD, Wiens S, Rotshtein P, Ohman A, Dolan RJ. 2004. Neural systems supporting interoceptive awareness. Nat Neurosci 7:189-195.

Dahl D, Bignami A. 1973. Immunochemical and immunofluorescence studies of the glial fibrillary acidic protein in vertebrates. Brain Res 61:279-293.

Dalgarno D, Klevit, RE, Levine, BA, Williams, RJP. 1984. The calcium receptor and trigger. Trends Pharmacol Sci 4:266-271.
Deecke VB, Ford JK, Spong P. 2000. Dialect change in resident killer whales: Implications for vocal learning and cultural transmission. Anim Behav 60:629-638.
DeFelipe J. 1993. Neocortical neuronal diversity: chemical heterogeneity revealed by colocalization studies of classic neurotransmitters, neuropeptides, calcium-binding proteins, and cell surface molecules. Cereb Cortex 3(4):273-289.
DeFelipe J. 1997. Types of neurons, synaptic connections and chemical characteristics of cells immunoreactive for calbindin-D28K, parvalbumin and calretinin in the neocortex. J Chem Neuroanat 14:1-19.
DeFelipe J, Hendry SH, Jones EG. 1989. Visualization of chandelier cell axons by parvalbumin immunoreactivity in monkey cerebral cortex. Proc Natl Acad Sci USA 86:2093-2097.
Delfour F, Marten K. 2001. Mirror image processing in three marine mammal species: Killer whales (*Orcinus orca*), false killer whales (*Pseudorca crassidens*), and California sea lions (*Zalophus californianus*). Behav Process 53:181-190.
D'Esposito M, Detre JA, Alsop DC, Shin RK, Atlas S, Grossman M. 1995. The neural basis of the central executive system of working memory. Nature 378:279-281.
Devinsky O, Morrell MJ, Vogt BA. 1995. Contributions of anterior cingulate cortex to behaviour. Brain 118:279-306.
Devue C, Collette F, Balteau E, Degueldre C, Luxen A, Maquet P, Bredart S. 2007. Here I am: The cortical correlates of visual self-recognition. Brain Res 1143:169-182.
Dickstein DL, Kabaso D, Rocher AB, Luebke JI, Wearne SL, Hof PR. 2007. Changes in the structural complexity of the aged brain. Aging cell 6(3):275-284.
Ding W, Wursig, B, Evans, WE. 1995. Whistles of bottlenose dolphins: comparisons among populations. Aquatic Mamm 21:65-77.
Divac I, Bjorklund A, Lindvall O, Passingham RE. 1978. Converging projections from the mediodorsal thalamic nucleus and mesencephalic dopaminergic neurons to the neocortex in three species. J Comp Neurol 180:59-71.
Dombrowski SM, Hilgetag CC, Barbas H. 2001. Quantitative architecture distinguishes prefrontal cortical systems in the rhesus monkey. Cereb Cortex 11:975-988.
Driesen NR, Leung HC, Calhoun VD, Constable RT, Gueorguieva R, Hoffman R, Skudlarski P, Goldman-Rakic PS, Krystal JH. 2008. Impairment of working memory maintenance and response in schizophrenia: Functional magnetic resonance imaging evidence. Biol Psychiatry 64:1026-1034.
Duan H, Wearne SL, Rocher AB, Macedo A, Morrison JH, Hof PR. 2003. Age-related dendritic and spine changes in corticocortically projecting neurons in macaque monkeys. Cereb Cortex 13:950-961.
Dyer CA, Hickey WF, Geisert EE Jr. 1991. Myelin/oligodendrocyte-specific protein: a novel surface membrane protein that associates with microtubules. J Neurosci Res 28:607-613.
Dyer CA, Matthieu JM. 1994. Antibodies to myelin/oligodendrocyte-specific protein and myelin/oligodendrocyte glycoprotein signal distinct changes in the organization of cultured oligodendroglial membrane sheets. J Neurochem 62:777-787.
Edds-Walton P. 1997. Acoustic communication signals of mysticetes whales. Bioacoustics 8:47-60.
Eickhoff SB, Schleicher A, Zilles K, Amunts K. 2006. The human parietal operculum. I. Cytoarchitectonic mapping of subdivisions. Cereb Cortex 16:254-267.
Eltringham S. 1999. The Hippos: Natural History and Conservation. London: Academic Press.
Eriksen N, Pakkenberg B. 2007. Total neocortical cell number in the mysticete brain. Anat Rec 290:83-95.

Fajardo C, Escobar MI, Buritica E, Arteaga G, Umbarila J, Casanova MF, Pimienta H. 2008. Von Economo neurons are present in the dorsolateral (dysgranular) prefrontal cortex of humans. Neurosci Lett 435:215-218.

Felleman DJ, Van Essen DC. 1991. Distributed hierarchical processing in the primate cerebral cortex. Cereb Cortex 1:1-47.

Ferry AT, Öngür D, An X, Price JL. 2000. Prefrontal cortical projections to the striatum in macaque monkeys: evidence for an organization related to prefrontal networks. J Comp Neurol 425:447-470.

Filimonoff IN. 1965. On the so-called rhinencephalon in the dolphin. J Hirnforsch 8:1-23.

Fitzgerald E. 2006. A bizarre new toothed mysticete (Cetacea) from Australia and the early evolution of baleen whales. Proc R Acad Sci B 273:2955-2963.

Fordyce R. 2008. Cetacean Evolution. In: Perrin WF WB, Thewissen JGM, editor. Encyclopedia of Marine Mammals. San Diego: Academic Press. p 201-207.

Fordyce RE. 2008. Cetacean Fossil Record. In: Perrin WF WB, Thewissen JGM, editor. Encyclopedia of Marine Mammals. San Diego: Academic Press. p 207-215.

Fordyce RE. 2002. *Simocetus rayi* (Odontoceti: Simocetidae)(new species, new genus, new family), a bizarre new archaic Oligocene dolphin from the Eastern North Pacific. Smithsonian Contrib Paleobiol 93:185-222.

Freedman LJ, Insel TR, Smith Y. 2000. Subcortical projections of area 25 (subgenual cortex) of the macaque monkey. J Comp Neurol 421:172-188.

Friede R. 1954. [Quantitative share of the glia in development of the cortex.]. Acta Anat 20:290-296.

Friede RL. 1963. The relationship of body size, nerve cell size, axon length, and glial density in the cerebellum. Proc Natl Acad Sci USA 49:187-193.

Friede RL, Van Houten WH. 1962. Neuronal extension and glial supply: functional significance of glia. Proc Natl Acad Sci USA 48:817-821.

Funahashi S, Bruce CJ, Goldman-Rakic PS. 1989. Mnemonic coding of visual space in the monkey's dorsolateral prefrontal cortex. Journal Neurophysiol 61:331-349.

Funahashi S, Bruce CJ, Goldman-Rakic PS. 1993. Dorsolateral prefrontal lesions and oculomotor delayed-response performance: evidence for mnemonic "scotomas". J Neurosci 13:1479-1497.

Fung C, Schleicher A, Kowalski T, Oelschläger HH. 2005. Mapping auditory cortex in the La Plata dolphin (*Pontoporia blainvillei*). Brain Res Bull 66:353-356.

Furutani R. 2008. Laminar and cytoarchitectonic features of the cerebral cortex in the Risso's dolphin (*Grampus griseus*), striped dolphin (*Stenella coeruleoalba*), and bottlenose dolphin (*Tursiops truncatus*). J Anat 213:241-248.

Fuster JM. 1993. Frontal lobes. Curr Opin Neurobiol 3:160-165.

Gallup G. 1970. Chimpanzees: Self-recognition. Science 167:86-87.

Gallup GG, McClure, MK, Hill, SD, Bundy,RA. 1971. Capacity for self-recognition in differentially reared chimpanzees. Psychol Rec 21:69-74.

Gallup GG. 1977. Absence of self-recognition in a monkey (*Macaca fascicularis*) following prolonged exposure to a mirror. Dev Psychobiol 10:281-284.

Gallup GG. 1982. Self-awareness and the emergence of mind in primates. Am J Primatol 2:237-248.

Gallup GG. 1985. Do minds exist in species other than our own? Neurosci Biobehav Rev 9:631-641.

Gallup GG, Jr., Wallnau LB, Suarez SD. 1980. Failure to find self-recognition in mother-infant and infant-infant rhesus monkey pairs. Folia Primatol 33:210-219.

Garey LJ, Leuba G. 1986. A quantitative study of neuronal and glial numerical density in the visual cortex of the bottlenose dolphin: Evidence for a specialized subarea and changes with age. J Comp Neurol 247:491-496.

Garey LJ, Takacs J, Revishchin AV, Hamori J. 1989. Quantitative distribution of GABA-immunoreactive neurons in cetacean visual cortex is similar to that in land mammals. Brain Res 485:278-284.

Gatesy J. 1997. More DNA support for a Cetacea/Hippopotamidae clade: the blood-clotting protein gene γ-fibrinogen. Mol Biol Evol 14:537-543.

Geisler G, Sanders AE. 2003. Morphological evidence for the phylogeny of Cetacea. J Mamm Evol 10:23-129.

Geisler G, Uhen, MD. 2003. Morphological support for a close relationship between hippos and whales. J Verteb Paleontol 23:991-996.

Ghashghaei HT, Hilgetag CC, Barbas H. 2007. Sequence of information processing for emotions based on the anatomic dialogue between prefrontal cortex and amygdala. NeuroImage 34:905-923.

Giguere M, Goldman-Rakic PS. 1988. Mediodorsal nucleus: Areal, laminar, and tangential distribution of afferents and efferents in the frontal lobe of rhesus monkeys. J Comp Neurol 277:195-213.

Gihr M, Pilleri, G. 1969. Hirn-Körpergewichts-Beziehungen bei Cetaceen. Invest Cetacea 1:109-126.

Gilbert CD. 1983. Microcircuitry of the visual cortex. Ann Rev Neurosci 6:217-247.

Gingerich PD, Uhen MD. 1998. Likelihood estimation of the time of origin of cetacean and the time of divergence of Cetacea and Artiodactyla. Palaeo-Electronica 2:1-47.

Gingerich PD. 2005. Cetacea. In: KD Rose AJ, editor. Placental Mammals: Origin, Timing and Relationship of the Major Extant Clades. Baltimore: John Hopkins University Press. p 234-252.

Gingerich PD, ul-Haq M, Zalmout IS, Khan IH, Malkani MS. 2001. Origin of whales from early artiodactyls: hands and feet of Eocene Protocetidae from Pakistan. Science 293:2239-2242.

Glezer, II, Hof PR, Leranth C, Morgane PJ. 1993. Calcium-binding protein-containing neuronal populations in mammalian visual cortex: A comparative study in whales, insectivores, bats, rodents, and primates. Cereb Cortex 3:249-272.

Glezer, II, Hof PR, Morgane PJ. 1992. Calretinin-immunoreactive neurons in the primary visual cortex of dolphin and human brains. Brain Res 595:181-188.

Glezer, II, Hof PR, Morgane PJ. 1998. Comparative analysis of calcium-binding protein-immunoreactive neuronal populations in the auditory and visual systems of the bottlenose dolphin (*Tursiops truncatus*) and the macaque monkey (*Macaca fascicularis*). J Chem Neuroanat15:203-237.

Glezer, II, Morgane PJ. 1990. Ultrastructure of synapses and Golgi analysis of neurons in neocortex of the lateral gyrus (visual cortex) of the dolphin and pilot whale. Brain Res Bull 24:401-427.

Glezer, II, Morgane PJ. 1993. Primate brain measurements. Science 261:277-278.

Glezer II. 2002. Neural morphology. In: AR H, editor. Marine Mammal Biology: An Evolutionary Approach: Malden: Blackwell Science Ltd. p 98-115.

Goldman-Rakic, PS. 1988. Topography of cognition: Parallel distributed networks in primate association cortex. Ann Rev Neurosci 11:137-156.

Goldman-Rakic PS, Porrino LJ. 1985. The primate mediodorsal (MD) nucleus and its projection to the frontal lobe. J Comp Neurol 242:535-560.

Goldman-Rakic PS, Selemon LD. 1997. Functional and anatomical aspects of prefrontal pathology in schizophrenia. Schizophr Bull 23:437-458.

Goldman-Rakic, PS. 1995. Cellular basis of working memory. Neuron 14(3):477-485.

Gonchar Y, Burkhalter A. 1997. Three distinct families of GABAergic neurons in rat visual cortex. Cereb Cortex 7:347-358.

Gordon GR, Baimoukhametova DV, Hewitt SA, Rajapaksha WR, Fisher TE, Bains JS. 2005. Norepinephrine triggers release of glial ATP to increase postsynaptic efficacy. Nat Neurosci 8:1078-1086.

Graybiel AM, Aosaki T, Flaherty AW, Kimura M. 1994. The basal ganglia and adaptive motor control. Science 265:1826-1831.

Gundersen HJG. 1988. The nucleator. J Microsc 151:3-21.

Haber SN, Kunishio K, Mizobuchi M, Lynd-Balta E. 1995. The orbital and medial prefrontal circuit through the primate basal ganglia. J Neurosci 15:4851-4867.

Hakak Y, Walker JR, Li C, Wong WH, Davis KL, Buxbaum JD, Haroutunian V, Fienberg AA. 2001. Genome-wide expression analysis reveals dysregulation of myelination-related genes in chronic schizophrenia. Proc Natl Acad Sci USA 98:4746-4751.

Hakeem AY, Sherwood CC, Bonar CJ, Butti C, Hof PR, Allman JM. 2009. Von Economo neurons in the elephant brain. Anat Rec 292:242-248.

Hamilton LS, Altshuler LL, Townsend J, Bookheimer SY, Phillips OR, Fischer J, Woods RP, Mazziotta JC, Toga AW, Nuechterlein KH, Narr KL. 2009. Alterations in functional activation in euthymic bipolar disorder and schizophrenia during a working memory task. Hum Brain Mapp in press.

Harley HE, Roitblat HL, Nachtigall PE. 1996. Object representation in the bottlenose dolphin (*Tursiops truncatus*): integration of visual and echoic information. J Exp Psychol Anim Behav Process 22:164-174.

Hatanaka N, Tokuno H, Hamada I, Inase M, Ito Y, Imanishi M, Hasegawa N, Akazawa T, Nambu A, Takada M. 2003. Thalamocortical and intracortical connections of monkey cingulate motor areas. J Comp Neurol 462:121-138.

Haug H. 1987. Brain sizes, surfaces, and neuronal sizes of the cortex cerebri: A stereological investigation of man and his variability and a comparison with some mammals (primates, whales, marsupials, insectivores, and one elephant). Am J Anat 180:126-142.

Hawkins A, Olszewski J. 1957. Glia/nerve cell index for cortex of the whale. Science 126:76-77.

Haydon PG. 2001. Glia: Listening and talking to the synapse. Nat Rev Neurosci 2:185-193.

Haydon PG, Carmignoto G. 2006. Astrocyte control of synaptic transmission and neurovascular coupling. Physiol Rev 86:1009-1031.

Helweg D, Cato, DH, Jerkins PF, Garrigue, C, McCauley, RD. 1998. Geographic variation in south Pacific humpback whales songs. Behav Brain Sci 135:1-27.

Hendry SH, Jones EG. 1991. GABA neuronal subpopulations in cat primary auditory cortex: co-localization with calcium binding proteins. Brain Res 543:45-55.

Hendry SH, Jones EG, Emson PC, Lawson DE, Heizmann CW, Streit P. 1989. Two classes of cortical GABA neurons defined by differential calcium binding protein immunoreactivities. Exp Brain Res 76:467-472.

Hao J, Rapp PR, Janssen WGM, Lou W, Lasley BL, Hof PR, Morrison JH. 2007. Interactive effects of age and estrogen on cognition and pyramidal neurons in monkey prefrontal cortex. Proc Natl Acad Sci USA 104:11465-11470.

Hao J, Rapp PR, Leffler AE, Leffler SR, Janssen WGM, Lou W, McKay H, Roberts JA, Wearne SL, Hof PR, Morrison JH. 2006. Estrogen alters spine number and morphology in prefrontal cortex of aged female rhesus monkeys. J Neurosci 26:2571-2578.

Herculano-Houzel S, Lent R. 2005. Isotropic fractionator: A simple, rapid method for the quantification of total cell and neuron numbers in the brain. J Neurosci 25:2518-2521.

Herman L. 1975. Interference and short-term memory in the bottlenose dolphin. Anim Learn Behav 3:43-48.

Herman L. 1980. Cognitive characteristics of dolphins. In: Herman L, editor. Cetacean Behavior: Mechanisms and Functions: New York: Wiley and Sons.

Herman LM, Abichandani SL, Elhajj AN, Herman EY, Sanchez JL, Pack AA. 1999. Dolphins (*Tursiops truncatus*) comprehend the referential character of the human pointing gesture. J Comp Psychol 113:347-364.

Herman LM, Kuczaj SA 2nd, Holder MD. 1993. Responses to anomalous gestural sequences by a language-trained dolphin: Evidence for processing of semantic relations and syntactic information. J Exp Psychol 122:184-194.

Herman LM, Pack AA, Hoffmann-Kuhnt M. 1998. Seeing through sound: dolphins (*Tursiops truncatus*) perceive the spatial structure of objects through echolocation. J Comp Psychol 112:292-305.

Herman LM, Richards DG, Wolz JP. 1984. Comprehension of sentences by bottlenose dolphins. Cognition 16:129-219.

Hof PR, Bogaert YE, Rosenthal RE, Fiskum G. 1996. Distribution of neuronal populations containing neurofilament protein and calcium-binding proteins in the canine neocortex: Regional analysis and cell typology. J Chem Neuroanat 11:81-98.

Hof PR, Chanis R, Marino L. 2005. Cortical complexity in cetacean brains. Anat Rec 287:1142-1152.

Hof PR, Glezer, II, Archin N, Janssen WG, Morgane PJ, Morrison JH. 1992. The primary auditory cortex in cetacean and human brain: A comparative analysis of neurofilament protein-containing pyramidal neurons. Neurosci Lett 146:91-95.

Hof PR, Glezer, II, Condé F, Flagg RA, Rubin MB, Nimchinsky EA, Vogt Weisenhorn DM. 1999. Cellular distribution of the calcium-binding proteins parvalbumin, calbindin, and calretinin in the neocortex of mammals: Phylogenetic and developmental patterns. J Chem Neuroanat 16:77-116.

Hof PR, Glezer, II, Nimchinsky EA, Erwin JM. 2000a. Neurochemical and cellular specializations in the mammalian neocortex reflect phylogenetic relationships: Evidence from primates, cetaceans, and artiodactyls. Brain Behav Evol 55:300-310.

Hof PR, Glezer, II, Revishchin AV, Bouras C, Charnay Y, Morgane PJ. 1995a. Distribution of dopaminergic fibers and neurons in visual and auditory cortices of the harbor porpoise and pilot whale. Brain Res Bull 36:275-284.

Hof PR, Haroutunian V, Copland C, Davis KL, Buxbaum JD. 2002. Molecular and cellular evidence for an oligodendrocyte abnormality in schizophrenia. Neurochem Res 27(10):1193-1200.

Hof PR, Haroutunian V, Friedrich VL Jr., Byne W, Buitron C, Perl DP, Davis KL. 2003. Loss and altered spatial distribution of oligodendrocytes in the superior frontal gyrus in schizophrenia. Biol Psychiatry 53:1075-1085.

Hof PR, Morrison JH. 2004. The aging brain: morphomolecular senescence of cortical circuits. Trends Neurosci 27:607-613.

Hof PR, Mufson EJ, Morrison JH. 1995b. Human orbitofrontal cortex: cytoarchitecture and quantitative immunohistochemical parcellation. J Comp Neurol 359:48-68.

Hof PR, Nimchinsky EA. 1992. Regional distribution of neurofilament and calcium-binding proteins in the cingulate cortex of the macaque monkey. Cereb Cortex 2:456-467.

Hof PR, Nimchinsky EA, Young WG, Morrison JH. 2000b. Numbers of meynert and layer IVB cells in area V1: A stereologic analysis in young and aged macaque monkeys. J Comp Neurol 420:113-126.

Hof PR, Rosenthal RE, Fiskum G. 1996. Distribution of neurofilament protein and calcium-binding proteins parvalbumin, calbindin, and calretinin in the canine hippocampus. J Chem Neuroanat 11:1-12.

Hof PR, Sherwood CC. 2005. Morphomolecular neuronal phenotypes in the neocortex reflect phylogenetic relationships among certain mammalian orders. Anat Rec 287:1153-1163.
Hof PR, Van der Gucht E. 2007. Structure of the cerebral cortex of the humpback whale, *Megaptera novaeangliae* (Cetacea, Mysticeti, Balaenopteridae). Anat Rec 290:1-31.
Hooper S, Reiss, DR, Carter, M, MCCowan, B. 2006. Importance of contextual saliency on vocal imitation by bottlenose dolphins. Int J Comp Psycol 19:116-128.
Horner PJ, Palmer TD. 2003. New roles for astrocytes: The nightlife of an 'astrocyte'. La vida loca! Trends Neurosci 26:597-603.
Ishibashi T, Dakin KA, Stevens B, Lee PR, Kozlov SV, Stewart CL, Fields RD. 2006. Astrocytes promote myelination in response to electrical impulses. Neuron 49:823-832.
Ishii K, Yamaji S, Kitagaki H, Imamura T, Hirono N, Mori E. 1999. Regional cerebral blood flow difference between dementia with Lewy bodies and AD. Neurology 53:413-416.
Jacobowitz DM, Winsky L. 1991. Immunocytochemical localization of calretinin in the forebrain of the rat. J Comp Neurol 304:198-218.
Jacobs M, Galaburda, AM, McFarland, WL, Morgane, PJ.. 1984. The insular formations of the dolphin brain: quantitative cytoarchitectonic studies of the insular component of the limbic lobe. J Comp Neurol 225:396-432.
Jacobs MS, McFarland WL, Morgane PJ. 1979. The anatomy of the brain of the bottlenose dolphin (*Tursiops truncatus*). Rhinic lobe (Rhinencephalon): The archicortex. Brain Res Bull 4 Suppl 1:1-108.
Jacobs MS, Morgane PJ, McFarland WL. 1971. The anatomy of the brain of the bottlenose dolphin (*Tursiops truncatus*). Rhinic lobe (rhinencephalon). I. The paleocortex. J Comp Neurol 141:205-271.
Janik V, Denhardt, G, Todt, D. 1994. Signature whistle variation in a bottlenose dolphin, *Tursiops truncatus*. Behav Ecol Sociobiol 35:243-248.
Janik VM. 2000. Food-related bray calls in wild bottlenose dolphins (*Tursiops truncatus*). Proc Biol Soc267:923-927.
Jehee JF, Murre JM. 2008. The scalable mammalian brain: emergent distributions of glia and neurons. Biol Cybern 98:439-445.
Jerison H. 1973. Evolution of the brain and intelligence: Academic Press, New York.
Joel D, Weiner I. 1994. The organization of the basal ganglia-thalamocortical circuits: Open interconnected rather than closed segregated. Neuroscience 63:363-379.
Johnson TN, Rosvold HE, Mishkin M. 1968. Projections from behaviorally-defined sectors of the prefrontal cortex to the basal ganglia, septum, and diencephalon of the monkey. Exp Neurol 21:20-34.
Jürgens U. 1983. Afferent fibers to the cingular vocalization region in the squirrel monkey. Experimental neurology 80:395-409.
Kabaso D, Coskren PJ, Henry BI, Hof PR, Wearne SL. 2009. The electrotonic structure of pyramidal neurons contributing to prefrontal cortical circuits in macaque monkeys is significantly altered in aging. Cereb Cortex. In press.
Kang J, Jiang L, Goldman SA, Nedergaard M. 1998. Astrocyte-mediated potentiation of inhibitory synaptic transmission. Nat Neurosci 1:683-692.
Karnath HO, Baier B, Nagele T. 2005. Awareness of the functioning of one's own limbs mediated by the insular cortex? J Neurosci 25:7134-7138.
Kaufman JA, Paul LK, Manaye KF, Granstedt AE, Hof PR, Hakeem AY, Allman JM. 2008. Selective reduction of Von Economo neuron number in agenesis of the corpus callosum. Acta Neuropathol 116:479-489.
Kellogg ME, Burkett S, Dennis TR, Stone G, Gray BA, McGuire PM, Zori RT, Stanyon R. 2007. Chromosome painting in the manatee supports Afrotheria and Paenungulata. BMC Evol Biol 7:6.

Keogh MJ, Ridgway SH. 2008. Neuronal fiber composition of the corpus callosum within some odontocetes. Anat Rec 291:781-789.
Kesarev VS, Malofeeva LI. 1969. [Structural organization of the motor zone of the cerebral cortex in dolphins]. Arkhiv Anat Gistol Enbriol 56:48-55.
Kitchen A, Denton D, Brent L. 1996. Self-recognition and abstraction abilities in the common chimpanzee studied with distorting mirrors. Proc Natl Acad Sci USA 93:7405-7408.
Klima M. 1999. Development of the cetacean nasal skull. Adv Anat Embryol Cell Biol 149:1-143.
Kojima T. 1951. On the brain of the sperm whale (*Physeter catodon L.*). Sci Rep Whales Res Inst Tokyo 6:49 -72.
Kraus C, Pilleri G. 1969. Quantitative Untersuchungen über die Grosshirnrinde der Cetaceen. Invest Cetacea 1:127-150.
Kretsinger RH, Nockolds CE. 1973. Carp muscle calcium-binding protein. II. Structure determination and general description. J Biol Chem 248:3313-3326.
Krettek JE, Price JL. 1977. The cortical projections of the mediodorsal nucleus and adjacent thalamic nuclei in the rat. J Comp Neurol 171:157-191.
Kruger L. 1959. The thalamus of the dolphin (*Tursiops truncatus*) and comparison with other mammals. J Comp Neurol 3:133-194.
Krutzen M, Mann J, Heithaus MR, Connor RC, Bejder L, Sherwin WB. 2005. Cultural transmission of tool use in bottlenose dolphins. Proc Natl Acad Sci USA 102:8939-8943.
Kubota Y, Hattori R, Yui Y. 1994. Three distinct subpopulations of GABAergic neurons in rat frontal agranular cortex. Brain rRes 649:159-173.
Kumar S, Hedges SB. 1998. A molecular timescale for vertebrate evolution. Nature 392:917-920.
Kunishio K, Haber SN. 1994. Primate cingulostriatal projection: Limbic striatal versus sensorimotor striatal input. J Comp Neurol 350:337-356.
Kunzle H. 1978. An autoradiographic analysis of the efferent connections from premotor and adjacent prefrontal regions (areas 6 and 9) in *Macaca fascicularis*. Brain Behav Evol 15:185-234.
Ladygina TF, Mass AM, Supin A. 1978. [Multiple sensory projections in the dolphin cerebral cortex]. Zh Vyssh Nerv Deiat Im I P Pavlova 28:1047-1053.
Ladygina TF, Supin A. 1970. [Acoustic projection in the dolphin cerebral cortex]. Fiziol Zh SSSR Im 56:1554-1560.
Ladygina TF, Supin A. 1977. [Localization of the sensory projection areas in the cerebral cortex of the dolphin, Tursiops truncatus]. Zh Evol Biokhim Fiziol 13(6):712-718.
Langworthy O. 1932. A description of the central nervous system of the porpoise (*Tursiops truncatus*). J Comp Neurol 350:337-356.
Lende RA, Welker WI. 1972. An unusual sensory area in the cerebral neocortex of the bottlenose dolphin. Brain Res 45:555-560.
Leung HC, Gore JC, Goldman-Rakic PS. 2005. Differential anterior prefrontal activation during the recognition stage of a spatial working memory task. Cereb Cortex 15:1742-1749.
Lewis M, Sullivan MW, Stanger C, Weiss M. 1989. Self development and self-conscious emotions. Child Dev 60:146-156.
Lewit-Bentley A, Rety S. 2000. EF-hand calcium-binding proteins. Curr Opin Struct Biol 10:637-643.
Lidow MS, Song ZM. 2001. Primates exposed to cocaine *in utero* display reduced density and number of cerebral cortical neurons. J Comp Neurol 435:263-275.
LoTurco JJ. 2000. Neural circuits in the 21st century: synaptic networks of neurons and glia. Proc Natl Acad Sci USA 97:8196-8197.
Lu MT, Preston JB, Strick PL. 1994. Interconnections between the prefrontal cortex and the premotor areas in the frontal lobe. J Comp Neurol 341:375-392.

Luppino G, Rozzi S, Calzavara R, Matelli M. 2003. Prefrontal and agranular cingulate projections to the dorsal premotor areas F2 and F7 in the macaque monkey. Eur J Neurosci 17:559-578.

Lusseau D. 2007. Evidence for social role in a dolphin social network. Evol Ecol 21:357-366.

Lusseau D, Newman ME. 2004. Identifying the role that animals play in their social networks. Proc Biol Soc 271 Suppl 6:S477-S481.

Magistretti PJ. 2006. Neuron-glia metabolic coupling and plasticity. J Exp Biol 209:2304-2311.

Magistretti PJ. 2009. Role of glutamate in neuron-glia metabolic coupling. Am J Clin Nutr. Epub ahead of print.

Magistretti PJ, Allaman I. 2007. Glycogen: A Trojan horse for neurons. Nat Neurosci 10:1341-1342.

Manger P, Sum M, Szymanski M, Ridgway SH, Krubitzer L. 1998. Modular subdivisions of dolphin insular cortex: Does evolutionary history repeat itself? J Cognit Neurosci 10:153-166.

Manger PR. 2006. An examination of cetacean brain structure with a novel hypothesis correlating thermogenesis to the evolution of a big brain. Biol Rev 81:293-338.

Manger PR, Pillay P, Maseko BC, Bhagwandin A, Gravett N, Moon DJ, Jillani N, Hemingway J. 2009. Acquisition of brains from the African elephant (*Loxodonta africana*): Perfusion-fixation and dissection. J Neurosci Methods 179:16-21.

Maragakis NJ, Rothstein JD. 2006. Mechanisms of disease: Astrocytes in neurodegenerative disease. Nat Clin Pract 2:679-689.

Marino L. 1998. A comparison of encephalization between odontocete cetaceans and anthropoid primates. Brain Behav Evol 51:230-238.

Marino L. 2004. Dolphin cognition. Curr Biol 14:R910-911.

Marino L. 2008. Brain Size Evolution. In: Perrin WF WB, Thewissen JGM, editor. Encyclopedia of Marine Mammals. San Diego, CA: Academic Press. p 149-152.

Marino L, Butti C, Connor RC, Fordyce RE, Herman LM, Hof PR, Lefebvre L, Lusseau D, McCowan B, Nimchinsky EA, Pack AA, Reidenberg JS, Reiss D, Rendell L, Uhen MD, Van der Gucht E, Whitehead H. 2008. A claim in search of evidence: Reply to Manger's thermogenesis hypothesis of cetacean brain structure. Biol Rev 83:417-440.

Marino L, Connor RC, Fordyce RE, Herman LM, Hof PR, Lefebvre L, Lusseau D, McCowan B, Nimchinsky EA, Pack AA, Rendell L, Reidenberg JS, Reiss D, Uhen MD, Van der Gucht E, Whitehead H. 2007. Cetaceans have complex brains for complex cognition. PLoS Biol 5(5):e139.

Marino L, McShea DW, Uhen MD. 2004a. Origin and evolution of large brains in toothed whales. Anat Rec 281:1247-1255.

Marino L, Murphy TL, Deweerd AL, Morris JA, Fobbs AJ, Humblot N, Ridgway SH, Johnson JI. 2001a. Anatomy and three-dimensional reconstructions of the brain of the white whale (*Delphinapterus leucas*) from magnetic resonance images. Anat Rec 262:429-439.

Marino L, Murphy TL, Gozal L, Johnson JI. 2001b. Magnetic resonance imaging and three-dimensional reconstructions of the brain of a fetal common dolphin, *Delphinus delphis*. Anat Embryol 203:393-402.

Marino L, Rilling JK, Lin SK, Ridgway SH. 2000. Relative volume of the cerebellum in dolphins and comparison with anthropoid primates. Brain Behav Evol 56:204-211.

Marino L, Sherwood CC, Delman BN, Tang CY, Naidich TP, Hof PR. 2004b. Neuroanatomy of the killer whale (*Orcinus orca*) from magnetic resonance images. Anat Rec 281:1256-1263.

Marino L, Sudheimer K, McLellan WA, Johnson JI. 2004c. Neuroanatomical structure of the spinner dolphin (*Stenella longirostris orientalis*) brain from magnetic resonance images. Anat Rec 279:601-610.

Marino L, Sudheimer K, Pabst DA, McLellan WA, Johnson JI. 2003a. Magnetic resonance images of the brain of a dwarf sperm whale (*Kogia simus*). J Anat 203:57-76.

Marino L, Sudheimer K, Sarko D, Sirpenski G, Johnson JI. 2003b. Neuroanatomy of the harbor porpoise (*Phocoena phocoena*) from magnetic resonance images. J Morphol 257:308-347.

Marino L, Sudheimer KD, Murphy TL, Davis KK, Pabst DA, McLellan WA, Rilling JK, Johnson JI. 2001c. Anatomy and three-dimensional reconstructions of the brain of a bottlenose dolphin (*Tursiops truncatus*) from magnetic resonance images. Anat Rec 264:397-414.

Marino L, Sudheimer KD, Pabst DA, McLellan WA, Filsoof D, Johnson JI. 2002. Neuroanatomy of the common dolphin (*Delphinus delphis*) as revealed by magnetic resonance imaging (MRI). Anat Rec 268:411-429.

Marino L, Uhen MD, Pyenson ND, Frohlich B. 2003c. Reconstructing cetacean brain evolution using computed tomography. Anat Rec 272:107-117.

Markram H, Toledo-Rodriguez M, Wang Y, Gupta A, Silberberg G, Wu C. 2004. Interneurons of the neocortical inhibitory system. Nature reviews 5(10):793-807.

Markowitsch HJ, Pritzel M. 1979. Prefrontal cortex of the cat: Evidence for an additional area. Experientia 35:396-398.

Martinez-Guijarro FJ, Freund TF. 1992. Distribution of GABAergic interneurons immunoreactive for calretinin, calbindin D28K, and parvalbumin in the cerebral cortex of the lizard *Podarcis hispanica*. J Comp Neurol 322:449-460.

McCowan B, Reiss D. 1995. Whistle contour development in captive-born infants bottlenose dolphin (*Tursiops truncatus*): Role of learning. J Comp Psychol 109:242-260.

McCowan B, Reiss D. 2001. The fallacy of "signature whistles" in bottlenose dolphins: A comparative perspective of "signature information" in animal vocalization. Anim Behav 62:1151-1162.

McFarland WL, Morgane PJ, Jacobs MS. 1969. Ventricular system of the brain of the dolphin, *Tursiops truncatus*, with comparative anatomical observations and relations to brain specializations. J Comp Neurol 135:275-368.

Medalla M, Barbas H. 2009. Synapses with inhibitory neurons differentiate anterior cingulate from dorsolateral prefrontal pathways associated with cognitive control. Neuron 61:609-620.

Mennerick S, Zorumski CF. 1994. Glial contributions to excitatory neurotransmission in cultured hippocampal cells. Nature 368:59-62.

Mercado E 3rd, Herman LM, Pack AA. 2005. Song copying by humpback whales: themes and variations. Anim Cogn 8:93-102.

Mesulam MM, Mufson EJ. 1982a. Insula of the old world monkey. I. Architectonics in the insulo-orbito-temporal component of the paralimbic brain. J Comp Neurol 212:1-22.

Mesulam MM, Mufson EJ. 1982b. Insula of the old world monkey. III: Efferent cortical output and comments on function. J Comp Neurol 212:38-52.

Miller EK. 1999. The prefrontal cortex: Complex neural properties for complex behavior. Neuron 22:15-17.

Montie EW, Schneider G, Ketten DR, Marino L, Touhey KE, Hahn ME. 2008. Volumetric neuroimaging of the Atlantic white-sided dolphin (*Lagenorhynchus acutus*) brain from *in situ* magnetic resonance images. Anat Rec 291:263-282.

Montie EW, Schneider GE, Ketten DR, Marino L, Touhey KE, Hahn ME. 2007. Neuroanatomy of the subadult and fetal brain of the Atlantic white-sided dolphin (*Lagenorhynchus acutus*) from in situ magnetic resonance images. Anat Rec 290:1459-1479.

Morecraft RJ, McNeal DW, Stilwell-Morecraft KS, Gedney M, Ge J, Schroeder CM, van Hoesen GW. 2007. Amygdala interconnections with the cingulate motor cortex in the rhesus monkey. J Comp Neurol 500:134-165.

Morecraft RJ, Van Hoesen GW. 1992. Cingulate input to the primary and supplementary motor cortices in the rhesus monkey: Evidence for somatotopy in areas 24c and 23c. J Comp Neurol 322:471-489.

Morecraft RJ, Van Hoesen GW. 1993. Frontal granular cortex input to the cingulate (M3), supplementary (M2) and primary (M1) motor cortices in the rhesus monkey. J Comp Neurol 337:669-689.

Morgane P, Jacobs, MS, Galaburda, A. 1986. Evolutionary morphology of the dolphin brain. In: Schusterman R, Thomas, J, Wood, F, editor. Dolphin Cognition and Behavior. A Comparative Approach. Hillsdale, NJ: Lawrence Erlbaum Assoc.

Morgane P, Glezer I, Jacobs M. 1990. Comparative and evolutionary anatomy of the visual cortex of the dolphin. In: Jones EG, Peters A, editors. Cerebral Cortex, vol. 8B. New York: Plenum. p 215-262.

Morgane P, Jacobs M, McFarland W. 1980. The anatomy of the brain of the bottlenose dolphin (*Tursiops truncatus*). Surface configuration of the telencephalon of the bottlenose dolphin with comparative anatomical observations in four other cetaceans species. Brain Res Bull 5 Suppl 3:1-107.

Morgane PJ, Glezer, II, Jacobs MS. 1988. Visual cortex of the dolphin: An image analysis study. J Comp Neurol 273:3-25.

Morgane PJ, McFarland WL, Jacobs MS. 1982. The limbic lobe of the dolphin brain: A quantitative cytoarchitectonic study. J Hirnforsch 23:465-552.

Morrison JH, Hof PR. 1997. Life and death of neurons in the aging brain. Science 278:412-419.

Morrison JH, Hof PR. 2007. Life and death of neurons in the aging cerebral cortex. Int Rev Neurobiol 81:41-57.

Mufson EJ, Mesulam MM. 1982. Insula of the old world monkey. II: Afferent cortical input and comments on the claustrum. J Comp Neurol 212:23-37.

Mufson EJ, Mesulam MM. 1984. Thalamic connections of the insula in the rhesus monkey and comments on the paralimbic connectivity of the medial pulvinar nucleus. J Comp Neurol 227:109-120.

Mufson EJ, Mesulam MM, Pandya DN. 1981. Insular interconnections with the amygdala in the rhesus monkey. Neuroscience 6:1231-1248.

Muller-Preuss P, Jürgens U. 1976. Projections from the 'cingular' vocalization area in the squirrel monkey. Brain Res 103:29-43.

Muller-Preuss P, Newman JD, Jürgens U. 1980. Anatomical and physiological evidence for a relationship between the 'cingular' vocalization area and the auditory cortex in the squirrel monkey. Brain Res 202:307-315.

Musil SY, Olson CR. 1988. Organization of cortical and subcortical projections to anterior cingulate cortex in the cat. J Comp Neurol 272:203-218.

Mutschler I, Schulze-Bonhage A, Glauche V, Demandt E, Speck O, Ball T. 2007. A rapid sound-action association effect in human insular cortex. PLoS One 2(2):e259.

Mutschler I, Wieckhorst B, Kowalevski S, Derix J, Wentlandt J, Schulze-Bonhage A, Ball T. 2009. Functional organization of the human anterior insular cortex. Neurosci Lett 457:66-70.

Nedergaard M, Ransom B, Goldman SA. 2003. New roles for astrocytes: Redefining the functional architecture of the brain. Trends Neurosci 26:523-530.

Newman EA. 2003. New roles for astrocytes: Regulation of synaptic transmission. Trends Neurosci 26:536-542.

Newman EA, Zahs KR. 1998. Modulation of neuronal activity by glial cells in the retina. J Neurosci 18:4022-4028.

Nikaido M, Rooney AP, Okada N. 1999. Phylogenetic relationships among cetartiodactyls based on insertions of short and long interpersed elements: Hippopotamuses are the closest extant relatives of whales. Proc Natl Acad Sci USA 96:10261-10266.

Nimchinsky EA, Gilissen E, Allman JM, Perl DP, Erwin JM, Hof PR. 1999. A neuronal morphologic type unique to humans and great apes. Proc Natl Acad Sci USA 96:5268-5273.
Nimchinsky EA, Vogt BA, Morrison JH, Hof PR. 1995. Spindle neurons of the human anterior cingulate cortex. J Comp Neurol 355:27-37.
Nimchinsky EA, Vogt BA, Morrison JH, Hof PR. 1997. Neurofilament and calcium-binding proteins in the human cingulate cortex. J Comp Neurol 384:597-620.
Noad MJ, Cato DH, Bryden MM, Jenner MN, Jenner KC. 2000. Cultural revolution in whale songs. Nature 408:537.
Oelschläger HHA, Buhl E. 1985. Development and rudimentation of the peripheral olfactory system in the harbor porpoise, *Phocoena phocoena* (Mammalia: Cetacea). J Morphol 184:351-360.
Oelschläger HHA, Oelschläger J. 2008. Brain. In: Perrin WF WB, Thewissen JGM, editor. Encyclopedia of Marine Mammals. San Diego, CA: Academic Press. p 134-149.
Oelschläger HHA, Haas-Rioth M, Fung C, Ridgway SH, Knauth M. 2008. Morphology and evolutionary biology of the dolphin (*Delphinus sp.*) brain — MR imaging and conventional histology. Brain Behav Evol 71:68-86.
Oelschläger HHA, Kemp B. 1998. Ontogenesis of the sperm whale brain. J Comp Neurol 399:210-228.
O'Kusky J, Colonnier M. 1982. A laminar analysis of the number of neurons, glia, and synapses in the adult cortex (area 17) of adult macaque monkeys. J Comp Neurol 210:278-290.
O'Leary M, Gatesy J. 2007. Impact on increased character sampling on the phylogeny of Cetartiodactyla (Mammalia): Combined analysis including fossils. Cladistics 23:1-46.
Öngür D, An, X, Price, JL. 1998. Orbital and medial prefrontal cortical projections to the hypothalamus in macaque monkeys. J Comp Neurol 401:480-505.
Öngür D, An X, Price JL. 1998. Prefrontal cortical projections to the hypothalamus in macaque monkeys. J Comp Neurol 401:480-505.
Öngür D, Drevets WC, Price JL. 1998. Glial reduction in the subgenual prefrontal cortex in mood disorders. Proc Natl Acad Sci USA 95:13290-13295.
Öngür D, Ferry AT, Price JL. 2003. Architectonic subdivision of the human orbital and medial prefrontal cortex. J Comp Neurol 460:425-449.
Öngür D, Price JL. 2000. The organization of networks within the orbital and medial prefrontal cortex of rats, monkeys and humans. Cereb Cortex 10:206-219.
Pack AA, Herman LM. 1995. Sensory integration in the bottlenosed dolphin: immediate recognition of complex shapes across the senses of echolocation and vision. J Acoust Soc Am 98:722-733.
Pack AA, Herman LM. 2007. The dolphin's (*Tursiops truncatus*) understanding of human gazing and pointing: knowing what and where. J Comp Psychol 121:34-45.
Pack AA, Herman LM, Hoffmann-Kuhnt M, Branstetter BK. 2002. The object behind the echo: Dolphins (*Tursiops truncatus*) perceive object shape globally through echolocation. Behav Process 58:1-26.
Page TL, Einstein M, Duan H, He Y, Flores T, Rolshud D, Erwin JM, Wearne SL, Morrison JH, Hof PR. 2002. Morphological alterations in neurons forming corticocortical projections in the neocortex of aged Patas monkeys. Neurosci Lett 317:37-41.
Pakkenberg B, Pelvig D, Marner L, Bundgaard MJ, Gundersen HJG, Nyengaard JR, Regeur L. 2003. Aging and the human neocortex. Exp Gerontol 38:95-99.
Pandya DN, Kuypers HGJM. 1969. Cortico-cortical connections in the rhesus monkey. Brain Res 13:13-36.
Pandya DN, Van Hoesen GW, Mesulam MM. 1981. Efferent connections of the cingulate gyrus in the rhesus monkey. Exp Brain Res 42:319-330.

Papez J. 1937. A proposed mechanism of emotions. Arch Neurol Psychiat 38:725-743.
Parpura V, Haydon PG. 2000. Physiological astrocytic calcium levels stimulate glutamate release to modulate adjacent neurons. Proc Natl Acad Sci USA 97:8629-8634.
Parri R, Crunelli V. 2003. An astrocyte bridge from synapse to blood flow. Nat Neurosci 6:5-6.
Parvizi J, Van Hoesen GW, Buckwalter J, Damasio A. 2006. Neural connections of the posteromedial cortex in the macaque. Proc Natl Acad Sci USA 103:1563-1568.
Pascual O, Casper KB, Kubera C, Zhang J, Revilla-Sanchez R, Sul JY, Takano H, Moss SJ, McCarthy K, Haydon PG. 2005. Astrocytic purinergic signaling coordinates synaptic networks. Science 310:113-116.
Pearson RC, Brodal P, Gatter KC, Powell TP. 1982. The organization of the connections between the cortex and the claustrum in the monkey. Brain Res 234:435-441.
Pellerin L, Bouzier-Sore AK, Aubert A, Serres S, Merle M, Costalat R, Magistretti PJ. 2007. Activity-dependent regulation of energy metabolism by astrocytes: An update. Glia 55:1251-1262.
Pellerin L, Magistretti PJ. 2004. Neuroenergetics: Calling upon astrocytes to satisfy hungry neurons. Neuroscientist 10:53-62.
Persechini A, Moncrief ND, Kretsinger RH. 1989. The EF-hand family of calcium-modulated proteins. Trends Neurosci 12:462-467.
Petrides M. 1996. Specialized systems for the processing of mnemonic information within the primate frontal cortex. Philos Trans R Soc Biol Lond 351:1455-1461.
Petrides M, Alivisatos B, Evans AC. 1995. Functional activation of the human ventrolateral frontal cortex during mnemonic retrieval of verbal information. Proc Natl Acad Sci USA 92:5803-5807.
Pfrieger FW. 2009. Roles of glial cells in synapse development. Cell Mol Life Sci 66:2037-2047.
Pfrieger FW, Barres BA. 1997. Synaptic efficacy enhanced by glial cells in vitro. Science 277:1684-1687.
Piet R, Vargova L, Sykova E, Poulain DA, Oliet SH. 2004. Physiological contribution of the astrocytic environment of neurons to intersynaptic crosstalk. Proc Natl Acad Sci USA 101:2151-2155.
Platel H, Price C, Baron JC, Wise R, Lambert J, Frackowiak RS, Lechevalier B, Eustache F. 1997. The structural components of music perception. A functional anatomical study. Brain 120:229-243.
Plotnik JM, de Waal FB, Reiss D. 2006. Self-recognition in an Asian elephant. Proc Natl Acad Sci USA 103:17053-17057.
Poole J, Moss, CJ. 2008. Elephant sociality and complexity: The scientific evidence. In: Wemmer C CC, editor. Elephants and Ethics: Towards a Morality of Coexistence. Baltimore: John Hopkins University Press. p 69-98.
Popov VV, Supin A. 1976. [Detemination of the hearing characteristics of the dolphin by the evoked potential method]. Fiziol Zh SSSR Im 62:550-558.
Popov VV, Supin A. 1986. [Evoked potentials of the dolphin auditory cortex recorded from the body surface]. Dokl Akad Nauk SSSR 288:756-759.
Porrino LJ, Crane AM, Goldman-Rakic PS. 1981. Direct and indirect pathways from the amygdala to the frontal lobe in rhesus monkeys. J Comp Neurol 198:121-136.
Posada S, Colell M. 2007. Another gorilla (*Gorilla gorilla gorilla*) recognizes himself in a mirror. Am J Primatol 69:576-583.
Poth C, Fung C, Güntürkün O, Ridgway SH, Oelschläger HH. 2005. Neuron numbers in sensory cortices of five delphinids compared to a physeterid, the pygmy sperm whale. Brain Res Bull 66:357-360.

Povinelli D, Gordon, G, Gallup, GG, Eddy, TJ, Bierschwale, DT, Engstrom, MC, Perriloux, HK, Toxopeus, IB. 1997. Chimpanzees recognize themselves in mirrors. Anim Behav 53:1083-1088.

Povinelli DJ, DeBlois S. 1992. Young children's (*Homo sapiens*) understanding of knowledge formation in themselves and others. J Comp Psychol 106:228-238.

Povinelli DJ, Nelson KE, Boysen ST. 1990. Inferences about guessing and knowing by chimpanzees (*Pan troglodytes*). J Comp Psychol 104:203-210.

Preuss T. 1995. Do rats have prefrontal cortex? The Rose-Woolsey-Akert program reconsidered. J Cognit Neurosci 7:1-24.

Preuss TM, Goldman-Rakic PS. 1987. Crossed corticothalamic and thalamocortical connections of macaque prefrontal cortex. J Comp Neurol 257:269-281.

Price JL, Carmichael ST, Drevets WC. 1996. Networks related to the orbital and medial prefrontal cortex; a substrate for emotional behavior? Prog Brain Res 107:523-536.

Pritz-Hohmeier S, Hartig W, Behrmann G, Reichenbach A. 1994. Immunocytochemical demonstration of astrocytes and microglia in the whale brain. Neurosci Lett 167:59-62.

Rainville P, Duncan GH, Price DD, Carrier B, Bushnell MC. 1997. Pain affect encoded in human anterior cingulate but not somatosensory cortex. Science 277:968-971.

Rajkowska G, Goldman-Rakic PS. 1995. Cytoarchitectonic definition of prefrontal areas in the normal human cortex: I. Remapping of areas 9 and 46 using quantitative criteria. Cereb Cortex 5:307-322.

Raz N, Gunning FM, Head D, Dupuis JH, McQuain J, Briggs SD, Loken WJ, Thornton AE, Acker JD. 1997. Selective aging of the human cerebral cortex observed *in vivo*: Differential vulnerability of the prefrontal gray matter. Cereb Cortex 7:268-282.

Reep RL, Corwin JV, Hashimoto A, Watson RT. 1984. Afferent connections of medial precentral cortex in the rat. Neurosci Lett 44:247-252.

Reep RL, O'Shea TJ. 1990. Regional brain morphometry and lissencephaly in the Sirenia. Brain Behav Evol 35:185-194.

Reichenbach A. 1989. Glia:neuron index: Review and hypothesis to account for different values in various mammals. Glia 2:71-77.

Reiss D, Marino L. 2001. Mirror self-recognition in the bottlenose dolphin: A case of cognitive convergence. Proc Natl Acad Sci USA 98:5937-5942.

Reiss D, McCowan B. 1993. Spontaneous vocal mimicry and production by bottlenose dolphins (*Tursiops truncatus*): Evidence for vocal learning. J Comp Psychol 107:301-312.

Reidenberg JS. 2007. Anatomical adaptations of aquatic mammals. Anat Rec (Hoboken) 290(6):507-513.

Rempel-Clower NL, Barbas H. 1998. Topographic organization of connections between the hypothalamus and prefrontal cortex in the rhesus monkey. J Comp Neurol 398:393-419.

Ren JQ, Aika Y, Heizmann CW, Kosaka T. 1992. Quantitative analysis of neurons and glial cells in the rat somatosensory cortex, with special reference to GABAergic neurons and parvalbumin-containing neurons. Exp Brain Res 92:1-14.

Rendell L, Whitehead H. 2001. Culture in whales and dolphins. Behav Brain Sci 24:309-382.

Résibois A, Rogers JH. 1992. Calretinin in rat brain: An immunohistochemical study. Neuroscience 46:101-134.

Revishchin AV, Garey LJ. 1989. [Sources of thalamic afferent neurons, projecting into the suprasylvian gyrus of the dolphin cerebral cortex]. Neirofiziologiia 21:529-539.

Revishchin AV, Garey LJ. 1996. Mitochondrial distribution in visual and auditory cerebral cortex of the harbour porpoise. Brain Behav Evol 47:257-266.

Rice D. 2008. Classification. In: Perrin WF, Thewissen JGM, editors. Encyclopedia of Marine Mammals. San Diego, CA. p 234-238.

Richards DG, Wolz JP, Herman LM. 1984. Vocal mimicry of computer-generated sounds and vocal labeling of objects by a bottlenose dolphin, *Tursiops truncatus*. J Comp Psychol 98:10-28.

Ries E, Langworthy O. 1937. A study of the surface structure of the brain of the whale (*Balaenoptera physalus* and *Physeter catodon*). J Comp Neurol 68:1-47.

Rivara CB, Sherwood CC, Bouras C, Hof PR. 2003. Stereologic characterization and spatial distribution patterns of Betz cells in the human primary motor cortex. Anat Rec 270:137-151.

Rogers JH. 1992. Immunohistochemical markers in rat cortex: co-localization of calretinin and calbindin-D28k with neuropeptides and GABA. Brain Res 587:147-157.

Rose JE, Woolsey CN. 1948. Structure and relations of limbic cortex and anterior thalamic nuclei in rabbit and cat. J Comp Neurol 89:279-347.

Rosene DL, Van Hoesen GW. 1977. Hippocampal efferents reach widespread areas of cerebral cortex and amygdala in the rhesus monkey. Science 198:315-317.

Rottschy C, Eickhoff SB, Schleicher A, Mohlberg H, Kujovic M, Zilles K, Amunts K. 2007. Ventral visual cortex in humans: cytoarchitectonic mapping of two extrastriate areas. Hum Brain Mapp 28:1045-1059.

Salat DH, Greve DN, Pacheco JL, Quinn BT, Helmer KG, Buckner RL, Fischl B. 2009. Regional white matter volume differences in nondemented aging and Alzheimer's disease. NeuroImage 44:1247-1258.

Sanders GS, Gallup GG, Heinsen H, Hof PR, Schmitz C. 2002. Cognitive deficits, schizophrenia, and the anterior cingulate cortex. Trends Cogn Sci 6:190-192.

Santello M, Volterra A. 2009. Synaptic modulation by astrocytes via Ca^{2+}-dependent glutamate release. Neuroscience 158:253-259.

Sayigh L, Tyack, PL, Wells, RS, Scott, MD. 1990. Signature whistles of free-ranging bottlenose dolphins, *Tursiops truncatus*: Stability and mother-offspring comparison. Behav Ecol Sociobiol 26:247-260.

Sayigh L, Tyack, PL, Wells, RS, Scott, MD, Irvine, AB. 1995. Sex differences in signature whistle production of free-ranging bottlenose dolphin, *Tursiops truncatus*. Behav Ecol Sociobiol 36:171-177.

Scannell JW, Blakemore C, Young MP. 1995. Analysis of connectivity in the cat cerebral cortex. J Neurosci 15:1463-1483.

Schenker NM, Buxhoeveden DP, Blackmon WL, Amunts K, Zilles K, Semendeferi K. 2008. A comparative quantitative analysis of cytoarchitecture and minicolumnar organization in Broca's area in humans and great apes. J Comp Neurol 510:117-128.

Schleicher A, Amunts K, Geyer S, Morosan P, Zilles K. 1999. Observer-independent method for microstructural parcellation of cerebral cortex: A quantitative approach to cytoarchitectonics. NeuroImage 9:165-177.

Schleicher A, Zilles K. 1990. A quantitative approach to cytoarchitectonics: analysis of structural inhomogeneities in nervous tissue using an image analyser. J Microsc 157:367-381.

Schleicher A, Zilles K, Wree A. 1986. A quantitative approach to cytoarchitectonics: software and hardware aspects of a system for the evaluation and analysis of structural inhomogeneities in nervous tissue. J Neurosci Methods 18:221-235.

Schmitz C, Dafotakis M, Heinsen H, Mugrauer K, Niesel A, Popken GJ, Stephan M, Van de Berg WD, von Horsten S, Korr H. 2000. Use of cryostat sections from snap-frozen nervous tissue for combining stereological estimates with histological, cellular, or molecular analyses on adjacent sections. J Chem Neuroanat 20:21-29.

Schmitz C, Grolms N, Hof PR, Boehringer R, Glaser J, Korr H. 2002. Altered spatial arrangement of layer V pyramidal cells in the mouse brain following prenatal low-dose X-irradiation. A

stereological study using a novel three-dimensional analysis method to estimate the nearest neighbor distance distributions of cells in thick sections. Cereb Cortex 12(9):954-960.
Schmitz C, Hof PR. 2005. Design-based stereology in neuroscience. Neuroscience 130:813-831.
Schwerdtfeger WK, Oelschläger HA, Stephan H. 1984. Quantitative neuroanatomy of the brain of the La Plata dolphin, *Pontoporia blainvillei*. Anat Embryol 170:11-19.
Seeley WW. 2008. Selective functional, regional, and neuronal vulnerability in frontotemporal dementia. Curr Opin Neuro 21(6):701-707.
Seeley WW, Allman JM, Carlin DA, Crawford RK, Macedo MN, Greicius MD, Dearmond SJ, Miller BL. 2007. Divergent social functioning in behavioral variant frontotemporal dementia and Alzheimer disease: reciprocal networks and neuronal evolution. Alzheimer Dis Assoc Disord 21:S50-S57.
Seeley WW, Carlin DA, Allman JM, Macedo MN, Bush C, Miller BL, Dearmond SJ. 2006. Early frontotemporal dementia targets neurons unique to apes and humans. Ann Neurol 60:660-667.
Seeley WW, Crawford R, Rascovsky K, Kramer JH, Weiner M, Miller BL, Gorno-Tempini ML. 2008. Frontal paralimbic network atrophy in very mild behavioral variant frontotemporal dementia. Arch Neurol 65:249-255.
Seeley WW, Crawford RK, Zhou J, Miller BL, Greicius MD. 2009. Neurodegenerative diseases target large-scale human brain networks. Neuron 62:42-52.
Seeley WW, Menon V, Schatzberg AF, Keller J, Glover GH, Kenna H, Reiss AL, Greicius MD. 2007. Dissociable intrinsic connectivity networks for salience processing and executive control. J Neurosci 27:2349-2356.
Segal D, Koschnick JR, Slegers LH, Hof PR. 2007. Oligodendrocyte pathophysiology: A new view of schizophrenia. Int J Neuropsychopharmacol 10:503-511.
Selemon LD, Goldman-Rakic PS. 1988. Common cortical and subcortical targets of the dorsolateral prefrontal and posterior parietal cortices in the rhesus monkey: Evidence for a distributed neural network subserving spatially guided behavior. J Neurosci 8:4049-4068.
Shariff GA. 1953. Cell counts in the primate cerebral cortex. J Comp Neurol 98:381-400.
Shea B. 1983. Phyletic size change and brain/body allometry: A consideration based on the African pongids and other primates. Int J Primatol 4:33-62.
Shelley BP, Trimble MR. 2004. The insular lobe of Reil — its anatomico-functional, behavioural and neuropsychiatric attributes in humans — A review. World J Biol Psychiatry 5:176-200.
Sherwood CC, Lee PW, Rivara CB, Holloway RL, Gilissen EP, Simmons RM, Hakeem A, Allman JM, Erwin JM, Hof PR. 2003. Evolution of specialized pyramidal neurons in primate visual and motor cortex. Brain Behav Evol 61:28-44.
Sherwood CC, Stimpson CD, Butti C, Bonar CJ, Newton AL, Allman JM, Hof PR. 2009. Neocortical neuron types in Xenarthra and Afrotheria: Implications for brain evolution in mammals. Brain Struct Funct 213:301-328.
Sherwood CC, Stimpson CD, Raghanti MA, Wildman DE, Uddin M, Grossman LI, Goodman M, Redmond JC, Bonar CJ, Erwin JM, Hof PR. 2006. Evolution of increased glia-neuron ratios in the human frontal cortex. Proc Natl Acad Sci USA 103:13606-13611.
Shimamura M, Abe H, Nikaido M, Ohshima K, Okada N. 1999. Genealogy of families of SINEs in cetaceans and artiodactyls: The presence of a huge superfamily of tRNA(Glu)-derived families of SINEs. Mol Biol Evol 16:1046-1060.
Shin LM, Dougherty DD, Orr SP, Pitman RK, Lasko M, Macklin ML, Alpert NM, Fischman AJ, Rauch SL. 2000. Activation of anterior paralimbic structures during guilt-related script-driven imagery. Biol Psychiatry 48:43-50.
Shin LM, Whalen PJ, Pitman RK, Bush G, Macklin ML, Lasko NB, Orr SP, McInerney SC, Rauch SL. 2001. An fMRI study of anterior cingulate function in posttraumatic stress disorder. Biol Psychiatry 50:932-942.

Showers MJ, Lauer EW. 1961. Somatovisceral motor patterns in the insula. J Comp Neurol 117:107-115.
Simmonds M. 2006. Into the brains of whales. Appl Anim Behav Sci 100:103-116.
Singer T, Seymour B, O'Doherty J, Kaube H, Dolan RJ, Frith CD. 2004. Empathy for pain involves the affective but not sensory components of pain. Science 303:1157-1162.
Siwek DF, Pandya DN. 1991. Prefrontal projections to the mediodorsal nucleus of the thalamus in the rhesus monkey. J Comp Neurol 312:509-524.
Smith SJ. 1994. Neural signaling, neuromodulatory astrocytes. Curr Biol 4:807-810.
Sokolov VE, Ladygina TF, Supin A. 1972. [Localization of sensory zones in the dolphin cerebral cortex]. Dokl Akad Nauk SSSR 202:490-493.
Song H, Stevens CF, Gage FH. 2002. Astroglia induce neurogenesis from adult neural stem cells. Nature 417:39-44.
Stephan E, Pardo JV, Faris PL, Hartman BK, Kim SW, Ivanov EH, Daughters RS, Costello PA, Goodale RL. 2003. Functional neuroimaging of gastric distention. J Gastrointest Surg 7:740-749.
Stolzenburg JU, Reichenbach A, Neumann M. 1989. Size and density of glial and neuronal cells within the cerebral neocortex of various insectivorian species. Glia 2:78-84.
Suarez S, Gallup, GG. 1981. Self-recognition in chimpanzee and orangutans but not gorillas. J Hum Evol 10:175-188.
Takada M, Nambu A, Hatanaka N, Tachibana Y, Miyachi S, Taira M, Inase M. 2004. Organization of prefrontal outflow toward frontal motor-related areas in macaque monkeys. Eur J Neurosci 19:3328-3342.
Tandrup T, Gundersen HJG, Jensen EB. 1997. The optical rotator. J Microsc 186:108-120.
Tarpley RJ, Ridgway SH. 1994. Corpus callosum size in delphinid cetaceans. Brain Behav Evol 44:156-165.
Tayler C, Saayman, GS. 1973. Imitate behavior by Indian Ocean bottlenose dolphins (*Tursiops truncatus*) in captivity. Behavior 44:286-298.
Taylor S, Semionowicz DA, Davis KD. 2009. Two systems of resting state connectivity between insula and cingulate cortex. Human brain mapping in press.
Terreberry RR, Neafsey EJ. 1983. Rat medial frontal cortex: a visceral motor region with a direct projection to the solitary nucleus. Brain Res 278:245-249.
Thewissen JG, Cooper LN, Clementz MT, Bajpai S, Tiwari BN. 2007. Whales originated from aquatic artiodactyls in the Eocene epoch of India. Nature 450:1190-1194.
Thewissen JG, Williams EM, Roe LJ, Hussain ST. 2001. Skeletons of terrestrial cetaceans and the relationship of whales to artiodactyls. Nature 413:277-281.
Thompson RK, Herman LM. 1977. Memory for lists of sounds by the bottle-nosed dolphin: Convergence of memory processes with humans? Science 195:501-503.
Thomsen F, Franck D, Ford JK. 2001. Characteristics of whistles from the acoustic repertoire of resident killer whales (*Orcinus orca*) off Vancouver Island, British Columbia. J Acoust Soc Am 109:1240-1246.
Thomsen F, Franck D, Ford JK. 2002. On the communicative significance of whistles in wild killer whales (*Orcinus orca*). Naturwissenschaften 89:404-407.
Tkachev D, Mimmack ML, Ryan MM, Wayland M, Freeman T, Jones PB, Starkey M, Webster MJ, Yolken RH, Bahn S. 2003. Oligodendrocyte dysfunction in schizophrenia and bipolar disorder. Lancet 362:798-805.
Tower DB. 1954. Structural and functional organization of mammalian cerebral cortex; the correlation of neurone density with brain size; cortical neurone density in the fin whale (*Balaenoptera physalus* L.) with a note on the cortical neurone density in the Indian elephant. J Comp Neurol 101:19-51.

Tower DB, Elliott KA. 1952. Activity of acetylcholine system in cerebral cortex of various unanesthetized mammals. Am J Physiol 168:747-759.
Tower DB, Young OM. 1973. The activities of butyrylcholinesterase and carbonic anhydrase, the rate of anaerobic glycolysis, and the question of a constant density of glial cells in cerebral cortices of various mammalian species from mouse to whale. J Neurochem 20:269-278.
Tsacopoulos M, Magistretti PJ. 1996. Metabolic coupling between glia and neurons. J Neurosci 16:877-885.
Tschudin A, Call J, Dunbar RI, Harris G, van der Elst C. 2001. Comprehension of signs by dolphins (*Tursiops truncatus*). J Comp Psychol 115:100-105.
Tyack P. 1986. Whistle repertoires of two bottlenose dolphin, *Tursiops truncatus*: Mimicry of signature whistles? Behav Ecol Sociobiol 35:243-248.
Uhen M. 2004. Form, function and anatomy of *Dorudon atrox* (Mammalia:Cetacea): An archeocete from teh middle to late Eocene of Egypt. Univ Mich Pap Paleontol 34:1-222.
Ullian EM, Sapperstein SK, Christopherson KS, Barres BA. 2001. Control of synapse number by glia. Science 291:657-661.
Van Brederode JF, Mulligan KA, Hendrickson AE. 1990. Calcium-binding proteins as markers for subpopulations of GABAergic neurons in monkey striate cortex. J Comp Neurol 298:1-22.
Verney C, Derer P. 1995. Cajal-Retzius neurons in human cerebral cortex at midgestation show immunoreactivity for neurofilament and calcium-binding proteins. J Comp Neurol 359:144-153.
Vogt BA. 2005. Pain and emotion interactions in subregions of the cingulate gyrus. Nat Rev Neurosci 6:533-544.
Vogt BA, Berger GR, Derbyshire SW. 2003. Structural and functional dichotomy of human midcingulate cortex. Eur J Neurosci 18:3134-3144.
Vogt BA, Crino PB, Vogt LJ. 1992a. Reorganization of cingulate cortex in Alzheimer's disease: Neuron loss, neuritic plaques, and muscarinic receptor binding. Cereb Cortex 2:526-535.
Vogt BA, Finch DM, Olson CR. 1992b. Functional heterogeneity in cingulate cortex: The anterior executive and posterior evaluative regions. Cereb Cortex 2:435-443.
Vogt BA, Nimchinsky EA, Vogt LJ, Hof PR. 1995. Human cingulate cortex: Surface features, flat maps, and cytoarchitecture. J Comp Neurol 359:490-506.
Vogt BA, Pandya DN. 1987. Cingulate cortex of the rhesus monkey: II. Cortical afferents. J Comp Neurol 262:271-289.
Vogt BA, Pandya DN, Rosene DL. 1987. Cingulate cortex of the rhesus monkey: I. Cytoarchitecture and thalamic afferents. J Comp Neurol 262:256-270.
Vogt BA, Rosene DL, Pandya DN. 1979. Thalamic and cortical afferents differentiate anterior from posterior cingulate cortex in the monkey. Science 204:205-207.
Vogt BA, Vogt LJ, Perl DP, Hof PR. 2001. Cytology of human caudomedial cingulate, retrosplenial, and caudal parahippocampal cortices. J Comp Neurol 438(3):353-376.
Vogt LJ, Vogt BA, Sikes RW. 1992c. Limbic thalamus in rabbit: Architecture, projections to cingulate cortex and distribution of muscarinic acetylcholine, GABAA, and opioid receptors. J Comp Neurol 319:205-217.
Vogt Weisenhorn DM, Prieto EW, Celio MR. 1994. Localization of calretinin in cells of layer I (Cajal-Retzius cells) of the developing cortex of the rat. Dev Brain Res 82:293-297.
von Economo C, Koskinas, GN. 1925. Die Cytoarchitektonik der Hirnrinde des erwachsenen Menschen. Berlin: Springer.
von Economo C. 1926. Eine neue Art Spezialzellen des Lobus cinguli and Lobus insulae. Zschr ges Neurol Psychiat 100:706 -712.
Wang SS, Shultz JR, Burish MJ, Harrison KH, Hof PR, Towns LC, Wagers MW, Wyatt KD. 2008. Functional trade-offs in white matter axonal scaling. J Neurosci 28:4047-4056.

Wang Y, Matsuzaka Y, Shima K, Tanji J. 2004. Cingulate cortical cells projecting to monkey frontal eye field and primary motor cortex. NeuroReport 15:1559-1563.

Wang Y, Shima K, Sawamura H, Tanji J. 2001. Spatial distribution of cingulate cells projecting to the primary, supplementary, and pre-supplementary motor areas: a retrograde multiple labeling study in the macaque monkey. Neurosci Res 39:39-49.

Watson KK, Jones TK, Allman JM. 2006. Dendritic architecture of the von Economo neurons. Neuroscience 141:1107-1112.

Weinberger DR. 1993. A connectionist approach to the prefrontal cortex. J Neuropsychiatry Clin Neurosci 5:241-253.

Wender R, Brown AM, Fern R, Swanson RA, Farrell K, Ransom BR. 2000. Astrocytic glycogen influences axon function and survival during glucose deprivation in central white matter. J Neurosci 20:6804-6810.

West MJ, Slomianka L, Gundersen HJG. 1991. Unbiased stereological estimation of the total number of neurons in thesubdivisions of the rat hippocampus using the optical fractionator. Anat Rec 231:482-497.

Weston EM, Lister AM. 2009. Insular dwarfism in hippos and a model for brain size reduction in *Homo floresiensis*. Nature 459:85-88.

Whalen PJ, Bush G, McNally RJ, Wilhelm S, McInerney SC, Jenike MA, Rauch SL. 1998. The emotional counting Stroop paradigm: a functional magnetic resonance imaging probe of the anterior cingulate affective division. Biol Psychiatry 44:1219-1228.

Willett CJ, Gwyn DG, Rutherford JG, Leslie RA. 1986. Cortical projections to the nucleus of the tractus solitarius: An HRP study in the cat. Brain Res Bull 16:497-505.

Xiao D, Barbas H. 2002. Pathways for emotions and memory I. Input and output zones linking the anterior thalamic nuclei with prefrontal cortices in the rhesus monkey. Thalamus Relat Syst 2:21-32.

Xiao D, Barbas H. 2002. Pathways for emotions and memory II. Afferent input to the anterior thalamic nuclei from prefrontal, temporal, hypothalamic areas and the basal ganglia in the rhesus monkey. Thalamus Relat Syst 2:33-48.

Zhang JM, Wang HK, Ye CQ, Ge W, Chen Y, Jiang ZL, Wu CP, Poo MM, Duan S. 2003. ATP released by astrocytes mediates glutamatergic activity-dependent heterosynaptic suppression. Neuron 40:971-982.

Zhang K, Sejnowski TJ. 2000. A universal scaling law between gray matter and white matter of cerebral cortex. Proc Natl Acad Sci USA 97:5621-5626.

Zola-Morgan S, Squire LR. 1993. Neuroanatomy of memory. Annu Rev Neurosci 16:547-563.